

# **Quadrotor Team Modeling and Control for DLO Transportation**

**By**

**Julián Estévez Sanz**

Submitted to the department of Computer Science and Artificial Intelligence in partial fulfillment of the requirements for the degree of Doctor of Philosophy

*PhD Advisor:*

Prof. Manuel Graña Romay  
at The University of the Basque Country (UPV/EHU)

Euskal Herriko Unibertsitatea  
Universidad del País Vasco  
Donostia - San Sebastián  
2016



**AUTORIZACION DEL/LA DIRECTOR/A DE TESIS  
PARA SU PRESENTACION**

Dr. MANUEL M. GRAÑA ROMAY con N.I.F. 15932620Z como Director de la Tesis Doctoral: *Quadrotor Modeling and Control for DLO Transportation* realizada en el Programa de Doctorado en Ingeniería Informática por el Doctorando D. JULIÁN ESTÉVEZ SANZ, autorizo la presentación de la citada Tesis Doctoral, dado que reúne las condiciones necesarias para su defensa.

En DONOSTIA a 16 de mayo de 2016

EL DIRECTOR DE LA TESIS

Fdo.: \_\_\_\_\_



## CONFORMIDAD DEL DEPARTAMENTO

El Consejo del Departamento de CIENCIAS DE LA COMPUTACIÓN E INTELIGENCIA ARTIFICIAL en reunión celebrada el día \_\_\_ de \_\_\_\_\_ de 201\_\_ ha acordado dar la conformidad a la admisión a trámite de presentación de la Tesis Doctoral titulada: *Quadrotor Modeling and Control for DLO Transportation* dirigida por el Dr. MANUEL M. GRAÑA ROMAY y presentada por Don JULIÁN ESTÉVEZ SANZ ante este Departamento.

En DONOSTIA a \_\_\_ de \_\_\_\_\_ de 201\_\_

VºBº DIRECTOR/A DEL DEPARTAMENTO

SECRETARIO/A DEL DEPARTAMENTO

Fdo.:\_\_\_\_\_

Fdo.:\_\_\_\_\_



## **AUTORIZACIÓN DE LA COMISIÓN ACADÉMICA DEL PROGRAMA DE DOCTORADO**

La Comisión Académica del Programa de Doctorado en Ingeniería Informática en reunión celebrada el día \_\_\_\_ de \_\_\_\_\_ de 201\_\_\_\_, ha acordado dar la conformidad a la presentación de la Tesis Doctoral titulada: *Quadrotor Modeling and Control for DLO Transportation* dirigida por el Dr. MANUEL M. GRAÑA ROMAY y presentada por D. JULIÁN ESTÉVEZ SANZ adscrito al Departamento CIENCIAS DE LA COMPUTACIÓN E INTELIGENCIA ARTIFICIAL

En DONOSTIA a \_\_\_\_ de \_\_\_\_\_ de \_\_\_\_\_

EL MIEMBRO DE LA COMISIÓN ACADÉMICA RESPONSABLE DEL  
PROGRAMA DE DOCTORADO

Fdo.: \_\_\_\_\_





## **ACTA DE GRADO DE DOCTOR O DOCTORA** **ACTA DE DEFENSA DE TESIS DOCTORAL**

DOCTORANDO/A **D. Julián Estévez Sanz**

TITULO DE LA TESIS: *Quadrotor Modeling and Control for DLO Transportation*

El Tribunal designado por la Comisión de Postgrado de la UPV/EHU para calificar la Tesis Doctoral arriba indicada y reunido en el día de la fecha, una vez efectuada la defensa por el/la doctorando/a y contestadas las objeciones y/o sugerencias que se le han formulado, ha otorgado por \_\_\_\_\_ la calificación de:  
*unanimidad ó mayoría*

--

SOBRESALIENTE / NOTABLE / APROBADO / NO APTO

Idioma/s de defensa (en caso de más de un idioma, especificar porcentaje defendido en cada idioma):

Castellano \_\_\_\_\_

Euskera \_\_\_\_\_

Otros Idiomas (especificar cuál/cuales y porcentaje) \_\_\_\_\_

En \_\_\_\_\_ a \_\_\_\_\_ de \_\_\_\_\_ de \_\_\_\_\_

EL/LA PRESIDENTE/A,

EL/LA SECRETARIO/A,

Fdo.:

Fdo.:

Dr/a: \_\_\_\_\_

Dr/a: \_\_\_\_\_

VOCAL 1º,

VOCAL 2º,

VOCAL 3º,

Fdo.:

Fdo.:

Fdo.:

Dr/a: \_\_\_\_\_ Dr/a: \_\_\_\_\_ Dr/a: \_\_\_\_\_

EL/LA DOCTORANDO/A,

Fdo.: \_\_\_\_\_



## **Acknowledgments**

*Third time lucky, and it is sure that would have been not possible without Prof. Manuel Graña. During this time, both of us had to learn to rely on each other and overcome all the inquisitive reviewers. Thanks specially for getting me enjoy this job and research field.*

*I want to thank all the GIC members I shared a word with for widening the habitual researchers' activities, and living experiences I would not have imagined to do along my PhD process.*

*I am very grateful to my closest friends for always accepting "it is hard to say" to their "how is your thesis going?" question, and thanks to the Owl for lightning the path in different aspects of my life.*

*Finally, special thanks to my family and Amalia for their unconditional support and continous aid.*

*Julián Estévez Sanz*



# Quadrotor Modeling and Control for DLO Transportation

*by*

Julián Estévez Sanz

Submitted to the Department of Computer Science and Artificial Intelligence on May 16th, 2016, in partial fulfillment of the requirements for the degree of Doctor of Philosophy

## **Abstract**

This Thesis presents a proposal of a dynamic model for loading Deformable Linear Objects (DLO) with a team of quadrotors. Three factors play a role in this model: Dynamic model of the payload solid, dynamic model of the quadrotor for taking into account the passive dynamics of the DLO, and a control strategy for an efficient and robust transportation. We differentiate two tasks: (a) achieving a equi-workload spatial configuration of the quasy-stationary DLO-quadrotors system. (b) performing the transportation by horizontal displacement of the whole system. The transportation is a simple follow-the-leader maintaining a line strategy, but the local quadrotor controls must be robust enough to cope with all non-linear induced by the DLO and other external perturbations. Quadrotor controllers are designed in order to assure the system stability and quick convergence for the robust achievement of the current task. Offline and online control strategies are compared and tested in various experiments to compare their fitness to variable dynamic conditions of the system, including external wind disturbances and taking into account the scalability of the system.



# Contents

<b>1</b>	<b>Introduction</b>	<b>1</b>
1.1	Introduction . . . . .	1
1.2	Motivation . . . . .	2
1.3	Elementary definitions . . . . .	3
1.3.1	Deformable Linear Objects (DLO) . . . . .	3
1.3.2	Transport problem definition . . . . .	4
1.3.3	Quadrotor modeling and control . . . . .	4
1.4	Thesis goals . . . . .	5
1.5	Thesis contributions . . . . .	6
1.5.1	Publications achieved . . . . .	7
1.6	Thesis organization . . . . .	7
<b>2</b>	<b>State of the Art</b>	<b>9</b>
2.1	Some basic definitions . . . . .	9
2.2	Previous works on deformable linear objects models . . . . .	10
2.2.1	DLO modeling approaches . . . . .	10
2.2.2	Aerial payload transportation using DLO . . . . .	11
2.2.3	Catenaries . . . . .	14
2.3	Drone cooperative systems . . . . .	16
2.4	Quadrotor dynamic modeling . . . . .	17
2.4.1	Dynamic equations . . . . .	20
2.4.2	Wind disturbance model . . . . .	21
2.5	Control strategies . . . . .	21
2.5.1	PID tuning algorithms . . . . .	23
<b>3</b>	<b>Dynamical models</b>	<b>25</b>
3.1	Introduction . . . . .	25
3.2	Geometrical and dynamical DLO model . . . . .	26
3.3	Desired team spatial configuration . . . . .	27
3.4	Quadrotor modeling . . . . .	32

3.4.1	Coordinate frames . . . . .	32
3.4.2	Dynamic equations . . . . .	34
<b>4</b>	<b>Quadrotor control system</b>	<b>37</b>
4.1	Introduction . . . . .	37
4.2	General motion control for DLO transportation . . . . .	38
4.3	Inner control loop . . . . .	39
4.4	Offline inner control loop tuning . . . . .	41
4.4.1	Ziegler-Nichols algorithm . . . . .	41
4.4.2	Particle Swarm Optimization (PSO) . . . . .	41
4.5	Experiment 1 . . . . .	43
4.5.1	Results of <i>Experiment 1a</i> . . . . .	45
4.5.2	Results of <i>Experiment 1b</i> . . . . .	47
4.6	Conclusions . . . . .	50
<b>5</b>	<b>Transportation control</b>	<b>53</b>
5.1	Introduction . . . . .	53
5.2	Quadrotor team control model . . . . .	54
5.3	Outer-loop control . . . . .	54
5.4	Outer control loop adaptive tuning . . . . .	56
5.5	Heuristics for smooth behaviors . . . . .	58
5.6	Experiment 2 . . . . .	58
5.6.1	Results of <i>Experiment 2a</i> . . . . .	60
5.6.2	Results of <i>Experiment 2b</i> . . . . .	64
5.6.3	Results of <i>Experiment 2c</i> . . . . .	64
5.7	Experiment 3 . . . . .	64
5.7.1	Results of <i>Experiment 3a</i> . . . . .	69
5.7.2	Results of <i>Experiment 3b</i> . . . . .	69
5.8	Conclusions . . . . .	72
<b>6</b>	<b>Conclusions and Future Work</b>	<b>79</b>
6.1	Conclusions . . . . .	79
6.1.1	Aerial robots modeling for cooperative transportation of DLOs . . . . .	79
6.1.2	Offline control strategy . . . . .	79
6.1.3	Online adaptive control strategy . . . . .	80
6.2	Future Work . . . . .	80
6.2.1	System modeling . . . . .	80
6.2.2	Control strategy . . . . .	81



*CONTENTS*

xvii

**Bibliography**

**82**



# List of Figures

1.1	Stylized physical representation of three drones carrying a DLO which is approximated by two catenary curve sections. . . . .	2
1.2	Roll, pitch and yaw angles representation . . . . .	5
2.1	Model to transport a payload in three dimensions through the air described in [63] . . . . .	13
2.2	2013 model for DLO transportation through the air . . . . .	13
2.3	Hose model used in [81] . . . . .	14
2.4	Catenary curve modeling a DLO holding between robots A and B. . . . .	15
2.5	Plus (left) and cross (right) rotor configurations . . . . .	18
2.6	Plus configuration: pitch, roll and yaw controls, where red arrows indicate the relative rotor speed . . . . .	19
2.7	Inner and outer loop for attitude and position . . . . .	22
2.8	PID controller diagram . . . . .	23
3.1	Catenary parameters ( $I, J$ ) correspond to the catenary nodes . . . . .	27
3.2	Catenary and two robots system . . . . .	28
3.3	Catenary and three robots system. Initial state . . . . .	28
3.4	Plot of the differences with the desired state in Eq. 3.4. . . . .	29
3.5	Two fold catenary sustained by a three robots system. Initial (blue) and final (red) states. . . . .	31
3.6	Two fold catenary sustained by three robot in an asymmetric initial state. . . . .	31
3.7	Catenary and three robot asymmetric system. Intermediate and final states . . . . .	32
3.8	Equi-workload configurations for systems with 3, 4, and 5 quadrotors, having 2, 3, and 4 catenary sections . . . . .	33
3.9	Roll ( $\phi$ ), pitch ( $\theta$ ), yaw ( $\psi$ ) angles in a plus configuration quadrotor . . . . .	34
3.10	Coordinate systems and catenary tensions . . . . .	35
4.1	Two loops controllers for quadrotor position and orientation . . . . .	38

4.2	Roll ( $\phi$ ), pitch ( $\theta$ ), yaw ( $\psi$ ) angles in a plus configuration quadrotor	39
4.3	PID $Z$ controller . . . . .	40
4.4	PID $\phi$ controller . . . . .	40
4.5	PID $\theta$ controller . . . . .	40
4.6	PID $\psi$ controller . . . . .	41
4.7	Catenary and three robots system for <i>Experiment 1a</i> . Initial and final state . . . . .	44
4.8	Balanced catenary for <i>Experiment 1b</i> . . . . .	45
4.9	Response of middle quadrotor in Figure 4.7, position in the $Z$ coordinate (elevation) under ZN tuning control to achieve the desired state of robot equiloading. . . . .	46
4.10	Response of quadrotor B of Figure 4.7, vertical speed under ZN tuning control to achieve the desired state of robot equiloading. . . . .	46
4.11	Response of quadrotor vertical B of Figure 4.7, vertical acceleration under ZN tuning control to achieve the desired state of robot equiloading. . . . .	47
4.12	Response of quadrotor vertical B of Figure 4.7, vertical displacement under PSO tuning control to achieve the desired state of robot equiloading. Three different PD tuning combinations . . . . .	48
4.13	Response of quadrotor vertical B of Figure 4.7 $Z$ displacement. Three different convergence heights . . . . .	48
4.14	Response of quadrotor vertical B of Figure 4.7 vertical displacement under PSO for different dynamic parameters . . . . .	49
4.15	Response of quadrotor B of Figure 4.8, position in the $Z$ coordinate (elevation) under the PID control to achieve the desired state of robot equiloading after the extension of one of the catenaries due to change in cruise speed of the $C$ robot. . . . .	50
4.16	Time plot of the load supported by quadrotor B of Figure 4.8 after the extension of one of the catenaries due to change in cruise speed of the $C$ robot. . . . .	51
5.1	Follow-the-leader behavior parameters: distance ( $\lambda$ ) between quadrotors positions, and heading angular difference ( $\varphi$ ) parameters. . . . .	55
5.2	Membership functions of the fuzzy adaption rules of the PD control parameters . . . . .	56
5.3	Catenaries configuration for <i>Experiment 2</i> . . . . .	60
5.4	Dependence of overshoot in $X$ (image a) and $Y$ (image b) of robots $D1$ and $D2$ on the required distance when training the controllers by minimizing CF1 in <i>Experiment 2a</i> . . . . .	61

5.5	Dependence of overshoot in $X$ (image a) and $Y$ (image b) of robots $D1$ and $D2$ on the required distance when training the controllers by minimizing CF2 in <i>Experiment 2a</i> . . . . .	62
5.6	Trajectory of the three quadrotors in $(X, Y)$ space when the desired motion is (a) $(\Delta x, \Delta y) = (60, 30)$ , (b) $(\Delta x, \Delta y) = (140, 60)$ , for the controllers achieved with both cost functions CF1 (up) and CF2 (down). . . . .	63
5.7	$X$ (image a) and $Y$ (image b) trajectory of three quadrotors in <i>Experiment 2b</i> . . . . .	65
5.8	Thrust of $D1$ and $D2$ in <i>Experiment 2c</i> under no disturbances . . . . .	66
5.9	Trajectory and thrust of drones under controllers trained minimizing CF1 suffering wind disturbances in $X$ direction in <i>Experiment 2c</i> . . . . .	67
5.10	Trajectory and thrust of drones under controllers trained minimizing CF2 suffering wind disturbances in $X$ direction in <i>Experiment 2c</i> . . . . .	67
5.11	Path of the leader quadrotor for the <i>Experiment 3b</i> . . . . .	67
5.12	Comparison offline PSO optimal estimation of PD controller parameters vs online fuzzy modulated adaptive controller in <i>Experiment 3a</i> . a) Results without perturbations. b) Results under wind conditions. . . . .	70
5.13	Trajectories of a system of four quadrotors in <i>Experiment 3a</i> without disturbances. Each color line corresponds to the motion of a quadrotor. (a), offline PSO optimal parameter setting of the controller. (b), online fuzzy modulated adaptive controller. . . . .	71
5.14	Trajectories of a system of four drones in <i>Experiment 3b</i> . (a), offline PSO optimal parameter setting. (b), online fuzzy modulated adaptive controller. . . . .	73
5.15	Error of offline PSO optimal parameter setting versus online fuzzy modulated adaptive controller following a curve path in <i>Experiment 3b</i> , increasing the number of quadrotors in the system. a) plot without wind shear influence. b) wind frequency perturbation is set to its nominal value. . . . .	74
5.16	Exploration of wind shear frequency impact on navigation error of offline PSO optimal parameter setting versus online fuzzy modulated adaptive controller following the curve path in <i>Experiment 3b</i> with 4 drones . . . . .	75

5.17	Time evolution of reference (blue) and real (red) values of the $\theta$ and $\phi$ angles in a system of 3 quadrotors controlled by the fuzzy online adaptive algorithm in the setting of <i>Experiment 3b</i> , for no wind conditions. Left and right column plots correspond to the $\theta$ and $\phi$ angles of each robot, respectively. . . . .	76
5.18	Time evolution of reference (blue) and real (red) values of the distance between 3 quadrotors controlled by the fuzzy online adaptive algorithm in the setting of <i>Experiment 3b</i> , for no wind conditions.	77

# List of Tables

4.1	Ziegler-Nichols rules . . . . .	42
4.2	Values of standard parrot quadrotor physical parameters. . . . .	43
4.3	PSO parameters for <i>Experiment 1</i> . . . . .	47
4.4	Values of AR Parrot [47] . . . . .	49
5.1	PSO parameters for CF1 in <i>Experiment 2</i> . . . . .	59
5.2	Values of standard parrot . . . . .	68
5.3	Drones starting coordinates for <i>Experiment 3</i> . . . . .	68





# Chapter 1

## Introduction

### 1.1 Introduction

The growing availability of cheap and robust quadrotors is making feasible innovative applications. A recently proposed challenging task for Unmanned Aerial Vehicles (UAV) is the transportation of deformable linear objects (DLO) [2], i.e. cables, by a team of quadrotors, which can be extremely useful in emergency situations, such rescue operations in highly unstructured environments.

Controlling the motion of isolated quadrotors in obstacle free environments has been successfully achieved in the literature by optimized Proportional Integral Derivative (PID) controllers [65]. However, solution of the control of a team of quadrotors subject to non-linear interactions induced by a DLO hanging from them is far from being solved. In this regard, the works initiated in [31] and further developed in this Thesis open a new venue of research, directly related to efforts of control of cooperative teams of aerial robots under the non-linear dynamical interactions introduced by the DLO linking.

Modeling DLO kinematics is a complex task requiring a compromise between model accuracy and computational cost [108]. Computing its reaction to external forces involves careful modeling and optimization techniques. The DLO acts as a passive object that links otherwise isolated and independent quadrotors [28], introducing dynamic interactions among the robots in the form of non-linear constraints. Previous works have dealt with dynamic modeling of the process of transporting a DLO by a team of mobile robots on a 2D surface [29].

The physical configuration of an instance of the system with three quadrotors is represented in Figure 1.1, where three drones are sustaining a DLO hanging freely in the space in stationary state. Non stationary regimes correspond to take-off and landing of the robots, until they reach a height where the DLO does not touch any surface. The DLO in Figure 1.1 appears divided in two sections each hanging from

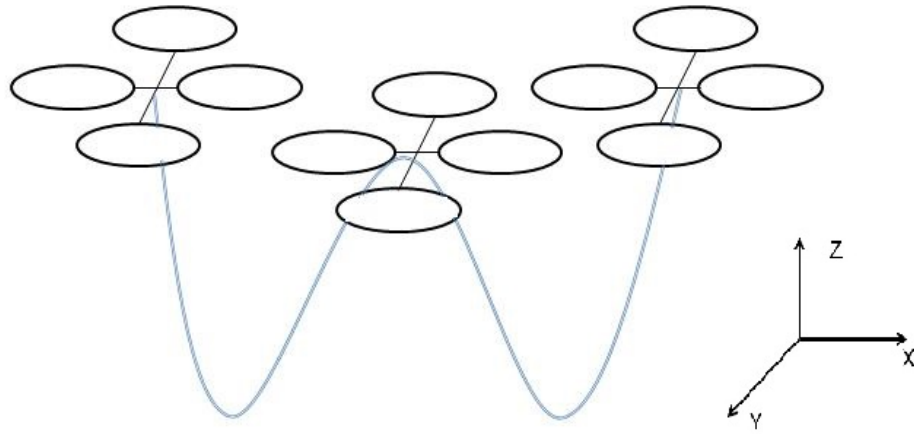


Figure 1.1: Stylized physical representation of three drones carrying a DLO which is approximated by two catenary curve sections.

a pair of quadrotors.

This introductory chapter aims to set the stage for the entire Thesis, providing some of the motivations for the research work performed, and some background ideas on each of the topics covered by the Thesis. Contributions of this Thesis are stated in this Chapter, too. The Chapter is organized as follows: Section 1.2 gives some motivation for the works carried out in the Thesis. Section 1.3.1 introduces deformable linear objects (DLO) models. Section 1.3.3 refers a general view of drone cooperative systems and introduces engineering control for drone systems. Section 1.4 summarizes the Thesis goals, which have been set along the years. Section 1.5 details achieved contributions. Section 1.5.1 enumerates the publications achieved. Section 1.6 describes the Thesis organization and content.

## 1.2 Motivation

Drone technology and business have experimented a great push from industry and research institutions. Most famous drone application remains photography, but surveillance and transport of different objects are revealing as big challenges for designers and researchers. One of the most important fact is that drones will need autonomy to perform their task with minimal human intervention. Thus, techniques for adapting drone parameters and behaviours to different conditions are needed, involving navigation, target detection, and coordination among other machines, humans or drones.

A drone cooperative system may help performing required industrial tasks in a shorter time and more efficiently. However, drone cooperative systems are not fully

studied. As more drones are included in the team, or the task complexity increases, the correct drone coordination becomes a key issue. There, control happens to be critic, as it involves aspects as whether control is decentralized or centralized, or rearranges for any incidence, such a single drone failure in the swarm, or changing outdoors perturbations. Thus, developing a robust control for these autonomous cooperative systems drones presents as a great technological and scientific challenge for researchers and industry.

Packet delivery is turning out promising drone application for society. Those packets are habitually represented as regular small boxes, but after the launch of this idea some years ago, now unexplored alternatives start to rise up. How would a swarm of drones be able to coordinate to transport a big packet? Or would a team of aerial robots be capable of loading a deformable solid that could change their dynamics continuously? In this Thesis, we combined the two previous mentioned points, and we developed a semi-autonomous cooperative drone system for the transport of deformable linear objects.

DLO aerial transportation presents a wide range of potential applications. Some of them are listed next:

- Tethered quadrotors, which permit a continuous energy supply [104]
- ETH Institute for Dynamic Systems and Control published a video where a team of quadrotors build autonomously a bridge made of ropes, which is later tested to support the crossing of a person. Their work was covered in [9] and [8], and the demo is located in their YouTube Channel <sup>1</sup>.
- Second, SAP Group and Service-drone companies together carried out in 2014 small tasks of a high-voltage line renewal with drones. Their video can be found in Youtube<sup>2</sup>.

## 1.3 Elementary definitions

We include here some definitions that are recurrent along the Thesis report.

### 1.3.1 Deformable Linear Objects (DLO)

A DLO can be considered a single dimensional solid which acts as a passive object with strong dynamics linking the quadrotors, and influencing their dynamics. There are several examples of DLO models [107] such as wires, cables and ropes, which have different applications in industry [41], i.e. medical robots [67]. DLO

---

<sup>1</sup><https://www.youtube.com/watch?v=CCDIuZUfETc>

<sup>2</sup><https://www.youtube.com/watch?v=Cb6DBu8pHO0>

geometrical and kinematics modeling is a complex task and requires a compromise between feasibility of the model and computational cost. Models of DLO have been developed specifically to model rope manipulation to produce knots [58],[84]. Vibration damping of DLO has been dealt with fuzzy control and sliding mode control [27]. Reproducing the motion of the DLO in response to a force involves careful modeling and optimization techniques [60],[25]. Linked Multicomponent Robotic Systems (L-MCRS) [28] are a special case of DLO manipulated by robots, whose dynamics have been studied in the case of ground mobile robots [29], achieving control by reinforcement learning [33][54].

### 1.3.2 Transport problem definition

The challenge of this Thesis work is to achieve robust navigation of a team of quadrotors while carrying a DLO hanging from them. Robustness means that we want the team to complete the task despite the perturbations introduced by the DLO non-linear independent dynamics or external perturbations, such as wind shear of various frequencies. Transportation means that the whole DLO is moved to another ground location from the initial one. We have identified two phases in this task. First, setting the drones and DLO in a spatial configuration that imposes the same workload to each quadrotor, an equi-workload configuration. Second, the transportation per se that implies the motion of the whole system in the XY plane.

To do research on how to solve this problem we needed to attack two fronts. One is the accurate modeling of the DLO quadrotors system to be able to simulate the system under diverse control and environmental conditions. The second is the design of robust control systems. If we assume quasi-stationary conditions the DLO can be modeled by sections of catenary curves, which allows very efficient implementations of the system simulation. We try to achieve robust control by adaptive control approaches.

### 1.3.3 Quadrotor modeling and control

Although cooperative robot systems for collective intelligence purposes are widely studied and big achievements are being obtained [83], cooperative drone systems for object transportation still remains an unexplored field. Few research groups have created cooperative transportations [89] for quadrotors, but they still keep two big differences with this Thesis: first, they do not attack the problem of deformable linear objects fully, and secondly, they do not develop an efficient strategy for their transportation.

There are four input forces (one *per* rotor) and six output states ( $x, y, z, \theta, \phi, \psi$ ). Therefore, a quadrotor is an underactuated aircraft and modeling a vehicle such this is not an easy task because of its complex structure. The aim is to develop

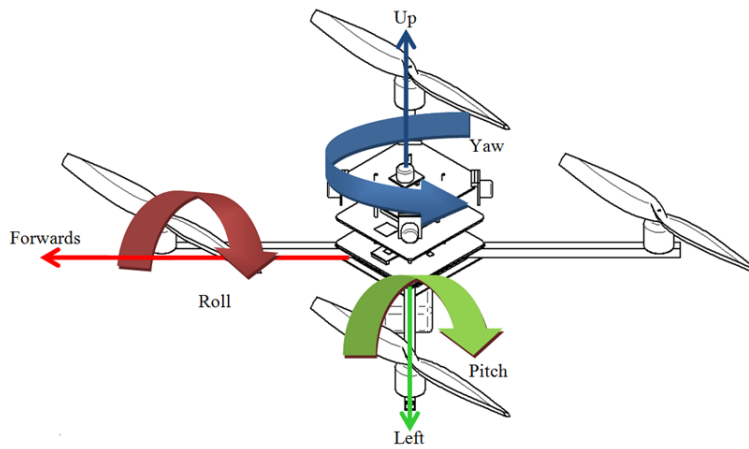


Figure 1.2: Roll, pitch and yaw angles representation

a model of the vehicle as realistic as possible. In the quadrotor, there are four rotors with fixed angles which represent four input forces that are basically the thrust generated by each propeller, which create moments simultaneously. These moments have been experimentally observed to be linearly dependent on the thrust forces at low speeds. The collective input is the sum of the thrusts of each motor. Pitch movement is obtained by increasing or reducing the speed of the rear motor while reducing or increasing the speed of the front motor. The roll movement is obtained similarly increasing or reducing the speeds on the right and left rotors. The yaw movement is obtained by varying the speed of the front and rear motors together while decreasing or increasing the speed of the lateral motors together. This should be done while keeping the total thrust constant. A representation of this model is shown in Figure 1.2.

The quadrotor dynamic modeling constrains the possibilities for engineering control strategies. In the bibliography, different alternatives are studied: PID controllers, LQR controllers, backstepping, robust, or optimal control algorithms, among others [118], [6]. In this Thesis, PID controllers were used. However, it is also necessary to obtain a good tuning methodology. The correct choice of these parameters must guarantee convergence, stability, and adaptability in different stress situations [57][100] [65].

## 1.4 Thesis goals

The main goal of this Thesis can be stated as follows:

1. Design of robust control systems for the transportation of a DLO by a team

of robots.

2. Experimental validation of the system under specific conditions.

From the operative point of view, we need to achieve specific goals:

1. Building an accurate dynamic simulation model of the DLO + quadrotor team, in order to validate the control proposal in repeatable and controlled conditions. To achieve this goal we need to:
  - (a) Propose an accurate model of the DLO dynamics, that would also be efficient from the computational cost aspect.
  - (b) Build simulation models of the quadrotor.
2. Propose an overall team control strategy, i.e. how the drones coordinate to achieve the transportation task.
3. Define a spatial configuration of the quadrotors in which the energy consumption is the same for all, avoiding early energy depletion by some robots.
4. Propose robust drone control that carries out the desired task under the load and perturbations induced by the DLO and external perturbations, such as wind.
  - (a) Offline tuning of the controllers
  - (b) Online adaptive tuning of the controllers

## 1.5 Thesis contributions

Pursuing the above goals, we have achieved several contributions. The main scientific results and contributions from this Thesis are the following:

1. We have proved that catenaries are suitable models for the dynamic representation of DLOs transportation by teams of quadrotors.
2. We have formalized a dynamic model that captures the dynamic behavior of the aerial robots together with the DLOs, which is adaptable to robots and DLOs with different physical and dynamic properties.
3. We have defined and computed the equi-workload spatial configuration, allowing equal energy consumption of all drones.

4. We have proposed and published an innovative way of transporting DLOs, considering the quadrotors payload and difference of relative heights among them.
5. Defined of a leader-following strategy that ensures that distance limits among drones is kept along a straight or curved path.
6. We have obtained both offline and online control strategies that ensure the rapid convergence of the system and its stability.

### 1.5.1 Publications achieved

- Estevez J., Lopez-Guede J. M., Graña M., (2014), “Quasi-stationary state transportation of a DLO with quadrotors”. *Robotics and Autonomous Systems*, Volume 63, Part 2, pp 187-194, ISSN 0921-8890.
- Lopez-Guede J. M., Estevez J., Graña J., Reinforcement Learning in Single Robot DLO Transport Task: A Physical Proof of Concept, SOCO 2015 .
- Estevez J., Lopez-Guede J. M., Graña M., (2015), Robust Control Tuning by PSO of Aerial Robots DLO Transportation. IWINAC 2015.
- Estevez J., Lopez-Guede J. M., Graña M., (2015), “Robust Control Tuning by PSO of Aerial Robots DLO Transportation”. *Bioinspired Computation in Artificial Systems* 9108, pp 291-300. Springer.
- Estevez J., Lopez-Guede J. M., Graña M., (2016), “Particle Swarm Optimization quadrotor control for cooperative aerial transportation of deformable linear objects”. *Cybernetics and Systems*. Vol. 47 (1-2), pp 4-16.
- Estevez J., Guisasola J., (2015) “El Taller del “Cuadrícóptero” en la Semana de la Ciencia. Divulgación de las aplicaciones científico-técnicas en la sociedad”. *Revista Alambique* (in press).
- Estevez J., Graña M., Lopez-Guede J.M., (2015), “Online fuzzy modulated adaptive PD control for cooperative aerial transportation of deformable linear objects”. *Integrated Computer-Aided Engineering* (submitted)

## 1.6 Thesis organization

The Thesis is organized as follows:

- Chapter 2 shows the State of the Art of the research lines. The aim of this chapter is to set the stage for different models and algorithms. Therefore, we cover in detail the literature for each aspect.

- Chapter 3 develops a dynamic model both for quadrotors and DLO. Here we propose the catenary model for DLO, and give the dynamic equations of the quadrotors. This chapter is the basis for the development of a motion control for the cooperative system. Quadrotors' dynamics are non-linear, and thus a precise and careful control is necessary. The control system is divided in two parts.
- Chapter 4 explains the equi-workload configuration and its computation. Then we introduce the PD controller for inner loop control for altitude control. We report computational experiments validating the approach.
- Chapter 5 discusses outer loop control for position control, proposing a novel fuzzy modulated adaptive tuning of the PD controllers. We report computational experiments comparing offline and online approaches, to validate our proposal.
- Chapter 6 ends with conclusions of the Thesis and some future work lines planned to work on after current phase.



## Chapter 2

# State of the Art

In this Chapter we gather descriptions of the state of the art of the two research lines mentioned in the introductory Chapter. The Chapter is structured as follows: Section 2.1 gives some basic definitions that will be used all along the Thesis. Section 2.2 presents a view of the state of the art on DLO modeling for different applications. Quadrotor modeling and control are divided in two sections: Section 2.3 introduces the antecedents and problems of cooperative robotic systems. Section 2.4 gives the dynamical description of the quadrotor. Section 2.5 gives some background of quadrotors control and adaptive strategies.

### 2.1 Some basic definitions

Let us recall some definitions.

- **Deformable Linear Object (DLO):** As the definition states, these solids can change their shape due to manipulation, representing a passive object. Due to the complexities of their representation, different simplifications are usually implemented for the simulation easiness.
- **Cosserat rods:** It is a physical model to represent DLO. The rod, which is assumed to undergo flexure about two principal axes, extension, shear and torsion, are described by a general geometrically exact theory.
- **Spline:** it is a numeric function that is piecewise-defined by polynomial functions, and which possesses a high degree of smoothness at the places where the polynomial pieces connect.
- **Cooperative behavior:** Given some task specified by a designer, a multiple-robot system displays cooperative behaviour if, due to some underlying mech-

anism (i.e., the “mechanism of cooperation”), there is an increase in the total utility of the system.

- **Catenary curve:** is the model of 2D rigid solid in quasi-stationary state, hanging freely from its two extremes.

## 2.2 Previous works on deformable linear objects models

Research on robotic manipulation has mainly focused on manipulating rigid objects so far. However, many important application domains require manipulating deformable objects, especially deformable linear objects (DLO), such as ropes, cables, and sutures. Such objects are very challenging to handle, as they can exhibit a great diversity of behaviors. However, models that fully show dynamics, graphic representation, material behaviour and deformation all together is an extreme difficult task and it requires a very high computational cost. Thus, different models have emerged where one or two of DLO properties are finely represented while sacrificing other ones, with a lower computational cost for online realistic simulations.

### 2.2.1 DLO modeling approaches

Two main representations are found in the bibliography: Cosserat rods and geometric splines. In the robotics community, several recent works use **Cosserat theory**. A Cosserat medium was first described in 1909 by Cosserat brothers. This medium is described by a set of oriented micro-solids. [74] first introduced Cosserat’s rod theory in computer graphics to model cantilever objects. This work first calculates the forces and torques iteratively along the rod discretization, and then evaluates the geometrical configuration in backward iterations using differential equations. [108] achieves a very accurate static solution of a cable simulation by considering it as a succession of oriented frames and by minimizing its potential energy; this approach is mechanically accurate, but demands a very high computation cost. He uses Lagrangean formulation for his calculus, which gets a fast computation method and visually realistic for low resolution rods. [41] formulates the dynamic model of an inextensible DLO using finite element model (FEM) and Lagrange motion equations including some dynamic effects, such as mass. The main drawback of these methods is that it is difficult to combine such models with constraints. Moreover, these methods need at least a reference point for calculation, which might not always be available in practical cases.

**Spline-based** techniques are still quite isolated within the physical animation literature. [101] initiated deformable models in Computer Graphics, including

## 2.2. PREVIOUS WORKS ON DEFORMABLE LINEAR OBJECTS MODELS 11

physics-based curves using a Lagrangian form of Newton's equation. [45] simply stated, created an algorithm that divides a curve in segments of constant curvature and solves the constrained energy minimization problem for a DLO manipulation path planning. Later, [67] extended this idea to 3D, and made the algorithm more scalable to a higher number of segments. To simulate a deformable object, we need to compute any physically plausible configuration; not only stable configurations. The emphasis is on efficiency in computing the response of an object to internal and external forces. [78] uses a spline of linear springs, while [51] and [18] use deformable splines for suture simulation in computer graphics, considering some subtle dynamic effects.

However, these approaches do not consider the dynamic non-linearities that DLO create when linked between different active agents. In order to model these effects, [79] developed dynamic NURBS, which is a combination of geometric splines and physical models. Recently, in many of this kind of applications **Geometric Dynamic Exact Splines** (GEDS) are used, [103]. GEDS simply explained, represent a sum of geometric splines and Cosserat rods. For instance, it is used in [29] and [54] for the modeling of the transportation of deformable linear objects with wheeled robots. However, the goal of this Thesis pursues the transportation of DLO through air, thus normally not considering transition states (taking off) or contact against walls.

### 2.2.2 Aerial payload transportation using DLO

One situation when DLO are involved in transportation is when the payload to be transported is connected to the robots by DLO, i.e. some kind of cable. Though the cable is deformable, when it is transmitting the force of the robot to the payload the DLO acts as a rigid solid. Nevertheless, we review here some approaches in the literature for the sake of completeness.

Though there are examples in the literature of robotic teams doing towing of payloads on the ground, there are significant differences between interacting with an object on the ground and in the air. The problem of swinging hanging payload manipulated by a robotic device has been studied for more than 30 years now. Certainly, in 1983 Gregory Starr [91] presented his work, *Swing-free transport of suspended objects with a robot manipulator*, later extended by [92], *Swing-Free Transport of Suspended Objects With a Path-Controlled Robot Manipulator*, where in both cases he used classical elementary applied mechanics equations for the system modeling. Despite the simplicity of the equations, his work led to several patents, such as [87, 44, 40, 39].

After this initial step, following works pushed on a further study on this task, searching for robotic trajectories for payload transportation [93], vibration reduc-

tion while performing this task [71], and development of control strategies for payload manipulators [32] [111] [73]. Most works focused their efforts on single cable aerial towing of a payload, which applications go from personal rescues with helicopter to heavy loads manipulation with cranes whose control is quite complex. First research works about UAVs transporting payloads appeared in late 90's [72][13]. In [23], the authors consider the problem of cooperative towing with a team of ground robots, where under quasi-static assumptions there is a unique solution to the motion of the object given the robot forces.

Specific studies of multi-rotors or drones transporting payloads has been studied by few research groups lately. [59] developed a cooperative transportation of a mass with helicopters with something similar to a DLO model. However, the lab led by Vijay Kumar at Pennsylvania University is one of the most prolific research groups in this topic, having published a series of works concerning the task of aerial transportation of cable-suspended payloads with multiple drones. Certainly, in 2010 [63] developed a model in three dimensions for the transportation of a payload via cables, illustrated in Figure 2.1 extracted from the paper. This cooperative aerial towing problem is similar to the problem of controlling cable-actuated parallel manipulators in three dimensions, where in the former the payload pose is affected by robot positions and in the latter pose control is accomplished by varying the lengths of multiple cable attachments. Moreover, three years later the same research group modelled the transportation of a DLO suspended from cables [43] [90][89], but with severe dynamic limitations according to the paper. The system is illustrated in Figure 2.2 under quasi-static conditions for the study. All the works from this group consider that the DLO joining the correspondent payload and the robot is always tense, so that it can almost be treated as a rigid bar that rotates around the quadrotor joint, which does not coincide totally with the mission of this Thesis. Observe in Figure 2.2 that the transported DLO seems to be rigid in the Z axis, because no catenary like curve appears between the points of attachment of the cables.

Researchers from other groups, such as [75] and [80], also developed a quadrotor system for a payload transportation with wires. Certainly, the payload was represented as a pendulum, and wires remained tense, similar to the previous works. Finally, [24] designed an adaptive controller for a quadrotor UAV transporting a point-mass payload connected by a flexible DLO modeled as serially-connected rigid links.

Thetered UAVs differ from the previous strategies presented in this section for DLO modeling. For instance, [105] used a basic model and a standard linear solid model for DLO, which are both based on the usage of springs and dumps for the simulation of stretched or relaxed DLO. [56] simplifies even more, and the DLO model employed in his research is simplified to an always-taut rope, and the effect

2.2. PREVIOUS WORKS ON DEFORMABLE LINEAR OBJECTS MODELS 13

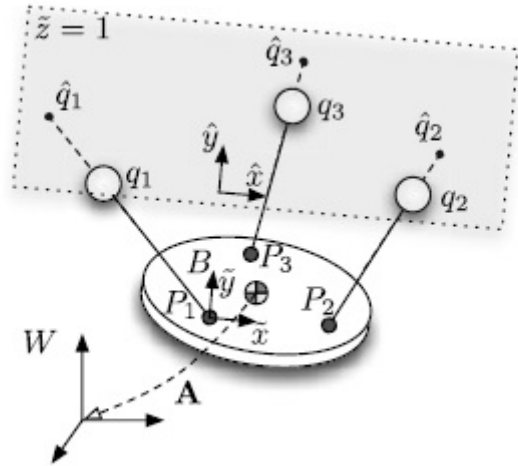


Figure 2.1: Model to transport a payload in three dimensions through the air described in [63]

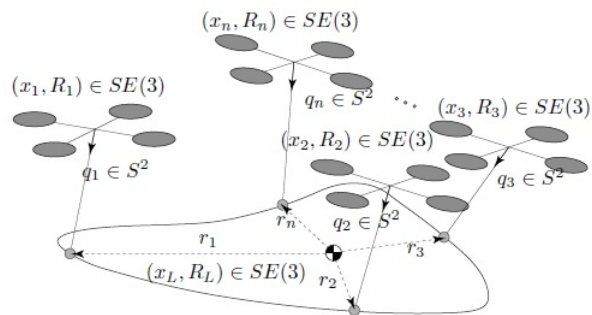


Figure 2.2: 2013 model for DLO transportation through the air

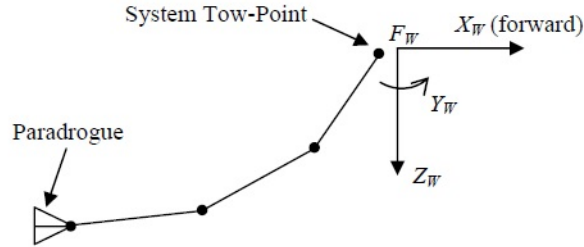


Figure 2.3: Hose model used in [81]

on the quadrotor is modeled as an axial tension in the DLO direction. As a last example of this diversity, [69] models a tethered UAV with an umbilical cable using Lagrangian coordinates, which is a cable which supplies required consumables to an apparatus.

Finally, air-hose refuelling considers too the problem of DLO modeling, even their starting hypothesis is not a solid transportation, but a solid link between two aircrafts at high speed. However, it is also assumed to suffer serious kinematic and dynamic constraints, as steady state and static movements due to movements of the airplanes. Certainly, [81] modeled the hose as a link-connected system, where the DLO is made up of a finite number of cylindrically-shaped, rigid links connected with frictionless spherical joints, as seen in Figure 2.3.

### 2.2.3 Catenaries

Catenaries are a broadly known element of classic Applied Mechanics. Mathematically, the catenary curve is the graph of the hyperbolic cosine function. The surface of revolution of the catenary curve, the catenoid, is a minimal surface of revolution. The mathematical properties of the catenary curve were first studied by Robert Hooke in the 1670s, and its equation was derived by Leibniz, Huygens and Johann Bernoulli in 1691. Catenaries and related curves are used in architecture and engineering in the design of bridges and arches, so that forces do not result in bending moments. Besides, they are also used for the study of the mechanic behaviour of long hanging cable structures, such as high voltage lines.

The expression of a catenary curve between nodes  $A$  and  $B$ , illustrated in Figure 2.4, is given by:

$$y - y_0 = a \cdot \cosh\left(\frac{x - x_0}{a}\right), \quad (2.1)$$

This equation is defined in the main reference frame given by axes  $(X, Y)$  in Figure

## 2.2. PREVIOUS WORKS ON DEFORMABLE LINEAR OBJECTS MODELS 15

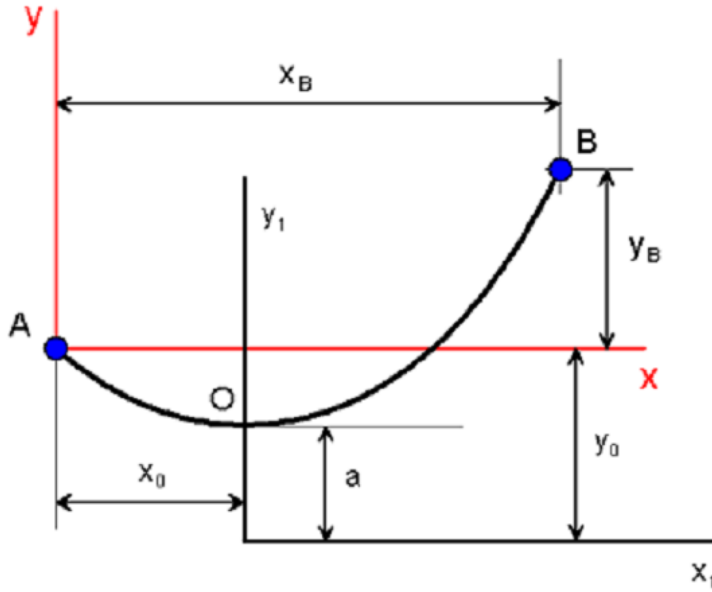


Figure 2.4: Catenary curve modeling a DLO holding between robots A and B.

2.4. The parameter  $a$  is the height from the lowest point of the catenary to the secondary reference frame give by new axes  $(X_1, Y_1)$ . The parameter  $a$  depends on  $w$  (weight per length unit of the catenary solid) and  $T_0$  (the horizontal tension of the catenary) according to Eq. (2.2):

$$a = \frac{T_0}{w}. \quad (2.2)$$

The tension exerted by the catenary on nodes A and B of Figure 2.4 can be calculated with expressions based on the previous formula.

$$T_A = w \cdot y_0$$

$$T_B = w(y_B + y_0)$$

However, this tension is tangent to the catenary in each point, while we are interested in the vertical and horizontal tension, as transmitting load to the quadrotors supporting the catenary at these points:

$$\begin{aligned} T_A^y &= T_A \sin(\alpha_A) & T_A^h &= T_A \cos(\alpha_A) \\ T_B^y &= T_B \sin(\alpha_B) & T_B^h &= T_B \cos(\alpha_B) \end{aligned}, \quad (2.3)$$

where  $\alpha$  are the tangent angles in each point of the catenary, which are always non-negative, taking values in the range  $[0, \frac{\pi}{2}]$ , being  $\alpha = 0$  at the lowest point of the catenary.

The high aspect ratio of thin objects, such as paper and cloth, and linear objects, such as wire and thread, often causes instability in the computation of deformed shapes. Thus, various modeling techniques have been adapted for thin or linear objects. For example, the deformed shape of a thread suspended by two points has been analyzed using calculus of variations and it has been found that the shape can be described by a catenary [42]. In these approaches, the material properties are not considered; only the mass and quasi-static effects are considered. As this element is a rigid solid, deformations due to collisions cannot be modelled with such manner.

However, its usage as DLO modeling for robotics is only applied to cable-driven parallel robots, such as in [62] [48], who proposed an elastic catenary model for this kind of robots. On the other hand, [94], [4] and [37] perform a good analysis of effects of catenary joints and assumed hypothesis and considerations, both in 2D and 3D. Besides, the computer graphics cost, even in online simulations, is extremely low. [55] proposes a model for catenaries torsion and aerodynamic effect inspired for hanging bridges. In summary, the application of catenaries to DLO transportation with quadrotors is an innovative contribution of this Thesis to the State of the Art.

### 2.3 Drone cooperative systems

The study of multiple-robot systems naturally extends research done on single-robot systems, but it is also a discipline unto itself. Multiple-robot systems can accomplish tasks that no single robot can accomplish, since ultimately a single robot, no matter how capable, is spatially limited:

- Tasks may be inherently too complex (or impossible) for a single robot to accomplish, or performance benefits can be gained from using multiple robots.
- Building and using several simple robots can be easier, cheaper, more flexible and more fault-tolerant than having a single powerful robot for each separate task. Scalability is rewarded.
- The constructive, synthetic approach inherent in cooperative mobile robotics can possibly yield insights into fundamental problems in the social sciences (organization theory, economics, cognitive psychology), and life sciences (theoretical biology, animal ethology).
- In case of payload transportation, sharing the load among a number of drones turns the system into a more energy efficient one.



In the literature, [21] and [76] provide a good study of the early antecedents and framework of this kind of systems. Coordination and interactions of multiple intelligent agents have been actively studied in the field of distributed artificial intelligence since the early 1970's [12]. In the late 1980's, the robotics research community became very active in cooperative robotics, beginning with projects such as CEBOT [34], SWARM [11], ACTRESS [7], and GOFER [20].

First research works about aerial cooperative robotic systems appeared in mid 90's [112], and this activity heavily increased in next decade, being of special interest for patrolling, fault-tolerant cooperation, swarm control, role assignment, multi-robot path planning, exploration and mapping, perimeter surveillance, and nowadays, collaborative learning.

In terms of practical value, one of the greatest benefits of the cooperative system is that it can provide users with superior information. However, developing such an autonomous cooperative system is quite challenging because of technical and operation issues such as decision making, formation, path planning, to be solved. Control of the system might be centralized or decentralized.

- **Centralized:** means that all the information about the aerial robots is sent to a single server where the controls are calculated for each aerial robot and sent back
- **Decentralized:** means that no central server exists, so that each aerial robot computes its own control based only on information from other aerial robots within a particular spatial range of itself. The situation is far from ideal under the computational perspective because the number of aerial robots that can be within range at a given time is bounded and therefore so is the time the algorithm will take to run, regardless of the total number of aerial robots involved.

## 2.4 Quadrotor dynamic modeling

A quadrotor is an agile flying vehicle, able to attain the full range of motions. It is propelled by four rotors symmetrically disposed across its center. They have smaller dimension and simple fabrication than conventional helicopters. Generally, it should be classified as a rotary-wing aircraft according to its capability of hover, perform horizontal flight, and vertical take-off and landing (VTOL). In the decade of 1920, prototypes of manned quadrotors were introduced for the first time; however, the development of this new type of air vehicle was interrupted for several decades due to various reasons such as mechanical complexity, large size and weight, and difficulties in achieving robust stable control, especially. Only in recent years a great deal of interests and efforts have been attracted on it; a quadrotor

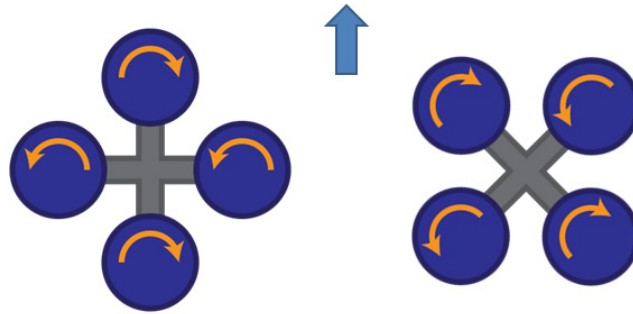


Figure 2.5: Plus (left) and cross (right) rotor configurations

has become a more feasible vehicle for practical application, such as search-and-rescue and emergency response. As a small, unmanned aerial vehicle (UAV), it has versatile forms from 0.3 to 4 kg. Up to now, only some large quadrotors already have sufficient payload capacity and flight range to undertake a number of indoor and outdoor applications, like Bell Boeing Quad TiltRotor and so forth [114].

For the specific purposes including academic research, commercial usage, and even military aim, many research groups or institutions have fabricated various quadrotors, such as the X4-flyer, OS4, STARMAC, and Pixhawk which have become the shining stars mentioned on the network, magazines, and all kinds of academic journals. In addition, numerous cooperation projects exist among contributions from RC hobbyists, universities, and corporations.

Typically, the structure of a quadrotor is composed of four rotors attached at the ends of arms under a symmetric crossed frame. The forces and moments acting on the quadrotor are given by rotors driven by the motors. According to the orientation of the blades, relative to the body coordinate system, there are two basic types of quadrotor configurations: plus and cross-configurations shown in Figure 2.5. Arrow is pointing the forward motion direction.

In the plus configuration, each pair of blades, spinning in the same clockwise or counter-clockwise direction, coordinate the  $x$  and  $y$  directions of the quadrotor. On the other hand, in cross-configuration two rotors are on the right side and two on the left. In contrast with the plus configuration, for the same desired motion, the cross-configuration provides higher momentum which can increase the maneuverability performance, as each motion requires all four blades to vary their rotation speed. And so it does with the attitude control. This Thesis makes use of plus configuration.

Basic control sequences of plus-configuration are shown in Figure 2.6. The quadrotor's translational motion depends on the tilting of rotorcraft platform to-

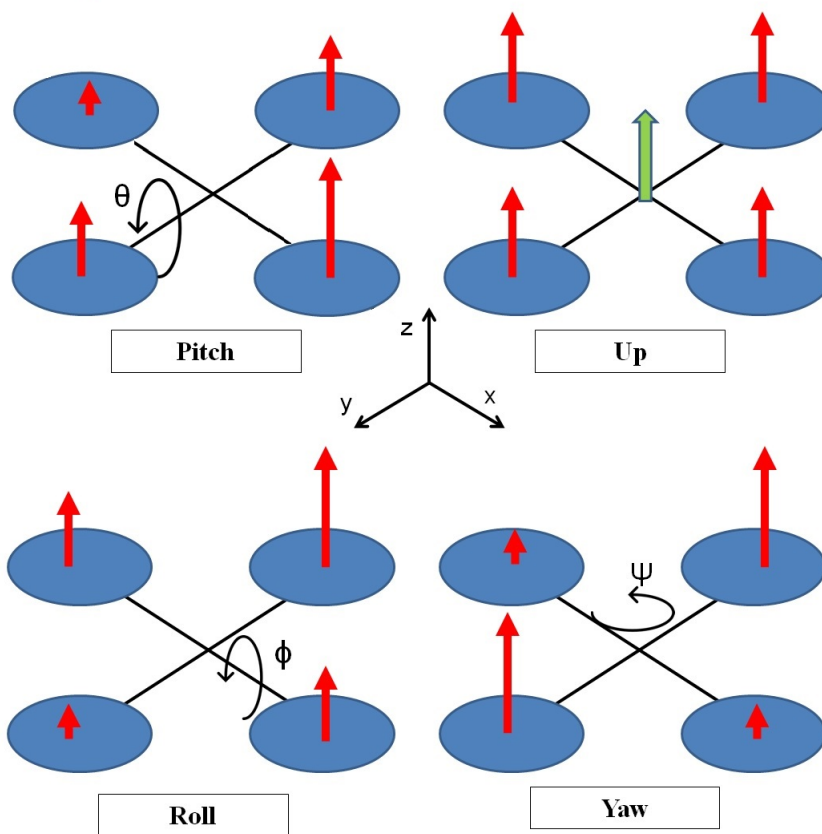


Figure 2.6: Plus configuration: pitch, roll and yaw controls, where red arrows indicate the relative rotor speed

wards the desired orientation. The quadrotor has six degrees of freedom (DOF) to be controlled by four inputs; therefore it is an underactuated system. In principle, a quadrotor is dynamically unstable and therefore careful control is necessary to make it stable. Two main dynamic simulation approaches are widely accepted in the literature for quadrotors:

- 1) Euler–Lagrange approach
- 2) Newton-Euler approach

Both methods lead to obtain same results in simulations, although Euler-Lagrange is considered to have the advantage that it takes the same form in any system of generalized coordinates, and it is better suited to generalizations and control adding. Typically two reference-frames are necessary to define the quadrotor's dynamics: a body-fixed frame and Earth-fixed frame. However, exact and rigorous formulas derived from these approaches are fairly complex for control purposes, and thus some simplifications are implemented in most research works. These simplified formulas are the ones that appear in this section.

### 2.4.1 Dynamic equations

Let us consider the coordinate system as  $\{x, y, z, \phi, \theta, \psi\}$ , which represent the Earth frame of reference coordinates  $x, y$  and  $z$ , and angles  $\phi, \theta, \psi$  are referenced to the body frame of the UAV. However, we have 6 degrees-of-freedom and only 4 inputs and controllable torques. Hence, a quadrotor is a highly non-linear apparatus. In these conditions, expressions for the control all the variables are as follows:

$$\left\{ \begin{array}{l} \ddot{\phi} = \frac{U_2}{I_{xx}} \\ \ddot{\theta} = \frac{U_3}{I_{yy}} \\ \ddot{\psi} = \frac{U_4}{I_{zz}} \end{array} \right\}, \quad (2.4)$$

$$\left\{ \begin{array}{l} U_1 = b(\Omega_1^2 + \Omega_2^2 + \Omega_3^2 + \Omega_4^2), \\ U_2 = l \cdot b(-\Omega_2^2 + \Omega_4^2), \\ U_3 = l \cdot b(-\Omega_1^2 - \Omega_3^2), \\ U_4 = d(-\Omega_1^2 + \Omega_2^2 - \Omega_3^2 + \Omega_4^2) \end{array} \right\}, \quad (2.5)$$

where parameter  $b$  is the propeller thrust coefficient, and  $d$  is the drag.

$$\left\{ \begin{array}{l} \ddot{x} = \frac{(-\cos \phi \sin \theta \cos \psi - \sin \phi \sin \psi)}{m} U_1 \\ \ddot{y} = \frac{(-\cos \phi \sin \theta \sin \psi - \sin \phi \cos \psi)}{m} U_1 \\ \ddot{z} = \frac{(\cos \phi \cos \theta) U_1}{m} - g \end{array} \right\}, \quad (2.6)$$

Eq. 2.4 represent the angular acceleration of the quadrotor angles; eq. 2.5 describe the total thrust and non-conservative torque of the quadrotor in each angle:

$U_2$ ,  $U_3$  and  $U_4$  are, respectively, roll, pitch and yaw torques, and  $\Omega_i^2$  is the squared speed of the  $i$ -th propeller; and finally eq. 2.6 relates  $x$ ,  $y$  and  $z$  absolute with the total thrust,  $U_1$ , which is always perpendicular to the body-fixed frame and thus is necessary the 3D-rotation matrix to transform the reference system. Rotation matrix is shown in eq.2.7:

$$\begin{bmatrix} \cos \psi \cos \theta & -\sin \psi \cos \phi + \cos \psi \sin \theta \sin \phi & \sin \psi \sin \phi + \cos \psi \sin \theta \cos \phi \\ \sin \psi \cos \theta & \cos \psi \cos \phi + \sin \psi \sin \theta \sin \phi & -\cos \psi \sin \phi + \sin \psi \sin \theta \cos \phi \\ -\sin \theta & \cos \theta \sin \phi & \cos \theta \cos \phi \end{bmatrix} \quad (2.7)$$

Assumptions made for this formulation are the following:

- The structure is supposed rigid, and symmetrical.
- The CoG and the body fixed frame origin are assumed to coincide.
- The propellers are supposed rigid.
- Thrust and drag are proportional to the square of propeller's speed.
- Coriolis and aerodynamic terms are neglected.
- Small angles approximation is used for linearizing angular accelerations.

### 2.4.2 Wind disturbance model

We carried out model tests of robust horizontal motion of the quadrotor system under wind disturbances. Most research works simulate wind as a constant more or less intense force. However, it is much more realistic to model wind shear as a sinusoidal [70] disturbance. It is a tough test for aerial vehicles, because the control system may resonate with the wind fluctuations, inducing unstable behaviors. Therefore, the sinusoidal model of eq. 2.8 was the chosen for this work [70, 38].

$$d(t) = D_1 + D_2 \sin(\omega t), \quad (2.8)$$

## 2.5 Control strategies

As can be observed in the equations of Section 2.4, the dynamic model of the quadrotor shows that is an under-actuated and strongly coupled system, where translational motion depends on the change of attitude angles. For this reason, the control system can be divided into the outer-loop translation controller and

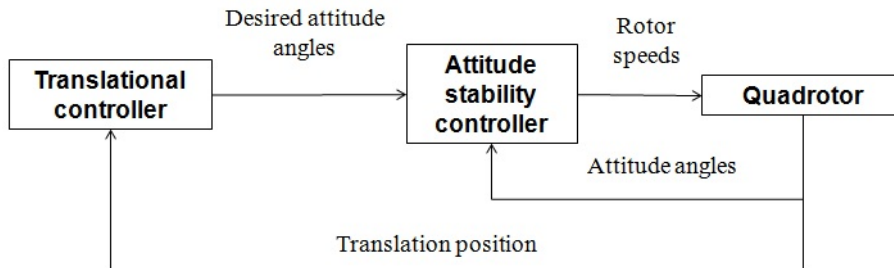


Figure 2.7: Inner and outer loop for attitude and position

inner-loop attitude controller [36] in a close-loop cascade feedback circuit (Figure 2.7).

Quadrotor controllers last instance is to obtain a rapid convergence, stability, smoothness, disturbance rejection and a good path planning following for the system. Due to the quadrotor intrinsic dynamic instability and non-linearity, control strategy election is not a minor task in the design [85]. A good summary and comparison of some of the most used control methods for autonomous quadrotors are presented in [118], including:

- Proportional Integral Derivative (PID)
- Linear Quadratic Regulator/Gaussian-LQR/G
- Sliding Mode Control (SMC)
- Backstepping Control
- Adaptive Control Algorithms
- Robust Control Algorithms
- Optimal Control Algorithms
- Feedback Linearization
- Fuzzy Logic and Artificial Neural Network
- Hybrid Control algorithms

In this Thesis' works we choose PID control for quadrotors on the basis on feasibility for industry applications, bibliography studies, simplicity and robustness for our quadrotor cooperative system. [106], [95], [14], [68] among others defend and demonstrate the advantages of PID configuration for autonomous quadrotor

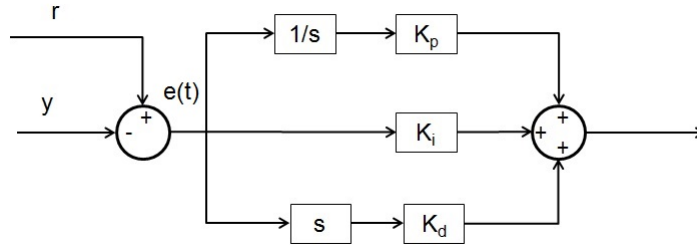


Figure 2.8: PID controller diagram

systems against others. That way, the tuning of the control system reduces to the tuning of PID controllers discussed next.

### 2.5.1 PID tuning algorithms

The PID controller was first introduced in 1939 in the industry and has been successfully used as controller in many processes until today. The basic function of the controller is to execute an algorithm using the information from input variables, to compute the output variable value minimizing the difference between the control output variable and the setpoint. The term ‘PID’ is an acronym for *proportional*, *integral*, and *derivative*. The PID controller circuit is represented in Figure 2.8.

In Laplace and time domain, the traditional PID structure can be rewritten according to equation 2.9 and 2.10 respectively:

$$u(s) = (K_P + \frac{K_I}{s} + K_D s)e(s) \quad (2.9)$$

$$u(t) = K_P e(t) + K_I \int e(t) dt + K_D \frac{de(t)}{dt} \quad (2.10)$$

PID *proportional*, *integral*, and *derivative* terms are represented by the corresponding gains  $K_P$ ,  $K_I$ ,  $K_D$ . The popularity of such kind of controller is due to their functional simplicity and reliability. They provide robust and reliable performance for most systems and the PID parameters may be tuned to ensure a satisfactory closed loop performance. A PID controller improves the transient response of a system by reducing the overshoot, and by shortening the stabilization time of the system. However, the PID loop must be properly tuned for a proper performance [1].

Various tuning methods have been discussed in the literature for finding out the parameters of a PID controller [98]. The most used tuning methods include Ziegler Nichols (ZN), relay auto-tuning (RA), pole placement and internal model control (IMC). [19] proposed a PID self-tuning controller based on pole placement method

for controlling an aluminum rolling mill. [117] proposed tuning of PID controller with time integral performance criteria, where ZN method was used to determining the controller parameters. [88] proposed a controller with a fuzzy model for air-conditioning system.

Different control schemes using PID controllers have been discussed in the literature by various researchers. [77] proposed an internal model based robust inversion feed-forward and feedback control approach for LPV system while [114] presented a discrete feed-forward and feedback optimal tracking control scheme for a steel jacket plat subjected to external wave force. [116] presented a comparative analysis between a single-loop control system and a cascade control system for a third-order process. [115] proposed model matching methods and approximate dynamic inversion techniques for designing feed-forward controllers. A feed-forward velocity control scheme for a DC motor based on the inverse dynamic model has been presented in the literature by [10]. A robust cascade control system has been implemented for controlling central air-conditioning system by [109]. [64] proposed a feed-forward control law based upon the concept of control equilibrium point.

Genetic Algorithm (GA) was proposed as an effective solution for the search in the space of parameters for the optimal parameter setting. The fundamental components of GA are encoding, reproduction, crossover and mutation [99]. It has been shown that GA could produce better results in PID tuning than the primitive tuning methods [49] having stochastic global searching characteristics that mimicking the process of natural evolution. Later, a set of new intelligent approaches called swarm intelligence tuning, such as Ant Colony Optimization, Particle Swarm Optimization (PSO) (first introduced by Kennedy and Eberhart in 1995 [46]), Bacterial Foraging optimization algorithm were introduced which could produce an effective characteristics of positive feedback, search mechanism, distributed computation and constructive greedy heuristic for simpler, efficient and faster tuning than primitive and other evolutionary tuning approaches for having improved characteristics like dynamic adjustment inertia weight factors, etc. Positive feedback search produces advantageous results, distributive computation can be used to avoid premature convergence and greedy heuristic is helpful to find the solution of early stages of search process.



## Chapter 3

# Dynamical models

### 3.1 Introduction

In this Chapter, we describe the dynamic models for the simulation of the aerial DLO transportation with quadrotors that will be used to tune and test the controllers for such task. As discussed in the state of the art of Chapter 2, there are different approaches for modeling DLO, inspired in different disciplines such as medicine, engineering, robotics, or computer graphics. However, most proposed models are subjected to certain modeling and behaviour restrictions due to the big complexity and cost of processing. Our proposal is a novel way of modeling the DLO allowing to simulate the its transportation by aerial robots, i.e. quadrotors. Different quadrotor demos have shown that DLO transportation is feasible, however in this Thesis we are concerned with developing robust control strategies.

The DLO model allows accurate modeling of the influence of DLO in quadrotor dynamics in terms of thrust, weight or any other parameter that affects quadrotor behaviour. Different quadrotor models exist, although they normally do not take into account the attachment of any payload. And as a final constraint, the modified quadrotor dynamics must admit any kind of engineering control which assures that DLO transportation converges and happens smoothly.

The Chapter contents is as follows: Section 3.2 presents the modeling of the DLO as a collection of catenary curves, and its dynamical model, i.e. the resulting forces exerted on the quadrotors. Section 3.3 presents the derivation of the spatial (vertical) configuration of the quadrotor team where all the drones are supporting the same load, and, thus, consuming the same quantity of energy. Section 3.4 presents the dynamical model of the quadrotor, focused on the vertical dimension to achieve the equi-workload spatial configuration.

### 3.2 Geometrical and dynamical DLO model

This section contains the description of the geometric and dynamical model of the DLO and the team of quadrotors carrying it. First, we justify and describe the DLO geometrical model by a composition of catenary curves. Secondly, we give the characterization of the desired equi-workload configuration, and its computation from the geometrical/dynamical model.

Previous works on DLO transportation by a team of robots [29] were based on a Generalized Dynamic Splines (GEDS) model of the DLO. GEDS are an extension of the Cosserat rods models to capture the dynamics of a DLO. However, this approach has several drawbacks. The most critical is that the length of the DLO changes according to the settings of the spline model parameters. This is unacceptable for the case considered in present Thesis, because this effect would introduce unreal random changes of altitude of the quadrotor UAVs. We will restrict our study in the Thesis to the quasi-stationary state, when the drones are at cruise height and the DLO is freely hanging at full length. In this situation, the DLO can be modeled as a catenary curve [16], or a collection of catenary curves sharing their extreme points, and the deformations induced by its transportation can be modeled by transformations between catenary curves. The catenary is the ideal hyperbolic shape of a DLO whose unique load is its own weight, corresponding to a quasi-stationary state. It is the model of a perfect 2D rigid solid at equilibrium. Two drones ( $n = 2$ ) can carry a catenary holding it at its end points (nodes). A long DLO divided in two sections, is transported by three drones ( $n = 3$ ), and henceforth, so that always  $n$  quadrotor UAVs carry a DLO composed of  $n - 1$  sections. Each section will be modeled as an independent catenary curve without consideration of bending effects at the joining point. The study presented in this Chapter assumes two sections at most, but results are easily extrapolated to a greater number of sections. Also, we deal with 2D catenary curves, but extension to 3D is immediate [22]. Collision with ground surfaces render the catenary model inaccurate. They happen in the phases of take off and landing.

For real life experimentation requiring visual feedback, we need to reformulate the conventional catenary model. This model, illustrated in Figure 3.1, is given by the following equations:

$$\left\{ \begin{array}{l} F_1 = -\frac{w \cdot l_y}{2 \cdot \lambda_0} \\ F_2 = \frac{w}{2} (-l_y \coth(\lambda_0) + L_0) \\ F_3 = -F_1 \\ F_4 = w \cdot L_0 - F_2 \end{array} \right. , \quad (3.1)$$

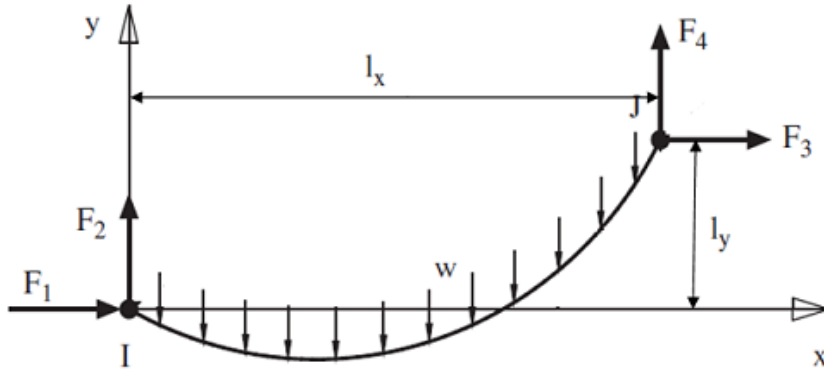


Figure 3.1: Catenary parameters  $(I, J)$  correspond to the catenary nodes

where the parameter  $\lambda_0$  takes values

$$\lambda_0 = \left\{ \begin{array}{ll} 10^6 & \text{if } (l_x^2 + l_y^2) = 0 \\ 0.2 & \text{if } (L_0^2 \leq l_x^2 + l_y^2 + l_z^2) \\ \sqrt{3 \left( \frac{L_0^2 - y^2}{l_x^2} - 1 \right)} & \text{if } (L_0^2 \geq l_x^2 + l_y^2 + l_z^2) \end{array} \right\}, \quad (3.2)$$

$L_0$  is the total length of the catenary, and  $F_1$ ,  $F_2$ ,  $F_3$ , and  $F_4$  are the projected components of cable tension in the  $(X, Y)$  axes at the extreme points. This model has the advantage of visually measurable parameters  $l_x$  and  $l_y$  allowing for visual servoing experiments [102]. The assumptions underlying Eqs. (3.1) and (3.2) are the following:

- The cable is a perfect not elongable solid (length is constant)
- The cross-sectional area of the cable is kept constant
- In Figure 3.1, node  $I$  is located at point  $(0, 0)$ , while node  $J$  is at point  $(l_x, l_y)$
- Material and cross sectional area is not taken into account.
- Inherent to catenary nature, only quasi-static situations are valid
- Torsion and bending moments are non-existent

### 3.3 Desired team spatial configuration

For practical reasons, we aim to have identical vertical forces exerted by the DLO on all quadrotors, so that energy expenditure is the same for all, which assures

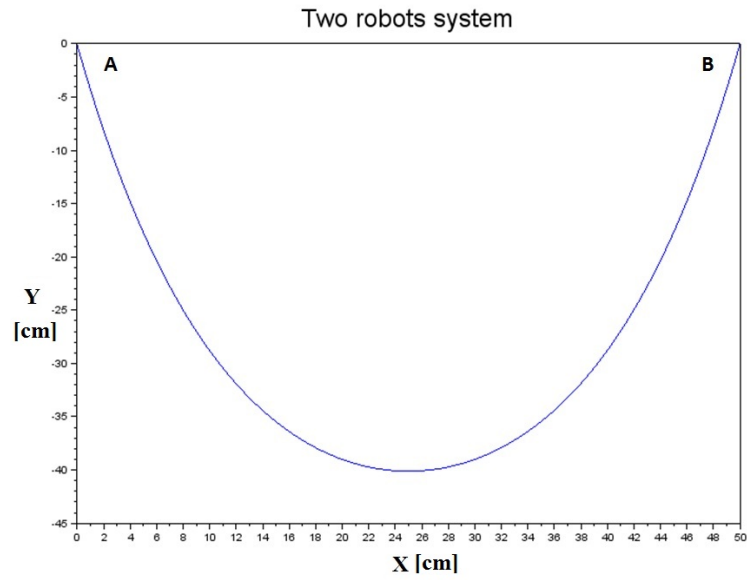


Figure 3.2: Catenary and two robots system

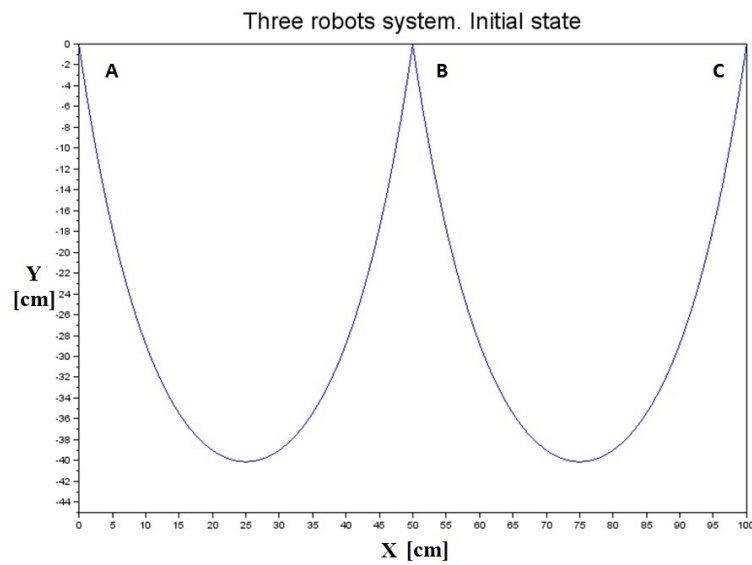


Figure 3.3: Catenary and three robots system. Initial state

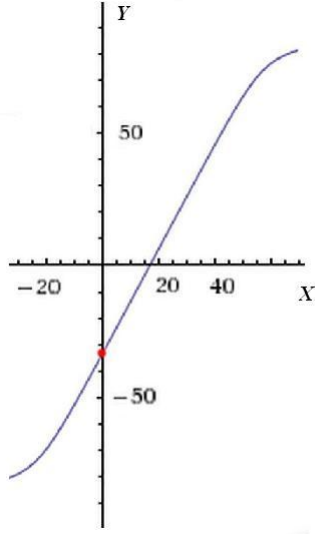


Figure 3.4: Plot of the differences with the desired state in Eq. 3.4.

that the autonomous life-span of equivalent drone models carrying the task will be almost the same and thus, avoiding early energy depletion by some quadrotor, which would result in failure of the collaborative task. In the simplest case, only one DLO section and two quadrotors, shown in Figure 3.2, the sought optimal state corresponds to identical heights of the extreme nodes. In case of a perturbation altering the height of either  $A$  or  $B$ , the only way to retrieve the optimal state of this system is to return the nodes to equal height.

Let us consider now the case with 3 robots. Then the DLO shape is modeled by two catenaries sharing one of the extreme points, as illustrated in Figure 3.3. The horizontal distance between each drone is  $l_x = 50\text{cm}$  and constant, and each catenary section measures  $L_0 = 100\text{cm}$ . The quadrotor located in node  $B$  supports twice the weight supported by the quadrotors located in nodes  $A$  and  $C$ . To achieve equal distribution of load in this system we need to make node  $B$  to support one third of the total weight of both catenaries; in order to get that, the variable to derivate is the difference in vertical height between node  $A$  and  $B$ . For the specific numerical data given above, the functional expression of the vertical tension at node  $B$  is as follows:

$$F_B(\Delta y, l_x) = \frac{w}{2} \left( -y \coth \left( \sqrt{3 \left( \frac{L_0^2 - (\Delta y)^2}{l_x^2} - 1 \right)} \right) + L_0 \right) \quad (3.3)$$

where  $\Delta y$  is the height difference between nodes  $A$  and  $B$  ( $C$  is supposed at the

same height as  $A$ ). Then the desired state is characterized by the following equality:

$$D_F = F_B(\Delta y, l_x) - \frac{(n-1) \cdot w \cdot L_0}{n} = 0 \quad (3.4)$$

Where  $n$  is the number of drones taking part in the cooperative transport system ( $n = 3$  in current example) and  $D_F$  represents the load difference among node  $B$  and any of the remaining nodes. Using the Newton-Raphson iterative method, minimization of this function converges quickly using the expression of the gradient of Eq. (3.3) for the specific numerical values of the parameters given above:

$$\frac{\partial}{\partial y} F_B(\Delta y, l_x) = F' = \frac{w}{2} \left( -\coth(A) - \frac{\sqrt{3} \cdot (\Delta y)^2 \cdot \frac{1}{\sinh^2(A)}}{l_x^2 \cdot A} \right), \quad (3.5)$$

where  $A$  is:

$$A = \sqrt{3 \cdot \left( \frac{L_0^2 - (\Delta y)^2}{l_x^2} \right) - 1}$$

In the plot shown in Figure 3.4 the  $X$  axis corresponds to variable  $D_F$  of Eq. (3.4), and the  $Y$  axis corresponds to  $\Delta y$ . The red dot represents the vertical displacement between catenary nodes  $\Delta y$  for which  $D_F = 0$ . This value is the height descent of the robot located at point  $B$  in order to reach a vertical load this node equal to those in  $A$  or  $C$ . The curve plotted in Figure 3.4 is obtained setting  $l_x = 50\text{cm}$ ,  $L_0 = 100\text{cm}$ , and  $w = 1\text{kg/m}$ . The desired state is shown in Figure 3.5 as the red configuration of the DLO, where the difference between nodes  $A$  and  $B$  is exactly the same as difference between  $B$  and  $C$ .

An asymmetric configuration is shown in Figure 3.6. In this case, the length of the left and right catenaries are  $100\text{cm}$  and  $110\text{cm}$ , respectively, and the horizontal distances between robots  $A$  and  $B$ , and robots  $B$  and  $C$  are different. To achieve a desired state of equal load on all robots from this initial configuration, we need to derive two different functions. First, height difference between node  $A$  and  $B$  is calculated so that vertical tension in  $A$  and  $B$  is equivalent to one third of the total DLO weight. Once this calculated, the height difference between node  $B$  and  $C$  is calculated so that vertical tension in  $C$  is one third of the total weight. The two equations are solved with Newton-Raphson algorithm. Figure 3.7 shows final state of the system, where blue line represents the initial state and red line represents the final state. Notice that nodes  $A$  and  $C$  are no longer at the same height in the desired state. Three different height points can be observed. We also show an evolution of intermediate states (green lines) of the system leading from the initial configuration to the desired one in 20 steps. Larger systems, with more drones, follow similar patterns. In Figure 3.8, the lengths of the catenaries are the same, hence new robots

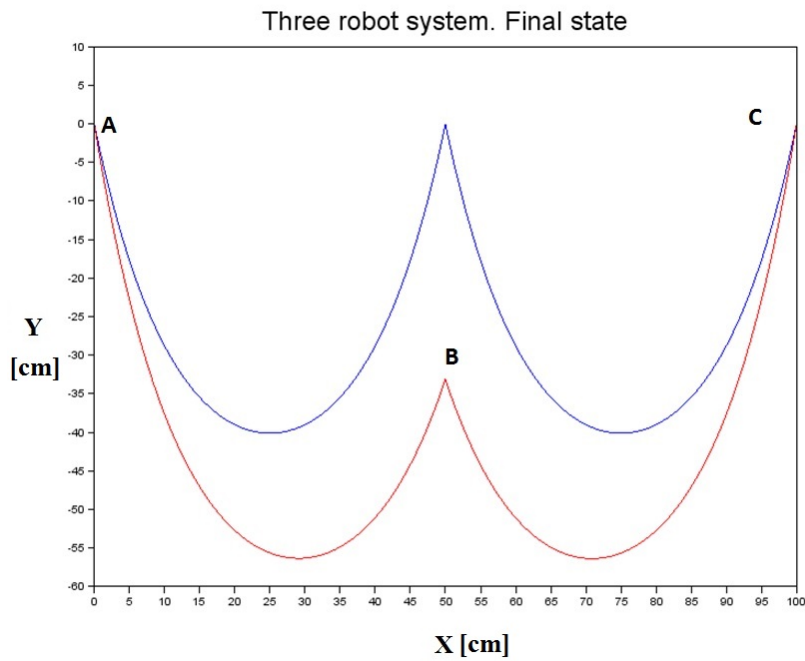


Figure 3.5: Two fold catenary sustained by a three robots system. Initial (blue) and final (red) states.

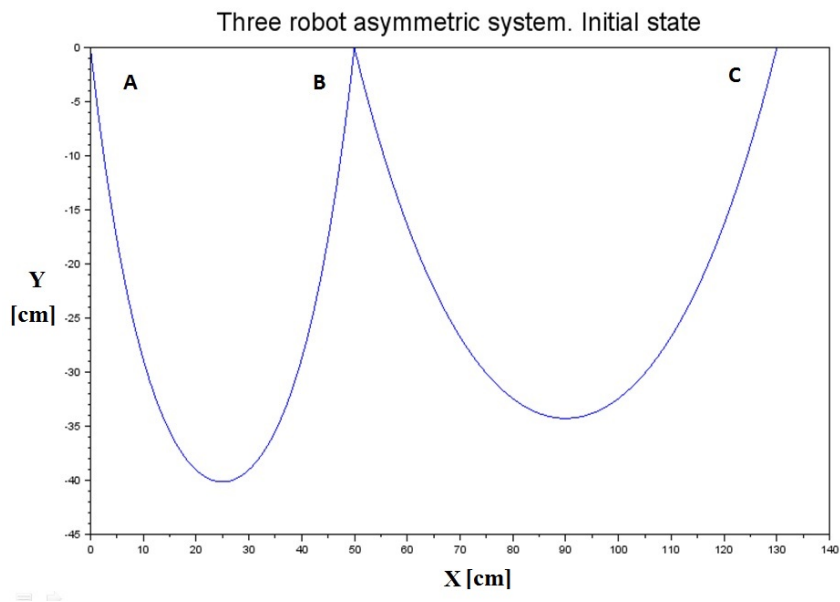


Figure 3.6: Two fold catenary sustained by three robot in an asymmetric initial state.

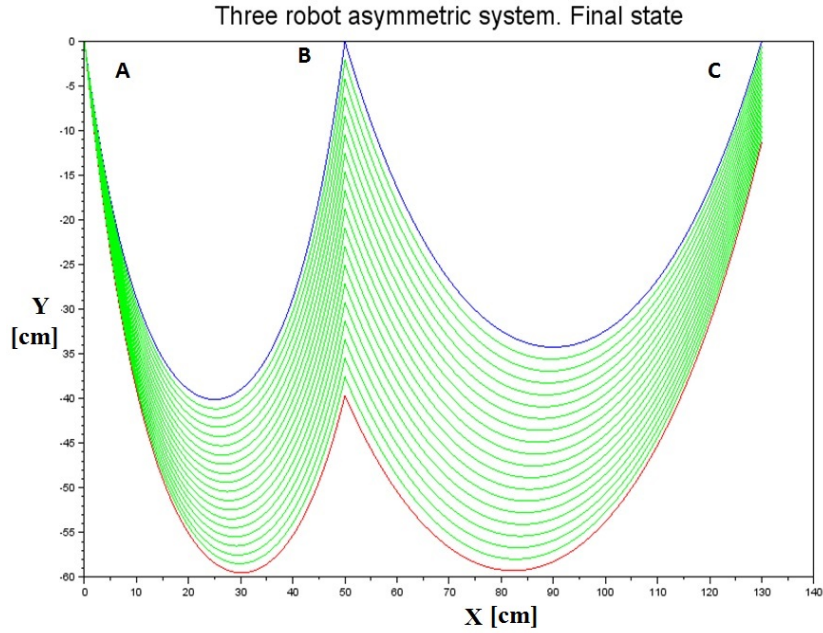


Figure 3.7: Catenary and three robot asymmetric system. Intermediate and final states

in the team add length to the DLO.

### 3.4 Quadrotor modeling

In this section we present the dynamical model of the quadrotor that is relevant for the task of achieving the equi-workload configuration. First we introduce the relevant coordinate frames, second the dynamic equations for the vertical motion used to achieve the equi-workload configuration.

#### 3.4.1 Coordinate frames

While the quadrotors are hovering, we can treat the catenary as being attached to stationary points through rigid rods and ball joints to arrive at the constraints [63]. The aim of this section is to relate the coordinates of one robot with the coordinates of the robots in the other nodes of the catenary. For this purpose, equations based on [42] will be used. Equations relate points  $(x_1, y_1)$  and  $(x_2, y_2)$  in the  $X - Y$  plane. Coordinates in node  $I$  keep steady, and  $x_2$  coordinate does change according to the model developed in Section 3.2.



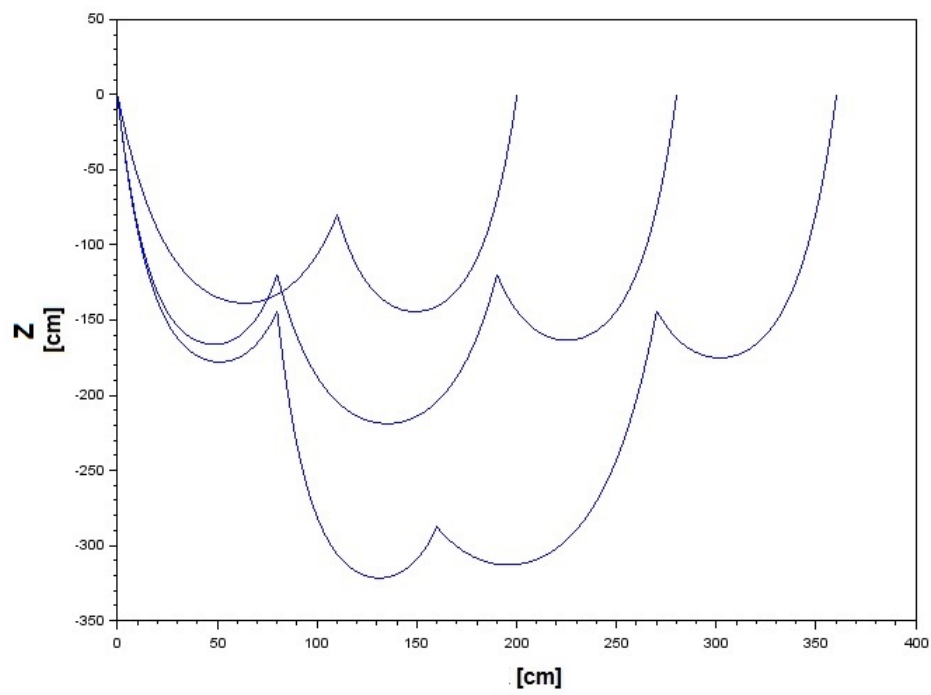


Figure 3.8: Equi-workload configurations for systems with 3, 4, and 5 quadrotors, having 2, 3, and 4 catenary sections

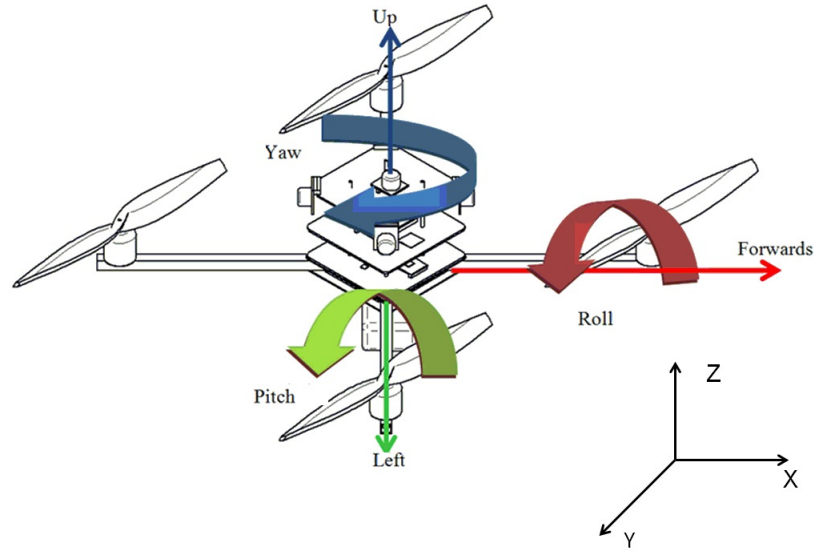


Figure 3.9: Roll ( $\phi$ ), pitch ( $\theta$ ), yaw ( $\psi$ ) angles in a plus configuration quadrotor

$$y_2 = y_1 - \frac{1}{w} \cdot \left( \sqrt{F_1^2 + (wL_0 - F_4)^2} - \sqrt{F_1^2 + F_4^2} \right) \quad (3.6)$$

Equation (3.6) implies the following assumptions on the behavior of the catenary and the limitations of this model:

- Funicular equilibrium of the deformed element: Once deformed, the catenary element adopts the equilibrium configuration corresponding to the final distribution of forces on the cable.
- The catenary does not elongate, and so it conserves the total unit weight after the displacements.

Equation (3.6) is the same whether the DLO is composed of a unique catenary or two. The formula is applied to nodes in the same catenary.

### 3.4.2 Dynamic equations

Angles  $\phi$ ,  $\theta$ , and  $\psi$  represent the Euler angles referring the Earth inertial frame with respect to the body-fixed frame ( $\phi$ ,  $\theta$ , and  $\psi$  represent the rotation along axis  $Y$ ,  $X$  and  $Z$  respectively, as shown in Figures 3.10 and 3.9, and  $Z$  represents the height of the quadrotor with respect to Earth frame of reference. Eq. 3.7 are the linear and angular accelerations of the system dofs including the presence of the catenaries  $A$  and  $B$  tensions ( $V$ ,  $H$  subindexes represent vertical and horizontal

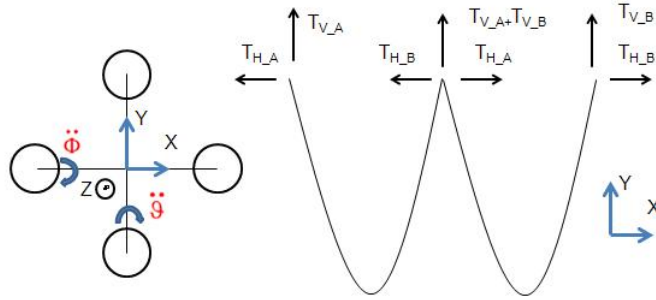


Figure 3.10: Coordinate systems and catenary tensions

components respectively, represented in Figure 3.10), which are obtained by the classical applied mechanics formulas for catenaries. Note that the approximation in eq. 3.7 is valid only for small angles and small rotational velocities, and equations are specified for the central drone, as the rest are affected only by tension components on their own catenary section.  $d_{GC}$  is the vertical distance from the attachment point of the catenary to the gravitational center of the drone, which is assumed to be  $10cm$ . Take into account that  $Z$  coordinate for the drone is  $Y$  coordinate for the catenary, while  $X$  remains the same for both systems, and represents the forwards direction.

$$\left\{ \begin{array}{l} \ddot{z} = -g - \frac{(T_{V,A} + T_{V,B})}{m} + (\cos \theta \cos \phi) \frac{U_1}{m}, \\ \ddot{\phi} = \frac{U_2}{I_{xx}}, \\ \ddot{\theta} = \frac{U_3}{I_{yy}} + \frac{(T_{H,A} - T_{H,B}) \cdot d_{GC}}{I_{yy}}, \\ \ddot{\psi} = \frac{U_4}{I_{zz}}. \end{array} \right. , \quad (3.7)$$

where  $U_1$ ,  $U_3$ , and  $U_4$  are control commands as defined in Chapter 2 that must be provided by the control loops.



## Chapter 4

# Quadrotor control system

### 4.1 Introduction

This chapter proposes and details the control structure for the dynamic model of the quadrotor described in Chapter 3. In essence, a quadrotor has a complex non-linear behaviour. It has 6 degrees of freedom, but we can only act on 4 different inputs, so any linear control will always be underdetermined. Although there are various control models from the technical literature that may be used, no one takes into account that the actual dynamic equations of the robot are modified by the DLO non-linear influence, and so a very robust control is crucial to achieve the DLO transportation that is the main goal in this Thesis.

This Chapter describes the equations and parameters needed to control the quadrotor and manage them to get to the final equilibrium position according to criteria presented in Chapter 3. Though there are proposals for quadrotor control using artificial neural networks [26], or optimal robust control [86], in this Chapter we attack the problem using classical Proportional Integral Derivative controllers, though we tune their parameters offline. In fact, a simplified Proportional Derivative controller (PD) [5] gives a good control response for this task. In this Chapter, we follow coordinate system and the modeling approach of quadrotor dynamics and kinematics proposed in [17] consisting of a collection of equations, involving spatial coordinates, local angles, torques, angular speed of rotors. Here, electric system modeling will not be taken into consideration as our focus is on the dynamical aspects of the system.

The contents of the Chapter are as follows: Section 4.2 overviews the general motion control strategy to achieve the DLO transportation. Section 4.3 describes the inner control loop. Section 4.4 describes the algorithms employed for offline inner control loop tuning. Section 4.5 reports the experimental results.

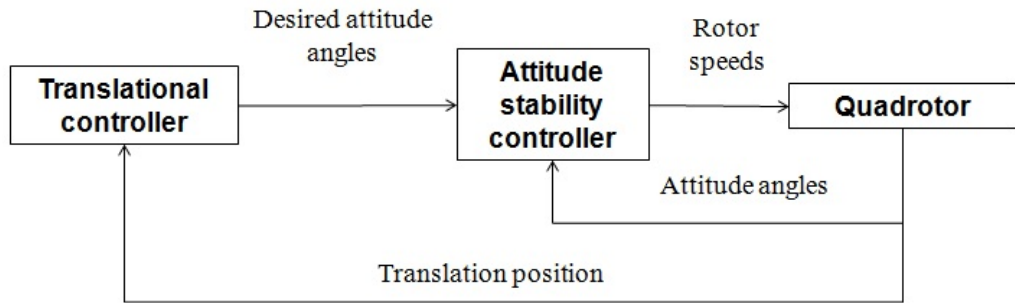


Figure 4.1: Two loops controllers for quadrotor position and orientation

## 4.2 General motion control for DLO transportation

Once reached the desired vertical position distribution configuration, with the quadrotors sustaining the DLO catenary sections at their energy consumption balanced equilibrium, quadrotors may start their horizontal or vertical motion. The system control strategy is decentralized, so each quadrotor control in the system is independent from the rest, and there are two controller loops in cascade configuration for each quadrotor:

- An inner control loop in charge of reaching the desired altitude and attitude. The controller acts on different torques and thrust of the quadrotor (attitude circuit).
- An outer control loop in charge of navigating to a specific point in space (position circuit), so that it calculates the desired rotor angles in order to move horizontally.

This two-loop structure is illustrated in Figure 4.1.

Current motion control loops structure is the same in all the drones that take part in the DLO transport task, and both altitude and position loop are PID/PD equipped. However, different tuning strategies have been tested to tune the controller parameters.

1. Inner control loop tuning is described in this Chapter 4. PID/PD parameters were obtained with an offline particle swarm optimization (PSO) tuning and classic Ziegler-Nichols rules.
2. Second, outer control loop is presented in Chapter 5, and an offline PSO tuning and an online adaptive fuzzy tuning methods were implemented to tune the parameters of this circuit.

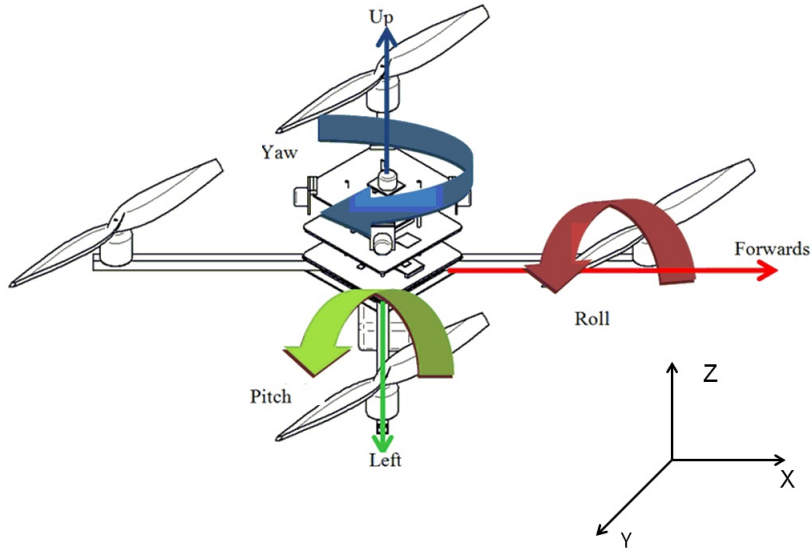


Figure 4.2: Roll ( $\phi$ ), pitch ( $\theta$ ), yaw ( $\psi$ ) angles in a plus configuration quadrotor

### 4.3 Inner control loop

We use four PD controllers for the roll, pitch, yaw and height, respectively, which are the degrees of freedom (dof) of each quadrotor [17]. The block diagrams specifying the control of the degrees of freedom of each quadrotor are shown in Figures 4.3, 4.4, 4.5, and 4.6. In the four control subsystems, the aim is that the real value of the degree of freedom reaches the desired value, denoted by a  $d$  subindex.  $K_P$ ,  $K_I$ , and  $K_D$  are the three PID control parameters to be tuned. Finally,  $I_{XX}$ ,  $I_{YY}$ ,  $I_{ZZ}$  [ $Nms^2$  or  $kgm^2$ ] are the body rotational moment of inertia around the  $X$ ,  $Y$  and  $Z$  axis.

The control system is scalable and can work with multiple drones. For greater simplicity, the  $\psi$  degree of freedom is set to 0, so we will deal with PD controllers. The methodology to tune PD parameters of the quadrotor is described in Section 4.4. In our experiments, all the quadrotors taking part in the system are equipped with the same inner-loop PD parameters. In order to find them, two different experiments are carried out. In *Experiment 1a*, we carry out a comparison between the two offline tuning methods. In *Experiment 1b*, the robustness of chosen parameters in *Experiment 1a* is tested.

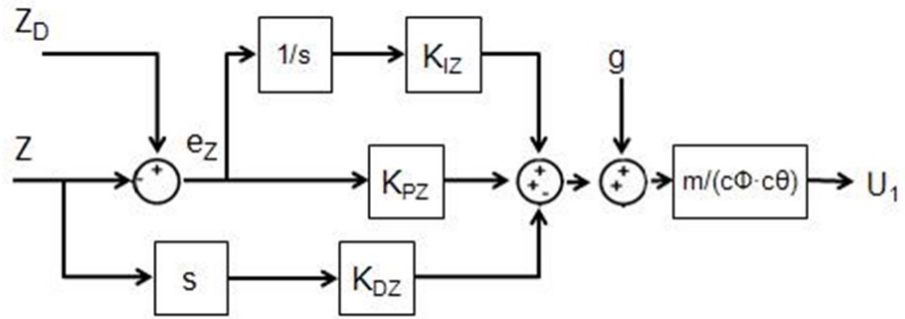
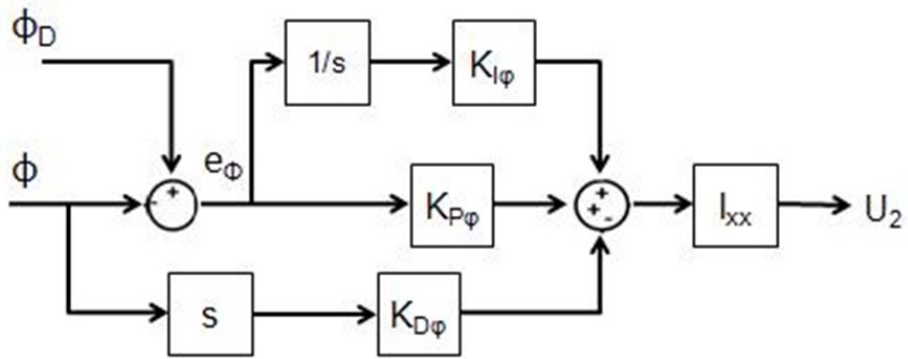
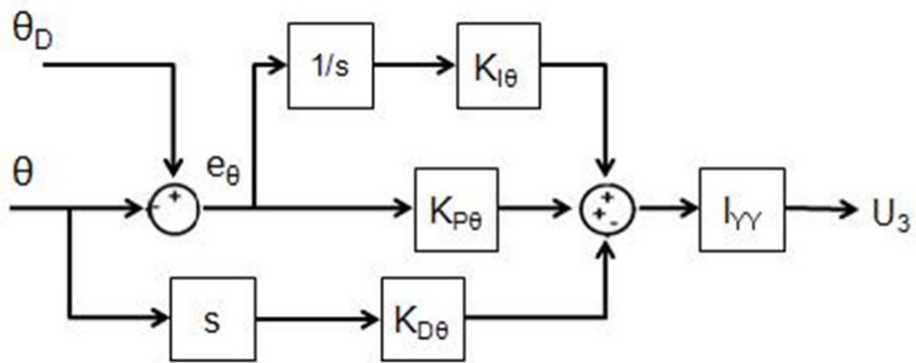
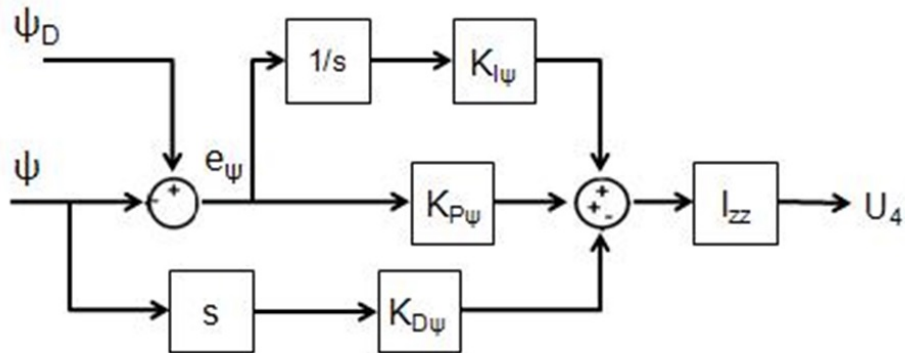


Figure 4.3: PID Z controller

Figure 4.4: PID  $\phi$  controllerFigure 4.5: PID  $\theta$  controller



Figure 4.6: PID  $\psi$  controller

## 4.4 Offline inner control loop tuning

Torque control is crucial so that quadrotors tend to the desired angles properly. We have compared the following parameter tuning methodologies:

- Ziegler-Nichols tuning (ZN): which is the classical approach to set PID parameters.
- Particle Swarm Optimization (PSO) algorithm: a novel algorithm based on metaheuristic optimization.

### 4.4.1 Ziegler-Nichols algorithm

This is a heuristic method of tuning a PID controller developed by John G. Ziegler and Nathaniel B. Nichols in 1942. It is performed as follows. First, setting the I and D gains to zero. Then, the P gain  $K_p$  is increased (from zero) until it reaches the ultimate gain  $K_u$ , at which the output of the control loop has stable and consistent oscillations. After that,  $K_u$  and the oscillation period  $T_u$  are used to set the P, I, and D gains depending on the type of controller used. Therefore, ZN is an offline tuning method. Its tuning rules are summarized in Table 4.1. Ziegler-Nichols has been widely used by industry and vendors traditionally, and it shows good results with linear and deterministic control systems. However, it might lack of robustness and the tuning is obtained with little knowledge of the system.

### 4.4.2 Particle Swarm Optimization (PSO)

This technique is a relatively recent heuristic search method whose mechanics are inspired by the swarming or collaborative behavior of biological populations,

<b>ZIEGLER-NICHOLS</b>			
<b>Control type</b>	$K_p$	$K_i$	$K_d$
P	$0.50K_u$	-	-
PI	$0.45K_u$	$1.2\frac{K_p}{T_u}$	-
PD	$0.8K_u$	-	$\frac{T_u}{8}$
PID	$0.60K_u$	$2\frac{K_p}{T_u}$	$\frac{K_p T_u}{8}$

Table 4.1: Ziegler-Nichols rules

which looks to search the objective value taking into account a cost function. In PSO, a set of particles are distributed randomly in a function and share information among each other, letting the rest of the particles direct to the particle that find the best solution in each iteration at a configurable speed, which makes reference to the mutation velocity of the algorithm. PSO algorithm can be used as a good offline optimization method because due to the number of particles involved in the algorithm, they avoid local minimums. For this reason, we propose it as an efficient PID tuning algorithm. In the literature, [66], [15], [3], and [96] among others defend the PSO advantages for quadrotor control system tuning.

The main steps in the PSO and selection process are as follows:

1. Initialize a population of particles with random positions and velocities in  $d$  dimensions of the problem space.
2. Evaluate the fitness of each particle in the swarm.
3. For every iteration, compare each particle's fitness with its previous best fitness ( $P_{best}$ ) obtained. If the current value is better than  $P_{best}$ , then set  $P_{best}$  equal to the current value and the  $P_{best}$  location equal to the current location in the  $d$ -dimensional space.
4. Compare  $P_{best}$  of particles with each other and update the swarm global best location with the greatest fitness ( $G_{best}$ )
5. Change the velocity and position of the particle according to equations 4.1 and 4.2 respectively,

$$V_{id} = \omega \cdot V_{id} + C_1 \cdot rand_1 (P_{id} - X_{id}) + C_2 \cdot rand_2 (P_{gd} - X_{id}) \quad (4.1)$$

$$X_{id} = X_{id} + V_{id} \quad (4.2)$$

where:

- (a)  $V_{id}$  and  $X_{id}$  represent the velocity and position of the  $i^{th}$  particle with

Parameter	Value
mass, $m$	0.5kg
length of the arm, $l$	25cm
rotational inertia moments $I_{xx} = I_{yy}$	$5 \cdot 10^{-3} [Nms^2]$
rotational inertia moments $I_{zz}$	$10^{-2} [Nms^2]$
propeller thrust coefficient, $b$	$3 \cdot 10^{-6} [Ns^2]$
drag, $d$	$1 \cdot 10^{-7} [Nms^2]$

Table 4.2: Values of standard parrot quadrotor physical parameters.

$d$  dimensions, respectively.  $rand_1$  and  $rand_2$  are two uniform random values, and  $\omega$  is the inertia weight.

- (b) The constants  $C_1$  and  $C_2$  in equations 4.1 and 4.2 are acceleration constants which changes the velocity of a particle towards  $P_{best}$  and  $G_{best}$ . This is, the mutation velocity.

Control subsystem takes the difference between the real and desired value of dofs in quadrotors. All the quadrotors of the DLO transportation team share the values of the four PD circuits ( $\phi$ ,  $\theta$ ,  $\psi$  and  $z$ ). The process to go from an initial vertical configuration to a vertical configuration of equal distribution of workload on the drones in the quadrotor cooperative system is the experimental framework where controllers tuning must be achieved. Results were published in [31] and [30].

## 4.5 Experiment 1

The settings of the simulations carried out to demonstrate the proposed control tuning experiment are as follows: Catenaries have the same weight per unit length ( $w$ ), which is  $1kg/m$ . We adopt standard values for mass and inertia moments of the quadrotors given in Table 5.2. Computational experiments were carried out using a discretization of the time variable. Time increment used to compute simulation steps is 0.1 seconds. Speed in the second experiment is specified by an array of values corresponding to each time instant.

The values for  $K_P$ ,  $K_I$ , and  $K_D$  are the same for the four PID controllers. We compute the values of these parameters with classical Ziegler-Nichols algorithm according to criteria in table 4.1, where  $K_u$  is the critical gain of the system and  $T_u$  is its correspondent period of time. In the present case,  $K_u = 12.5$  and  $T_u = 2.4s$ . Under these conditions,  $K_p = 2.5$ ,  $K_I = 2.08$ ,  $K_D = 1.98$ .

Two experiments are carried out in order to test the response of our system in two different situations:

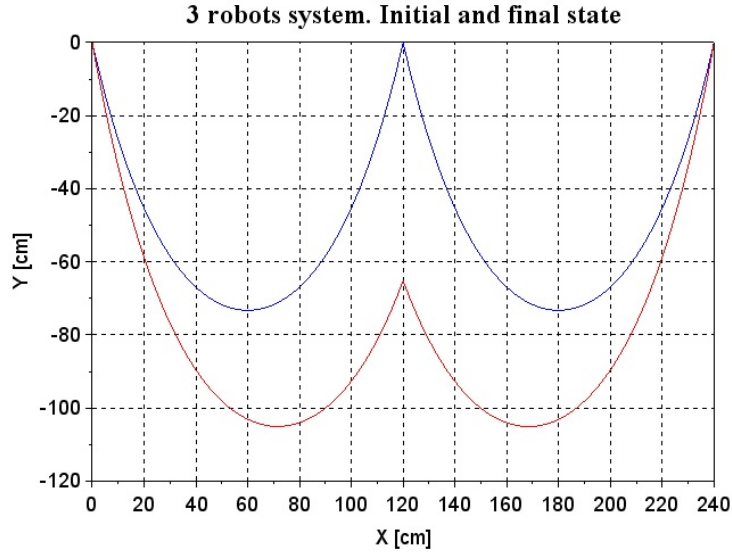
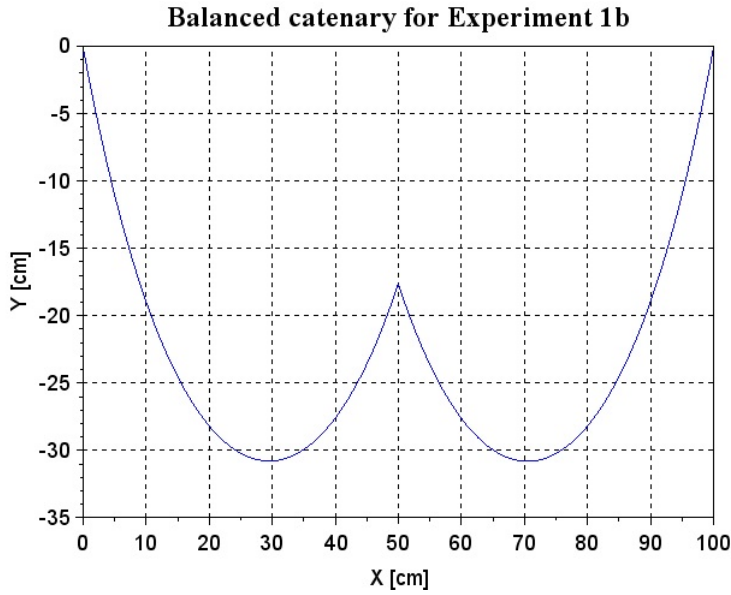


Figure 4.7: Catenary and three robots system for *Experiment 1a*. Initial and final state

- In *Experiment 1a*, we perform the basic tuning performance experiment. We have two catenaries in a symmetric configuration (as shown in Figure 4.7) measuring 200cm long each and with a horizontal distance between nodes of 120cm. The desired state of equal vertical force exerted to all quadrotors is achieved when the quadrotor in the central node height difference is  $\Delta y = 66.54\text{cm}$ . The control goal is to descend smoothly maintaining  $\phi$ ,  $\theta$ , and  $\psi = 0$  during all the descent, without position overshooting to the final position shown in Figure 4.7.
- In *Experiment 1b*, we test the recovery from a loss of the equi-workload configuration. We have two catenaries measuring 70cm long each, with a horizontal distance among the nodes of 50cm. The central drone is already in vertical equilibrium. In this configuration, the experiment consists in achieving the desired state in the following scenario: the three quadrotors are moving at the same speed horizontally, but one of them has a perturbation and moves during a small time lapse slightly faster. The system has a transitory regime from time 0s to 45s, during which quadrotors have a linear acceleration starting from 0 and reaching 0.5m/s. In the stationary regime, all quadrotors cruise at 0.5m/s, until one of them (C) has a sudden increase to 1.5m/s for a short period, coming back to 0.5m/s again. At each moment, desired pitch angle is 0.3 rads for three quadrotors. Due to this change in velocity, the vertical position of the middle quadrotor (B) must be corrected

Figure 4.8: Balanced catenary for *Experiment 1b*

to maintain the desired equi-workload distribution among drones.

#### 4.5.1 Results of *Experiment 1a*

**ZIEGLER-NICHOLS** The response of the middle quadrotor in  $Z$  coordinate is presented in Figure 4.9. It can be seen that the system converges to the desired state of equal load per robot approximately after 4 seconds, achieving an error between the desired height and the measured height close to zero. The vertical speed and acceleration of the drone are plotted in Figures 4.10 and 4.11.

**PSO** PSO parameters are stated in Table 4.3. In the majority of tests, most particles reached the optimum before 10 iterations. However, these particles present different velocities of convergence. In Figure 4.12, we plot the evolution of the central drone position for three different P-D tunings. We choose the combination of PD values ( $K_p = 4.6521$   $K_d = 10.1373$ ) in Figure 4.12 for ensuing tests, because it has the fastest convergence among the three alternatives. In this situation, different values of final height for the central drone were chosen, regardless of obtaining a statically balanced system. Results are shown in Figure 4.13. The next experiment tests the performance with different quadrotor dynamic parameters for a  $\Delta y = 66.54\text{cm}$ . The default parameter values in this article are standard (Table 5.2). The alternative parameters are commercial AR Drone Parrot's, reported in

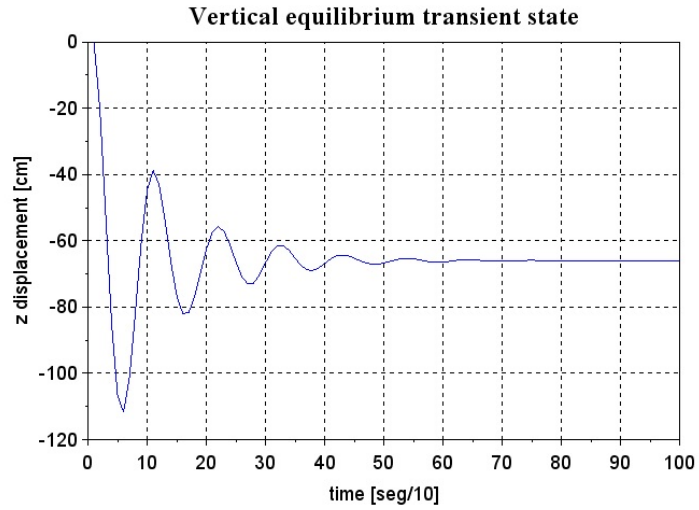


Figure 4.9: Response of middle quadrotor in Figure 4.7, position in the Z coordinate (elevation) under ZN tuning control to achieve the desired state of robot equilibrium.

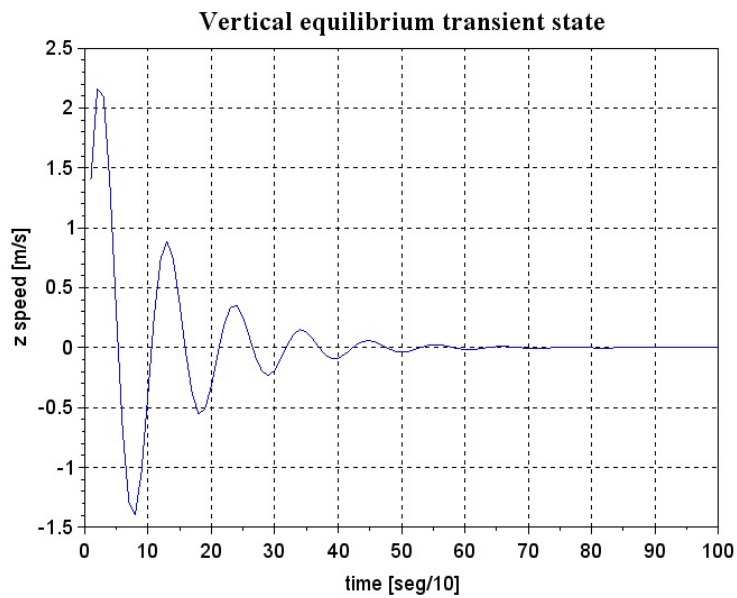


Figure 4.10: Response of quadrotor B of Figure 4.7, vertical speed under ZN tuning control to achieve the desired state of robot equilibrium.

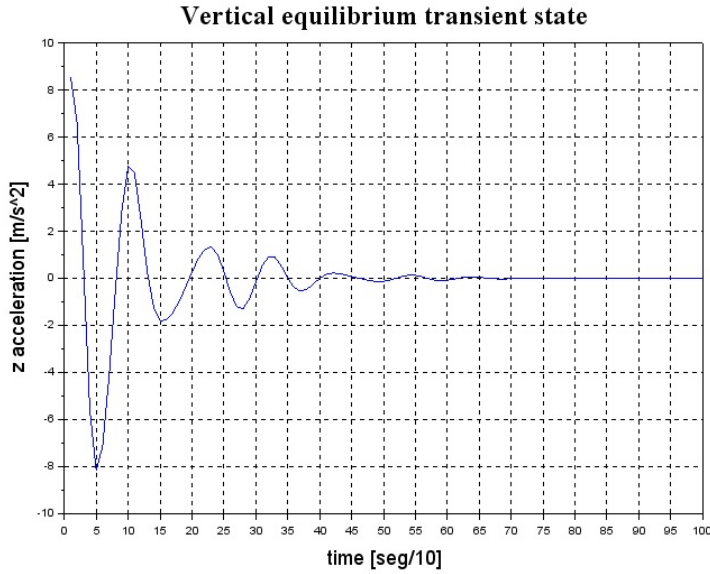


Figure 4.11: Response of quadrotor vertical  $B$  of Figure 4.7, vertical acceleration under ZN tuning control to achieve the desired state of robot equiloal.

Parameter	Value
number of particles	10
weight, $w$	1
$C_1$	2.5
$C_2$	2.5

Table 4.3: PSO parameters for *Experiment 1*

[47] (see Table 4.4). Convergence plot results are shown in Figure 4.14.

#### 4.5.2 Results of *Experiment 1b*

In this experiment, we focus on the responded of the central robot. There is no additional tuning of controller parameters. The horizontal speed of three drones is discretized in 50 position arrays which represent the  $X$  axis in next graphs. Three quadrotors start from  $0m/s$  till  $0.5m/s$ . However, the drone on the right accelerates from time 36 to 45 up to a speed of  $1.5m/s$ . The effect of this acceleration is that the distance between nodes  $B$  and  $C$  enlarges, so that load on  $B$  increases. To restore the state of equal load, the quadrotor in node  $B$  must accelerate to close the distance with  $C$  while descending to reduce its own load. Figure 4.15 shows the plot of the height of quadrotor in node  $B$  in time in response to this perturbation of the global system state. Figure 4.16 plots the evolution of the thrust supported by

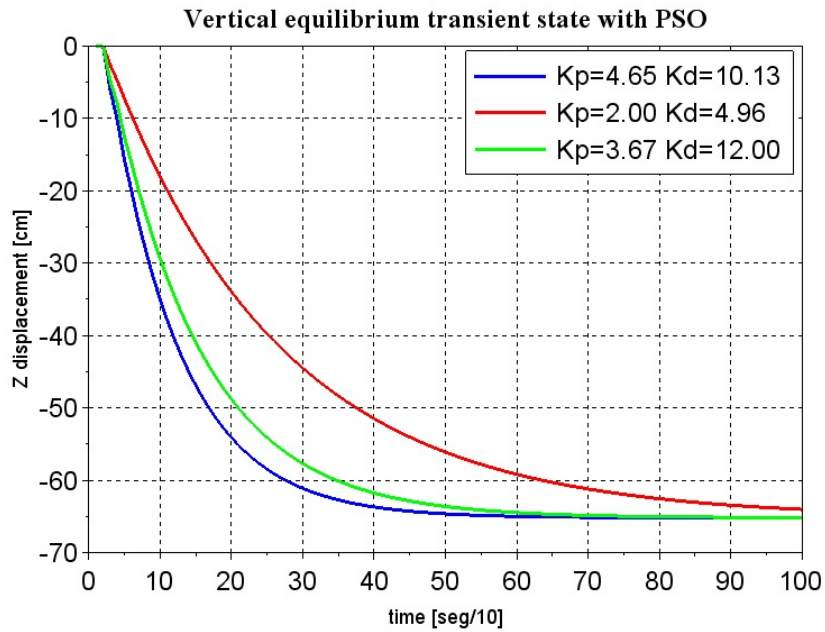


Figure 4.12: Response of quadrotor vertical B of Figure 4.7, vertical displacement under PSO tuning control to achieve the desired state of robot equilibrium. Three different PD tuning combinations

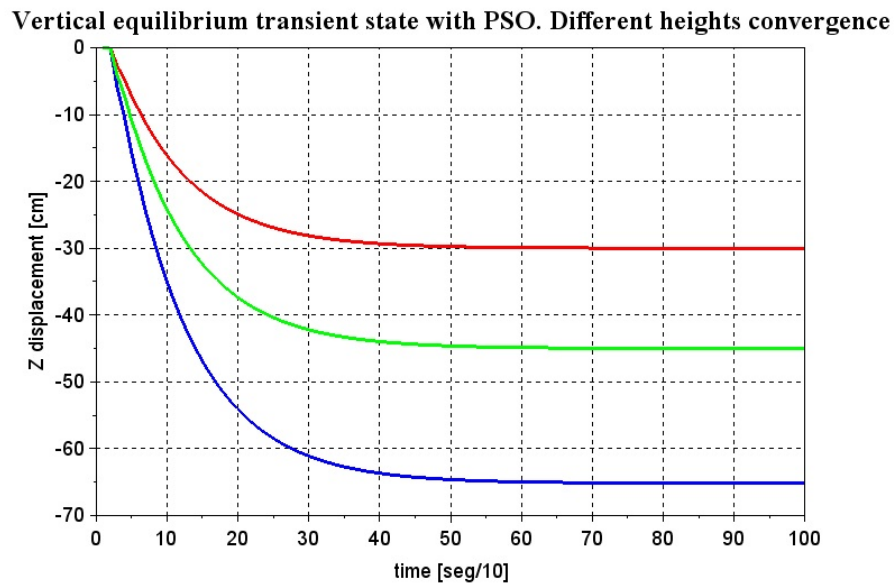


Figure 4.13: Response of quadrotor vertical B of Figure 4.7 Z displacement. Three different convergence heights



Parameter	Value
mass, $m$	0.38kg
length of the arm, $l$	17cm
rotational inertia moments, $I_{xx} = I_{yy}$	$86 \cdot 10^{-2} [Nms^2]$
rotational inertia moment, $I_{zz}$	$172 \cdot 10^{-2} [Nms^2]$
propeller thrust coefficient, $b$	$3.13 \cdot 10^{-5} [Ns^2]$
drag, $d$	$7.5 \cdot 10^{-7} [Nms^2]$

Table 4.4: Values of AR Parrot [47]

Vertical equilibrium transient state. Different dynamic parameters drones

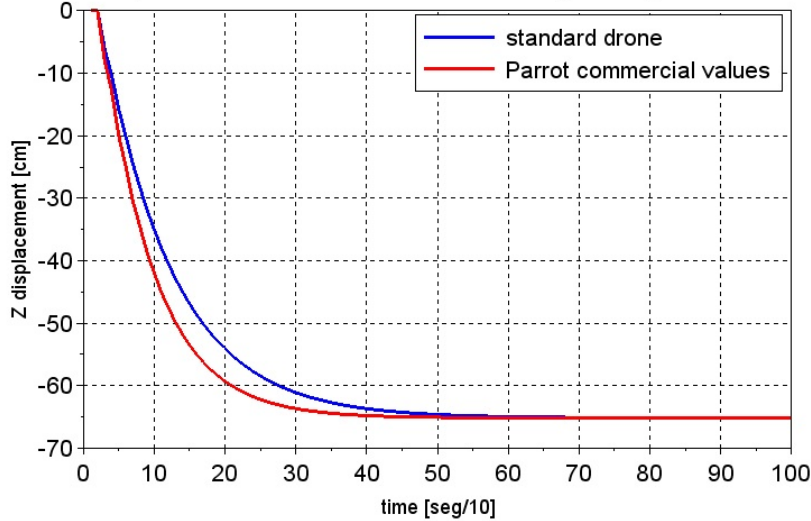


Figure 4.14: Response of quadrotor vertical B of Figure 4.7 vertical displacement under PSO for different dynamic parameters

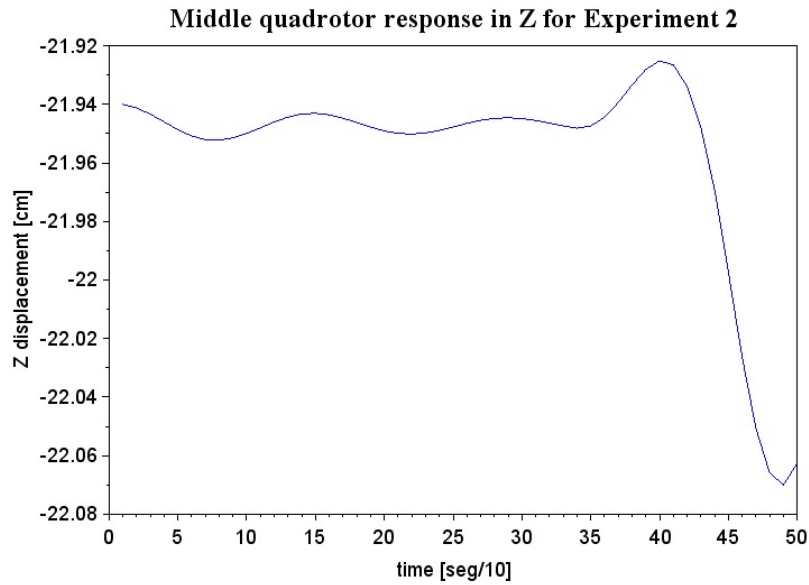


Figure 4.15: Response of quadrotor *B* of Figure 4.8, position in the *Z* coordinate (elevation) under the PID control to achieve the desired state of robot equiloading after the extension of one of the catenaries due to change in cruise speed of the *C* robot.

quadrotor in node *B*, which decreases when the quadrotor in node *C* accelerates.

## 4.6 Conclusions

In this Chapter we have introduced the general two loop control scheme for the quadrotors, one loop devoted to altitude control and the other to horizontal navigation. We have shown that offline tuning of PD controllers for the task of achieving the equi-workload can be efficiently carried out by PSO. The navigation control will be dealt with in the next chapter.

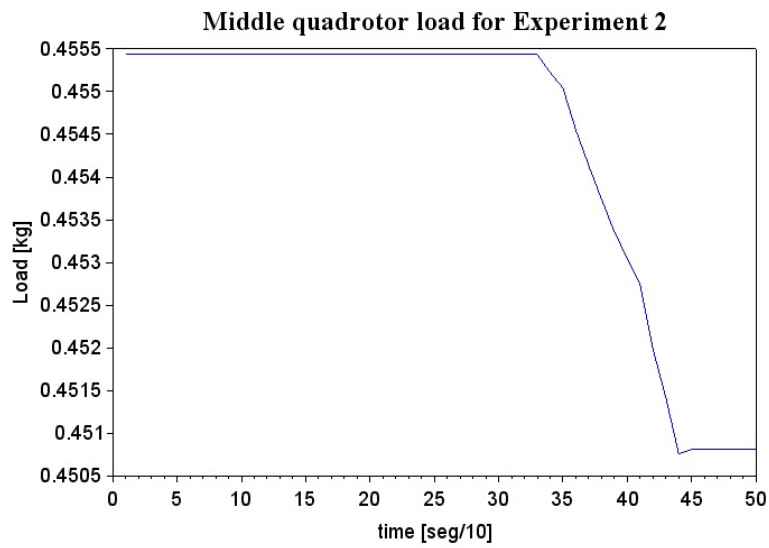


Figure 4.16: Time plot of the load supported by quadrotor *B* of Figure 4.8 after the extension of one of the catenaries due to change in cruise speed of the *C* robot.



## Chapter 5

# Transportation control

### 5.1 Introduction

This Chapter presents the second part of the quadrotor control structure for the task of team DLO transportation, which is in charge of tuning the outer-loop control, i.e. the navigation towards the goal position. As in Chapter 4, PID/PD controllers will be used for the outer-loop control configuration too. However, inner-loop tuning has been carried out offline in this Thesis, which has the advantage of adapting from scratch to different quadrotor dynamic parameters, catenary lengths, or height objectives. But it turns out that it might be not easily adapted to uncertain conditions, such as suffering variable wind perturbations along a path. PID is tailored to control linear stationary systems, but a team of quadrotors carrying a DLO is strongly non-linear and non-stationary, hence we propose an adaptive control whose implementation is explained in this Chapter. Simulation based experiments show the comparison between an offline and online tuning of outer-loop control under different stress conditions. Regarding the kind of PID controller, the integral control term has not been considered in the works of this Chapter due to the good response that the PD controller achieved in *Experiment 1a* in Chapter 4. Having comparable response quality, we prefer to work with a computationally simpler and easier to tune controller.

The content of the chapter is as follows: Section 5.2 presents the quadrotor team control strategy to achieve DLO transportation. Section 5.3 presents the outer control loop, which achieves the robust quadrotor motion to perform DLO transportation. Section 5.4 presents our online adaptive control using a fuzzy modulation in order to achieve outer loop controller tuning. Section 5.5 discusses some heuristics that we apply to obtain smooth system behavior. Section 5.6 describes the results of the DLO transportation simple scenario of line-following following a baseline approach of tuning the PD controllers with a PSO approach similar to

the one in Chapter 4. Section 5.7 presents the results of computational experiments with our proposed fuzzy modulated adaptive approach.

## 5.2 Quadrotor team control model

The team of quadrotors carrying the DLO will move in a line formation according to a leader following strategy [61, 82]. This strategy is defined in the horizontal subspace spanned by the  $XY$  axes, the  $Z$  axis position of the drone has been determined by the equilibrium position of the catenary. Control to achieve this equilibrium has been presented in Chapter 4. Polar coordinates could be used, however, this could lead to singularity points [52], therefore cartesian coordinates are used.

The desired position of a follower robot related to the leader robot is given by eq. 5.1, maintaining a constant distance and angle of following drone.

$$\begin{cases} x_F = x_L + \lambda_X \cos(\psi_L) - \lambda_Y \sin(\psi_L) \\ y_F = y_L + \lambda_X \sin(\psi_L) + \lambda_Y \cos(\psi_L) \end{cases}, \quad (5.1)$$

where  $L$  and  $F$  subindices denote the *leader* and *follower* parameters, respectively. Angle  $\psi$  is the orientation in the  $XY$  plane at each moment of the quadrotor produced by  $\theta$  and  $\phi$ . Factors  $\lambda_X$  and  $\lambda_Y$  are the projections of the constant distance  $\lambda$  on axes  $X$  and  $Y$ , respectively, according to eq. 5.2, where  $\varphi$  is a constant angle that the leader drone tries to keep with its follower(s):

$$\begin{cases} \lambda_X = \lambda \cos(\varphi) \\ \lambda_Y = \lambda \sin(\varphi) \end{cases}, \quad (5.2)$$

In our basic controller, we chose  $\varphi = \pi$ . This leader following strategy is summarized in Figure 5.1:

Thus,  $x_F$  and  $y_F$  are the desired  $x_d$  and  $y_d$  of eq. 5.4 for the follower drone(s), while the desired  $x$  and  $y$  values are the path equation points for the leader drone. Maintaining the catenary shape is an additional constraint for the model, because the entire dynamical system modeling is invalid for non-catenary curves. As a consequence, drones cannot get too near or too far from each other.

## 5.3 Outer-loop control

The outer control loop is responsible for calculating the desired values for each quadrotor angle ( $\theta_d, \phi_d$ ) according to equations 5.3 and 5.4. The control commands for the quadrotor to adapt its torques and thrust towards those desired values is the competence of inner control loop.

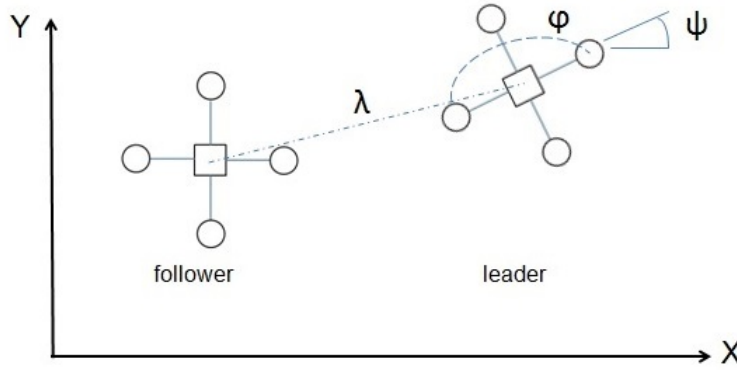


Figure 5.1: Follow-the-leader behavior parameters: distance ( $\lambda$ ) between quadrotors positions, and heading angular difference ( $\phi$ ) parameters.

Quadrotor displacement is achieved by an increase of the corresponding Euler angles. Simply stated, setting  $\psi$  angle to 0, while  $\theta$  and  $\phi$  angles are positive, produces a motion in the  $X, Y$  axes, respectively. Equations to find the desired angles follow the approach in [36], who sets a desired goal point in the space, and calculates the correspondent angle based on the actual quadrotor angle and the remaining distance to reach the ending position of the quadrotor, as follows:

$$\begin{cases} \phi_d = -\arcsin\left(\frac{u_y m}{U_1}\right) \\ \theta_d = \arcsin\left(\frac{u_x m}{U_1 \cos \phi}\right) \end{cases}, \quad (5.3)$$

where  $m$  is the mass of the quadrotor, and  $(u_x, u_y)$  are the motion commands in the  $X$  and  $Y$  axis, respectively. Angles are limited by a built-in saturator to 0.8 rads. The equations for the outer-loop control are given by the following expressions:

$$\begin{cases} u_x = \ddot{x}_d + K_{dx}(\dot{x}_d - \dot{x}) + K_{px}(x_d - x) \\ u_y = \ddot{y}_d + K_{dy}(\dot{y}_d - \dot{y}) + K_{py}(y_d - y) \end{cases}. \quad (5.4)$$

As can be appreciated in eq. 5.4, there are two independent PD controllers in outer-loop circuit: one corresponding to axis  $Y$  and dependent on  $\phi$ , and another relating to axis  $X$  and angle  $\theta$ . Each quadrotor of the system is controlled by independent PD controller for the outer loop-circuit. Given that they are independent, we can tune them separately.

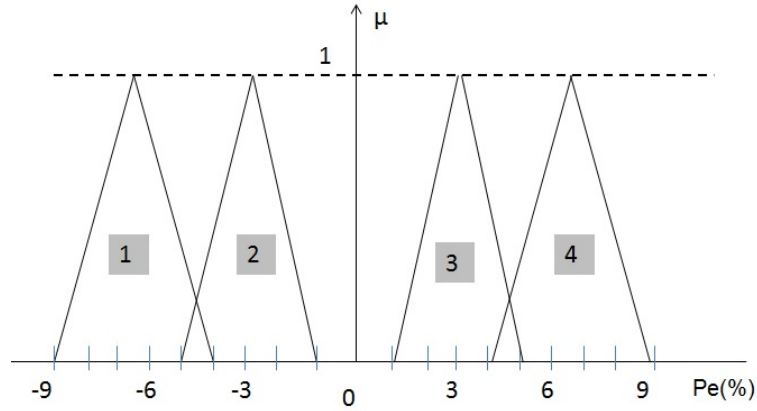


Figure 5.2: Membership functions of the fuzzy adaption rules of the PD control parameters

## 5.4 Outer control loop adaptive tuning

The parameter tuning of outer-loop PD controllers of each and all the quadrotors in the team is an online adaptive algorithm which combines fuzzy membership function activation and gradient descent like adaptation rule, achieving an online fuzzy controller [110, 113]. Takagi-Sugeno controllers [97] are built as *if – then* rules, where the antecedent are fuzzy logic expressions based on evidences modeled by fuzzy membership functions. The consequents are fuzzified actions or fuzzy variable assignments. Reasoning is carried out in the framework of a rule based expert systems. There has been some work about fuzzy logic applied for quadrotor systems for the optimization of stability and dynamics control [50][53][35], however there is no reference to team control performing a joint task.

The approach that we have implemented and successfully tested, consists in the adaptive estimation of the PD controller parameters by updating rules performing gradient descent on the perceived trajectory error. The degree of activation of such rules is modulated by fuzzy terms modeling the error into two fuzzy categories. Error modeling is based on the relative error between the real control signal and its reference:

$$Pe = \frac{Y_{ref} - Y_{real}}{Y_{ref}} \cdot 100, \quad (5.5)$$

where  $Y_{ref}$  is the reference position, and  $Y_{real}$  is the real quadrotor position. The proposed system has four error fuzzy categories dependent on the  $Pe$  value, which can be negative and positive, represented in Figure 5.2. The control variables are the angles  $\theta_d$  and  $\phi_d$ , determining the motion in the  $XY$  plane as discussed above.



We have a independent PD controller for each angle. Therefore, there are two error  $e(t)$  functions depending on the spatial coordinate to control, as shown in eq. 5.6:

$$\begin{cases} e_\phi(t) = \phi_d - \phi(t) \\ e_\theta(t) = \theta_d - \theta(t) \end{cases}, \quad (5.6)$$

where  $\phi_d$  and  $\theta_d$  are the desired values of the angles. Membership functions  $\mu_1(Pe(t))$  and  $\mu_4(Pe(t))$  modulate the activation of equation 5.7 that performs the adaptation of parameter  $K_p$ , while functions  $\mu_2(Pe(t))$  and  $\mu_3(Pe(t))$  modulate the activation of equation 5.8 that performing the adaptation of parameter  $K_d$ . The online parameter adaptation equations read as follows:

$$K_p(t+1) = K_p(t) + \alpha e(t) (\mu_1(Pe(t)) + \mu_4(Pe(t))) \quad (5.7)$$

$$K_d(t+1) = K_d(t) + \alpha e(t) (\mu_2(Pe(t)) + \mu_3(Pe(t))) \quad (5.8)$$

where  $\alpha$  is the adaptation factor,  $e(t)$  is the navigation error at each  $t$  moment, and  $\mu_k(Pe(t))$  is the  $k$ -th membership value function, which provides the activation strength of the adaptation function (note that the activation values are always between 0 and 1 due to the triangular shape of the membership functions specified in Figure 5.2, which have empty support intersections). The adaption factor  $\alpha$  is initialized with a value between 0 and 1 and remains constant until the end of the process. The online PD controller tuning is intended to allow the system to adapt to different trajectories, dynamic parameters of the quadrotors, and unknown catenary weight *per* length.

**Convergence of the fuzzy modulation approach** The online adaptation equations Eq. (5.7) and Eq. (5.8) are in fact instances of the general stochastic gradient descent algorithm applied in many neural network learning algorithms. It is well known that convergence of online stochastic gradient descent learning in stationary environments require that the gradient descent gain  $\alpha_t$  complies with conditions  $\sum_t \alpha_t^2 < \infty$  and  $\lim_{t \rightarrow \infty} \alpha_t = 0$ . However, if the environment is non-stationary the decay of the gradient descent gain freezes adaptation, so that after some time the system becomes insensitive to changes in the environment and, therefore, equivalent to an offline training/tuning algorithm. Hence we leave the gain fixed to a small constant value, so that adaptation is never stopped. Additionally, the membership function modulation factors further enhance convergence, because they focus the learning of the PID coefficients  $K_p$  and  $K_d$  according to the error magnitude. For greater error magnitude, the  $K_p$  coefficient is more affected, while fine tuning to small errors is achieved affecting the  $K_d$  coefficient. Lacking a formal analytical proof, the intu-

ition is that the process will not diverge because the overall gain is always smaller than 1. Empirical (simulated) experiments confirm that the approach works well.

## 5.5 Heuristics for smooth behaviors

In a multi-quadrotor system, there is no guarantee that all the robots will fly at the same speed, therefore inducing distance variations among catenary nodes, which may lead to system instability and collapse. In order to prevent that, two extra conditions are introduced in the model. For each leader-follower pair of drones:

- If the euclidean distance between drones overcomes a threshold, the leader's desired angles turn to 0 until the distance falls within the desired range again.
- If the euclidean distance between drones is shorter than a threshold, the follower's desired angles turn to 0 until the distance increases.

Besides,  $\varphi$  constant angle creates sharp path changes, and abrupt changes in catenary node distances. To achieve path smoothing we make  $\varphi$  variable, as follows:

$$\varphi = \pi - \frac{(\psi_L - \psi_F)}{2}, \quad (5.9)$$

where,  $\psi_L$  and  $\psi_F$  are the XY heading angles of the leader and follower robot respectively, in [rad].

## 5.6 Experiment 2

This section gives results on the baseline PD controller tuning by a PSO approach for the DLO transportation task, as in the tuning of the controller to achieve the equi-workload position in Chapter 4. We train a PD controller, which is applied to each of the four rotors in the quadrotor. The PSO cost function value is computed after the simulation of the system performing one instance of the task. Therefore, carrying the PD parameter tuning by PSO is very time consuming, involving thousands of simulations. Once the PD parameter values are chosen, robustness experiments are carried out.

The experimental system is composed of three quadrotors carrying a DLO in two sections of symmetric catenaries, with the robots flying in parallel. That is, three quadrotors must reach the  $(x_{0,i} + \Delta x, y_{0,i} + \Delta y)$  coordinates at the same time, where  $(x_{0,i}, y_{0,i})$  is the initial position of the  $i$ -th robot, and  $(x, y)$  is the displacement to the desired position. Robots are named  $D1$ ,  $D2$ , and  $D3$ .

Time increment used to compute simulation steps is 0.1 seconds. Specific values of system parameters in the experiment are: each catenary section has length

	CF1	CF2
Parameter	Value	Value
number of particles	15	4
weight, $w$	0.9	0.9
$C_1$	0.01	0.01
$C_2$	0.01	0.01

Table 5.1: PSO parameters for CF1 in *Experiment 2*

$L_0 = 300cm$ ; horizontal distance between drones is  $120cm$ , the weight parameter of the catenary is  $w = 0,005kg/cm$ . The system initial state for the simulation is set in its energy balanced configuration by maintaining drones  $D1$  and  $D3$  at the same height  $z_0$  and decreasing the middle drone  $D2$  to  $\Delta y = 99.9cm$ . During the experiments, though the horizontal distance between drones alters slightly in time, no correction of height is applied. Dynamic parameters of the quadrotors are assumed as in Table 5.2. Initial angles of three drones are all set to 0. Inner control loop PD parameters were tuned as explained in *Experiment 1* (Chapter 4), for this section are set to  $K_p = 140.66$  and  $K_d = 41.36$ . We denote  $(x_d, y_d)$  the desired final position of the leader drone.

We carried out three experiments in order to test the robustness of the obtained controller.

- *Experiment 2a*: Horizontal motion with no wind disturbances for the transportation of a DLO symmetric catenary.
- *Experiment 2b*: Horizontal motion with DLO sections between drones modeled by catenary sections of different length as shown in Figure 5.3, so that we have an unbalanced system,  $l_{x1} = 150cm$  and  $l_{x2} = 120cm$ . Height of point A (drone  $D2$ ) at balanced energy equilibrium configuration is  $\Delta y = 99.9cm$ .
- *Experiment 2c*: Horizontal motion with wind disturbance (along  $200cm$  in  $X$ ,  $90cm$  in  $Y$ ) of the same catenary in *Experiment 2a*. The equation of wind disturbance is:

$$d(t) = 3 + \sin\left(\frac{\pi}{4}t\right), \quad (5.10)$$

where  $t$  corresponds to the time variable used in the quadrotor model and  $d(t)$  is measured in *Newtons*[ $N$ ].

Minimization with PSO is performed setting constants as given in Table 5.1. Besides we test two strategies for the PSO:

- **CF1**: Optimize the PD parameters to minimize the overshoot of the quadrotor in  $X$  direction. Needed iterations for convergence are approximately 10. The

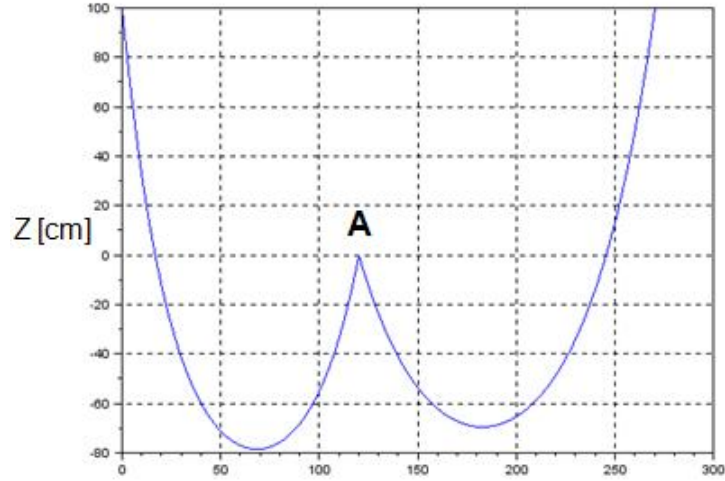


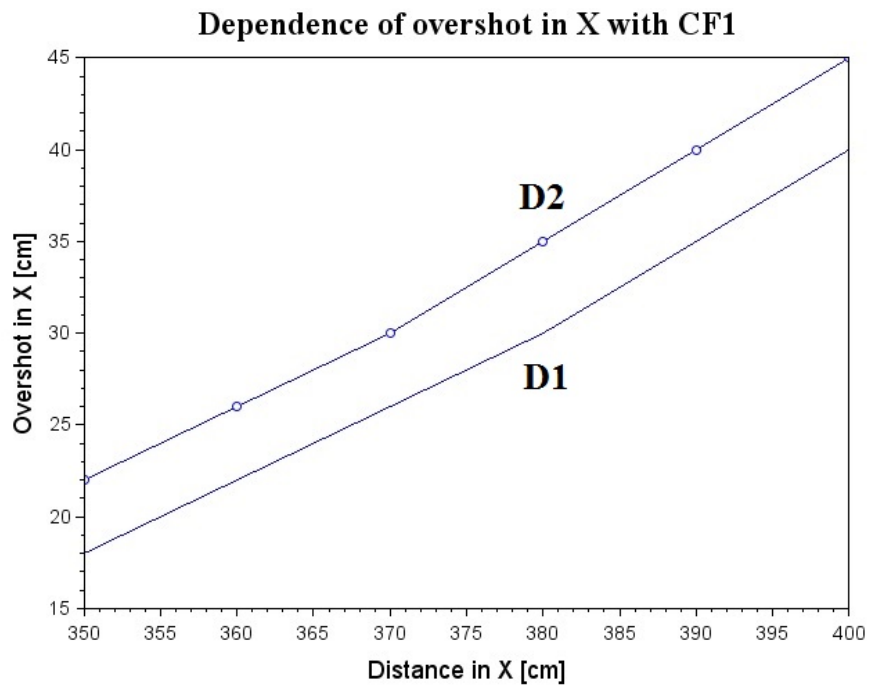
Figure 5.3: Catenaries configuration for *Experiment 2*

hypothesis underlying this function is that we can achieve optimal control using limited information.

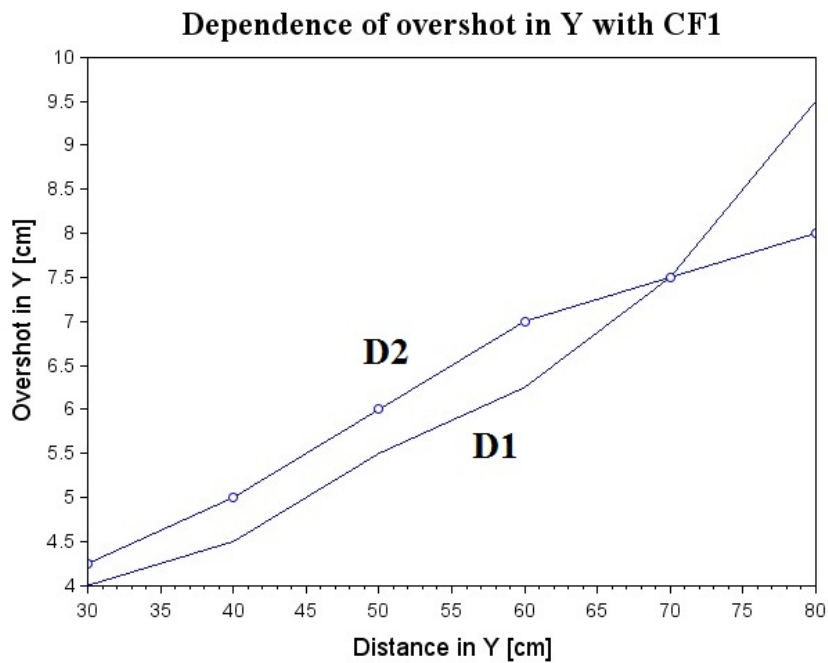
- **CF2:** Optimize the PD parameters to minimize the overshoot in  $(X, Y)$  plane. Number of needed iterations are about 15.

### 5.6.1 Results of *Experiment 2a*

Figures 5.4 and 5.5 plot the overshoot depending on the distance to be traversed by the robots carrying the DLO, for a given range of distances, when the design is achieved by minimizing cost functions specified according to CF1 and CF2, respectively. Distance is quite limited because the quadrotor model in the simulation does not have a specific thrust saturator. The control of robots  $D1$  and  $D2$  produce different overshoot relative to the target position depending on the cost function minimized to estimate the parameters (CF1 or CF2). Also, it can be noticed that  $D2$  has greater overshoot than  $D1$ , due to the combined effect of the DLO in both sectors. The controller designed minimizing cost function CF2 proves to be much more accurate in both directions. Robot  $D3$  has not been represented, as it behaves exactly the same as  $D1$ . To illustrate the detailed behavior of the robots we show in Figure 5.6 the trajectories of the robots in the  $XY$  plane for two specific goal displacements. It can be appreciated that PD controller parameters obtained by minimizing cost function CF2 provide much smoother trajectories, without overshoot.

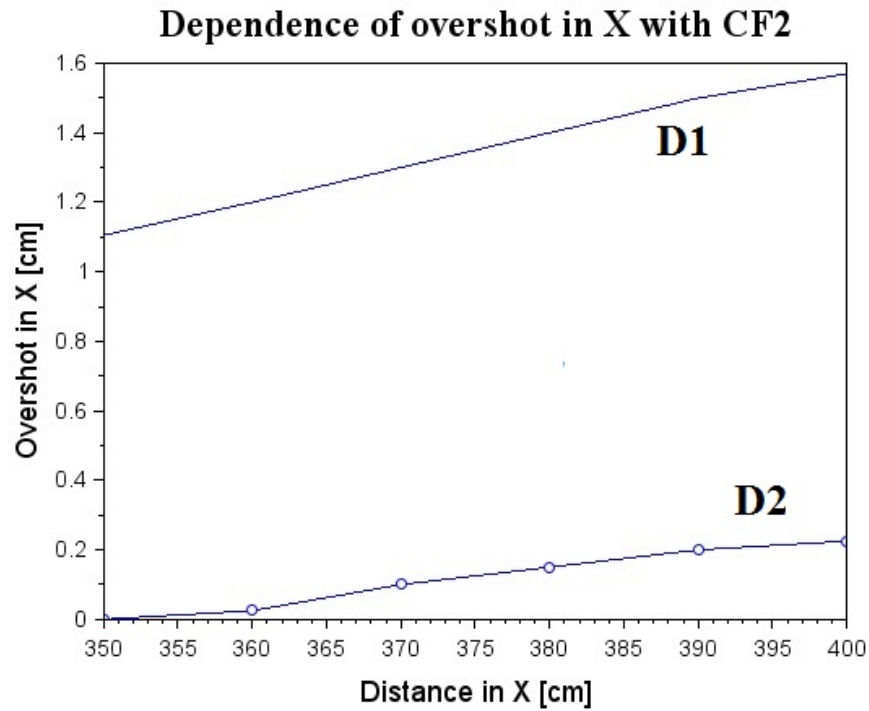


(a)

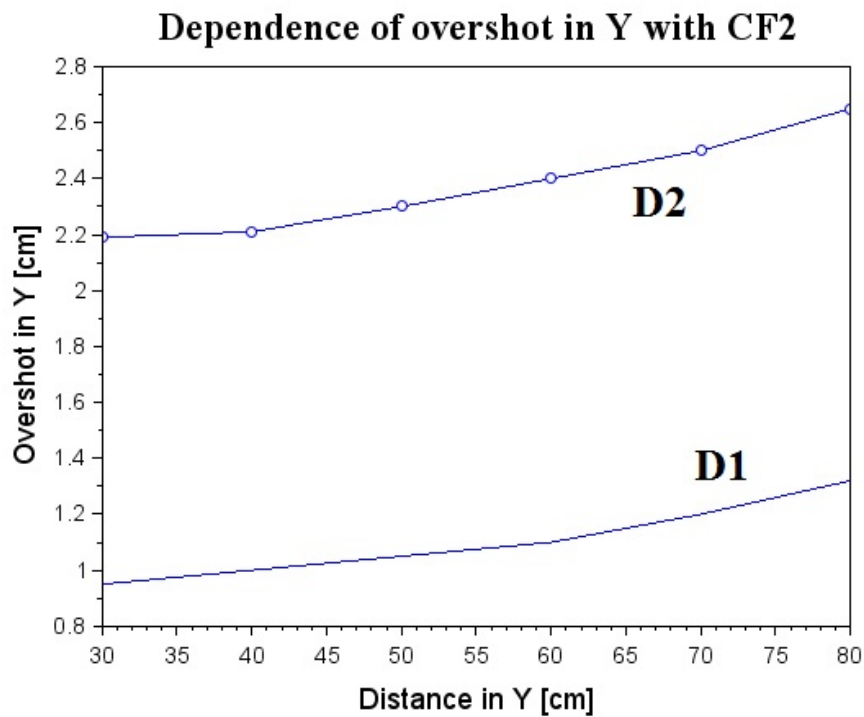


(b)

Figure 5.4: Dependence of overshoot in X (image a) and Y (image b) of robots D1 and D2 on the required distance when training the controllers by minimizing CF1 in *Experiment 2a*



(a)



(b)

Figure 5.5: Dependence of overshoot in X (image a) and Y (image b) of robots D1 and D2 on the required distance when training the controllers by minimizing CF2 in *Experiment 2a*

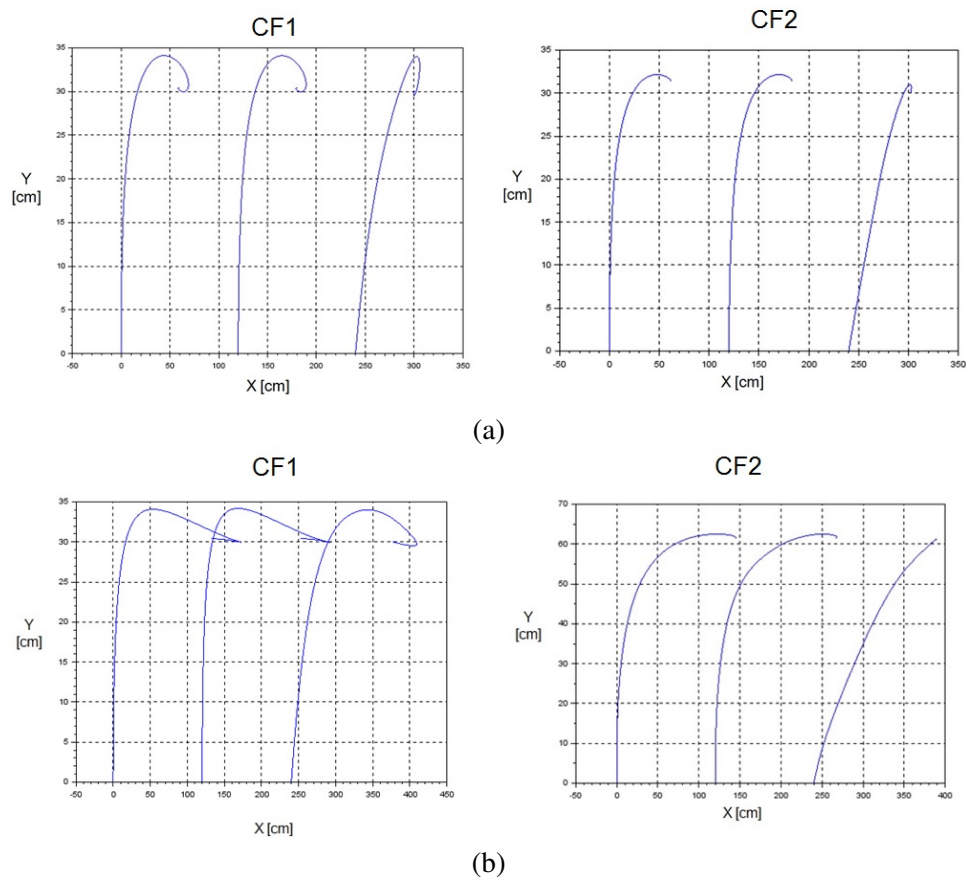


Figure 5.6: Trajectory of the three quadrotors in  $(X, Y)$  space when the desired motion is (a)  $(\Delta x, \Delta y) = (60, 30)$ , (b)  $(\Delta x, \Delta y) = (140, 60)$ , for the controllers achieved with both cost functions CF1 (up) and CF2 (down).

### 5.6.2 Results of *Experiment 2b*

Figure 5.7 shows the trajectory of the three drones carrying the unbalanced sectors of the DLO under controllers whose parameters are tuned minimizing CF1 or CF2. Again, controllers obtained minimizing CF2 provide much more smooth trajectories.

### 5.6.3 Results of *Experiment 2c*

This experiment tests the quadrotor system PD control performance under sinusoidal wind disturbances. In Figure 5.8 appears the time evolution of thrust of the system for controllers trained minimizing CF1 and CF2 when there are no wind disturbances. In the experiments with wind disturbances, the examination of the thrust response gives information on how the quadrotor is reacting to overcome the disturbance in order to accomplish the task. Figures 5.9 and 5.10 show the trajectory and the thrust of the three drones under disturbances in  $X$  direction with controllers trained minimizing CF1 and CF2, respectively. It can be appreciated that the system trained minimizing CF2 achieves smooth convergence and the thrust does stabilize soon.

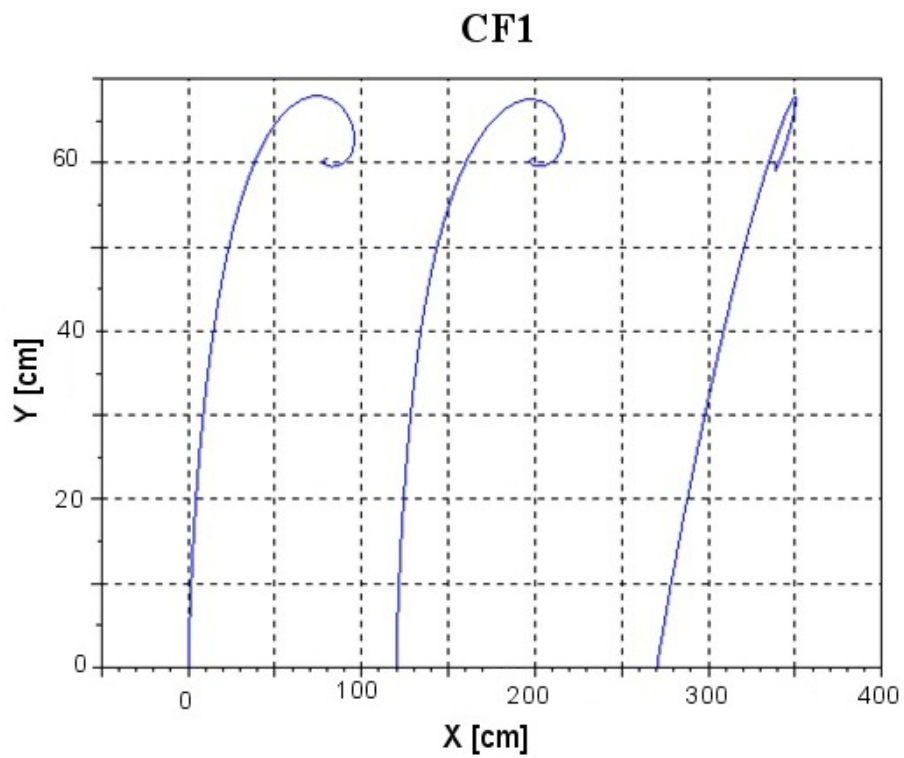
## 5.7 Experiment 3

Two computational experiments based on accurate simulations of the system have been carried out in order to test the efficiency and robustness of the adaptive fuzzy modulated tuning of the PD controllers. The benchmarking systems for comparison have the parameters PD controllers estimated offline by Particle Swarm Optimization (PSO) for attitude and motion control, as discussed in the previous section. The simulation experiments were carried out using a discretization of the time variable and all the simulations cover a time of 20s, including the transient state of the experiment. Time increment used to compute simulation steps is 0.1s. The experiments are as follows:

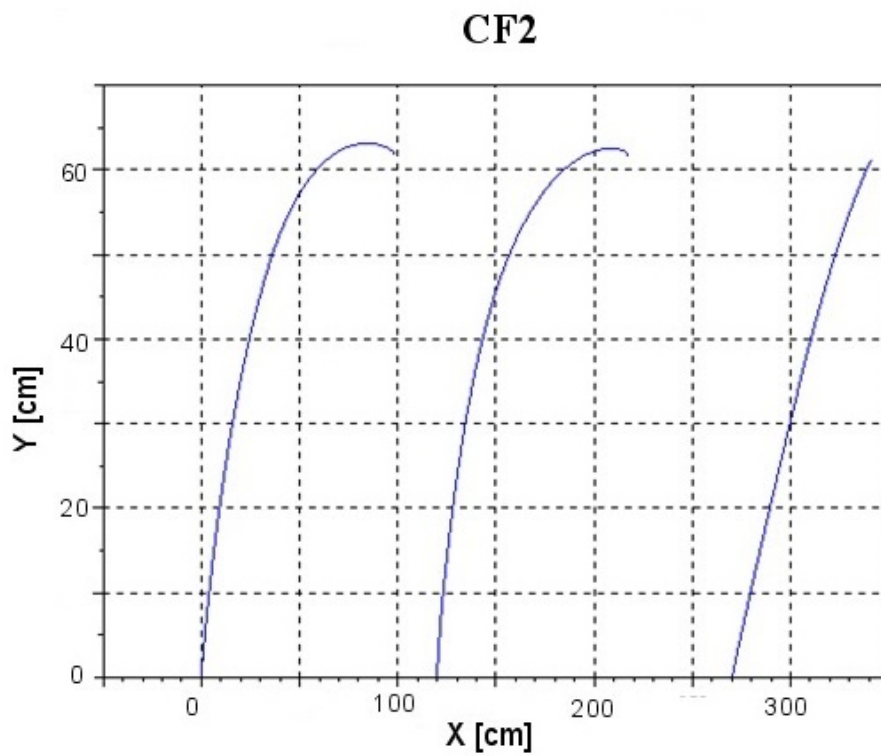
- *Experiment 3a*: The team follows a straight line carrying the DLO.
- *Experiment 3b*: It consists on a curve path to be completed by team of quadrotors carrying the DLO. The shape of this trajectory is shown in Figure 5.11.

Both experiments are carried out with and without wind disturbances. Initial horizontal distance between quadrotors is set different for each one, and the bal-



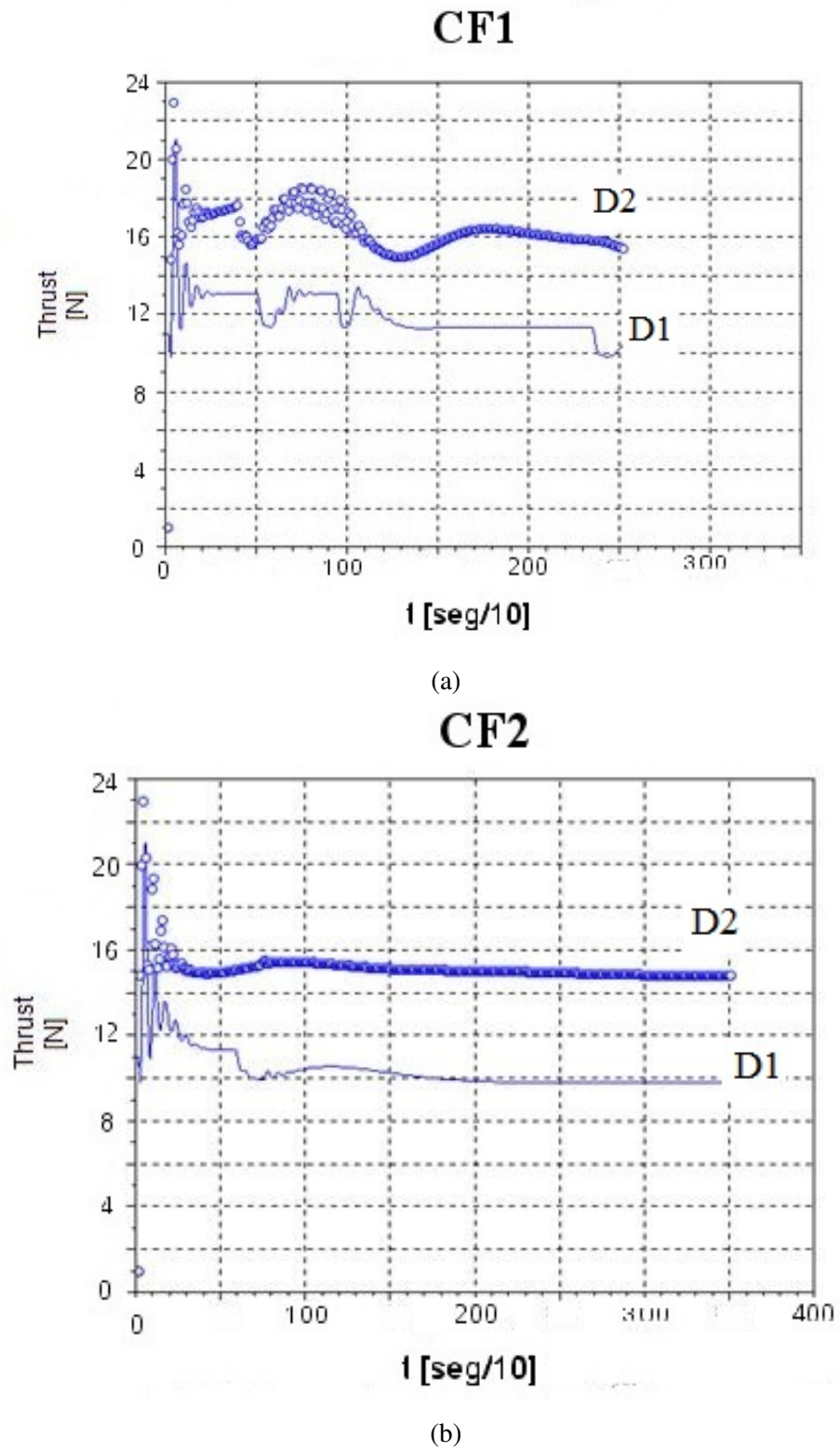


(a)



(b)

Figure 5.7: X (image a) and Y (image b) trajectory of three quadrotors in *Experiment 2b*

Figure 5.8: Thrust of  $D1$  and  $D2$  in *Experiment 2c* under no disturbances

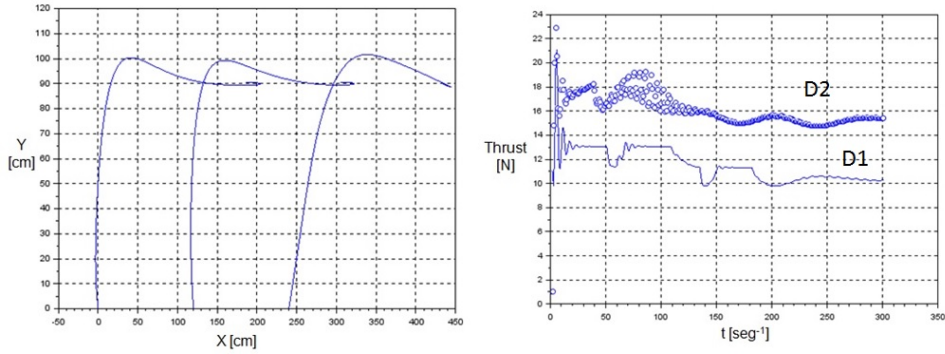


Figure 5.9: Trajectory and thrust of drones under controllers trained minimizing CF1 suffering wind disturbances in X direction in *Experiment 2c*

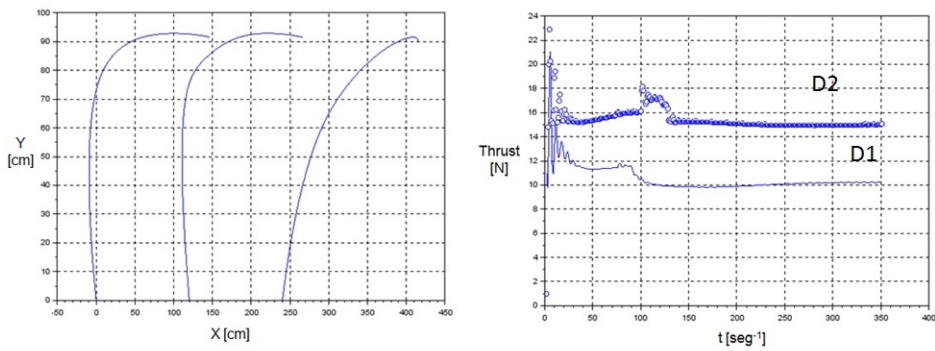


Figure 5.10: Trajectory and thrust of drones under controllers trained minimizing CF2 suffering wind disturbances in X direction in *Experiment 2c*

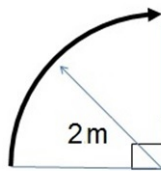


Figure 5.11: Path of the leader quadrotor for the *Experiment 3b*

Parameter	Value
mass, $m$	0.5kg
length of the arm, $l$	25cm
rotational inertia moments $I_{xx} = I_{yy}$	$5 \cdot 10^{-3} [Nms^2]$
rotational inertia moments $I_{zz}$	$10^{-2} [Nms^2]$
propeller thrust coefficient, $b$	$3 \cdot 10^{-6} [Ns^2]$
drag, $d$	$1 \cdot 10^{-7} [Nms^2]$

Table 5.2: Values of standard parrot

Coordinate	Value	Coordinate	Value
$(x_1, y_1)$	(240, 0)	$(x_4, y_4)$	(240, -280)
$(x_2, y_2)$	(240, -90)	$(x_5, y_5)$	(240, -360)
$(x_3, y_3)$	(240, -200)	$(x_6, y_6)$	(240, -450)

Table 5.3: Drones starting coordinates for *Experiment 3*

anced energy consumption spatial configuration is assumed to be maintained. Specific values of system parameters in the experiment are as follows: length of each catenary part of the DLO  $L_0 = 240cm$ ; the weight parameter of the solid is  $w = 0,005 [kg/cm]$ . During the experiments, though the horizontal distance between drones changes in time, no correction of height is applied. Reference distances among drones were all set to  $\lambda = 70 [cm]$ . Adaption factor is  $\alpha = 0.5$  for adaptive fuzzy modulated PD tuning. Mass and inertia moments of the quadrotors are assumed in Table 5.2. Initial angles of four drones are all set to 0. Inner-loop PD parameters are calculated as in previous experiments (see *Experiment 1a* of Chapter 4), which for experiments in this Chapter are set to  $K_p = 140.66$  and  $K_d = 41.36$ . Thrust of the drones is limited by hardware to  $20[N]$ . Initial PD parameter values for  $X$  and  $Y$  axes in all the drones are  $K_{px} = K_{py} = 0.22$ ;  $K_{dx} = K_{dy} = 0.76$ , respectively. Drone starting coordinates in the  $XY$  plane are stated in Table 5.3, where subindex 1 is used for the leader drone and the rest are the followers. Drone leader flight along the planned reference, followed by the rest of the drones. Conditions and parameter values are stated previously. The expression for wind disturbance is shown in eq. 5.11

$$d(t) = 2 + 2 \sin\left(\frac{\pi}{4}t\right), \quad (5.11)$$

with  $d(t)$  measured in  $[N]$ . Wind affects simultaneously to each and every quadrotor, nominal wind frequency is  $\omega = \frac{\pi}{4}$ , but in the robustness experiments we test a range of wind frequencies.

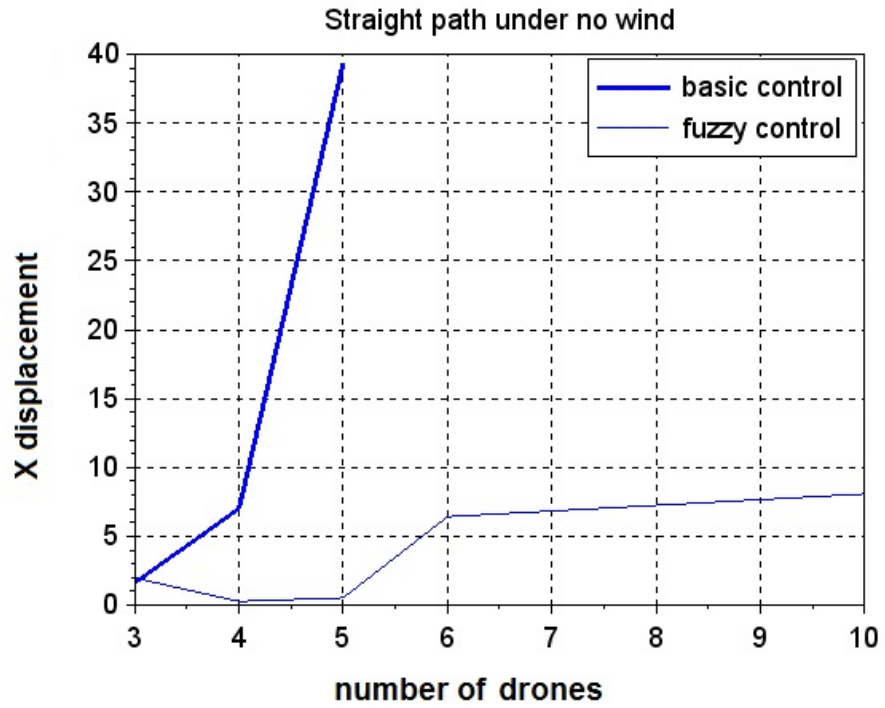
### 5.7.1 Results of *Experiment 3a*

A central question is the scalability of the control system. Could the controller cope with an increasing number of drones in the system? This question is answered in these experiments, by measuring the maximum deviation as the system size grows. Another relevant question is the robustness of the control against wind perturbations. Are there critical wind shear frequencies that overcome the control system? We explore the response over of a range of wind shear frequencies.

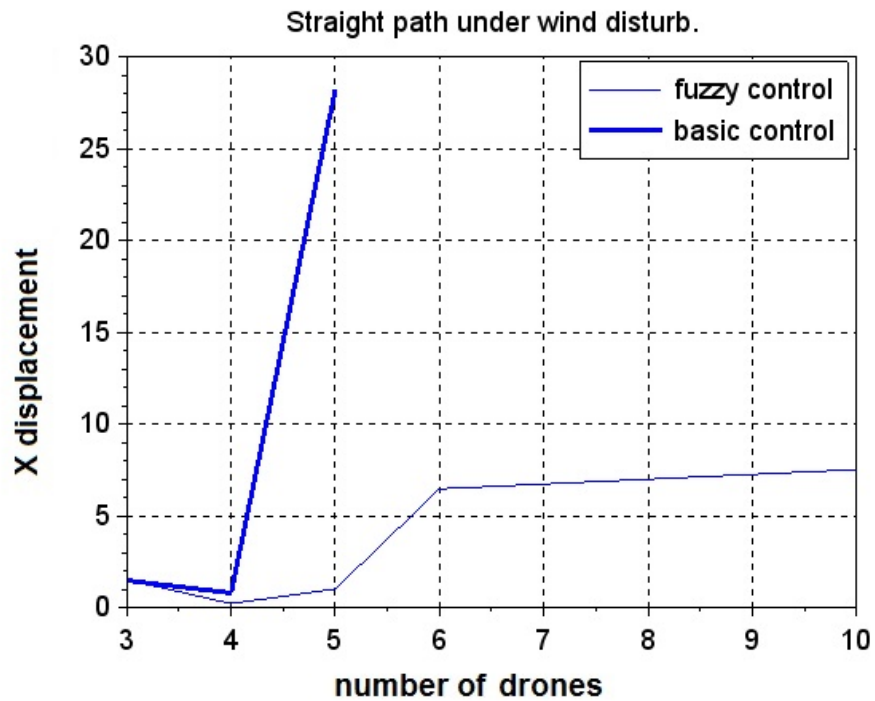
We implemented the experiment both with and without wind perturbations for systems with a different number of quadrotors, and we measured the maximum absolute displacement from the desired trajectory in the  $X$  axis for the last quadrotor. The main results of the *Experiment 3a* are shown on Figure 5.12. As can be seen, the PSO optimal offline control strategy, cannot complete the straight path with a formation of more than 5 quadrotors. This happens because the accumulating error makes the distance among the quadrotors excessive, breaking the catenary so that the DLO-quadrotors model is no longer valid. On the other hand, results for adaptive fuzzy controller shows robust control and bounded error with ten or more quadrotors, suffering little displacement in all the cases (with and without wind perturbation). To illustrate the behavior of the system, Figure 5.13 shows the trajectories of the drones in a system with 4 quadrotors under the PSO optimal offline and adaptive online fuzzy controller in the case without wind disturbances. It can be observed that the PSO offline trajectory has some fluctuations at the start, that induce some spurious trends until the end of the linear path.

### 5.7.2 Results of *Experiment 3b*

Figure 5.14 shows the trajectories of four quadrotors following the leader along the curve path of Figure 5.11, for the offline trained and online adaptive fuzzy controllers. It can be appreciated that the maneuver achieved by the adaptive fuzzy modulated controller is smooth and with little deviation from the leader path. On the other hand the PSO offline estimated parameters produce large oscillations at the beginning of the control, and some of the followers lose the leader path. To measure the efficiency of the model we use the maximum displacement in the  $X$  axis of the actual path relative to the desired curved path of the last quadrotor in the formation. Figure 5.15 plots the results of the tests for increasing numbers of quadrotor in the system. The PD controller tuned offline by PSO cannot deal with systems of more than five quadrotors, while our online fuzzy modulated adaptive controller is able to control teams of up to ten drones with small navigation error. If we include the wind shear perturbation in the simulations, the PSO optimized controller can not deal with more than four quadrotors, while the online fuzzy modulated adaptive controller is able to cope with the wind conditions though the

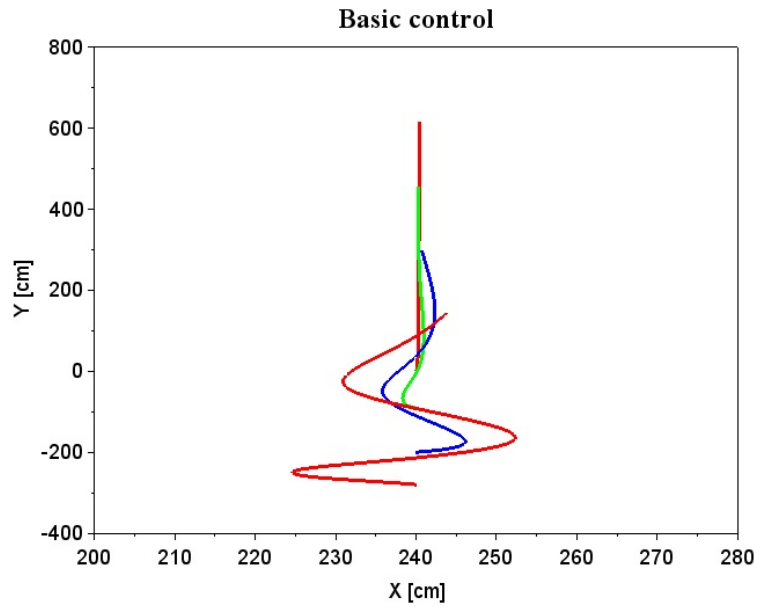


(a)

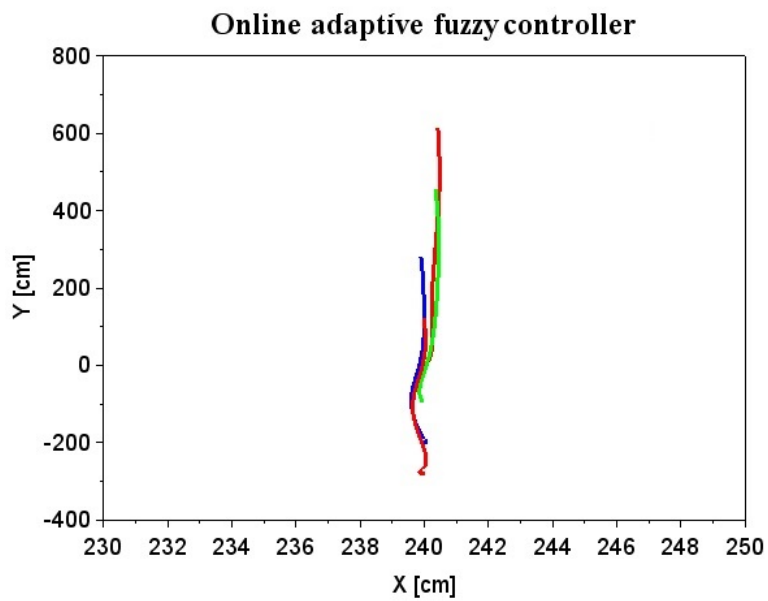


(b)

Figure 5.12: Comparison offline PSO optimal estimation of PD controller parameters vs online fuzzy modulated adaptive controller in *Experiment 3a*. a) Results without perturbations. b) Results under wind conditions.



(a)



(b)

Figure 5.13: Trajectories of a system of four quadrotors in *Experiment 3a* without disturbances. Each color line corresponds to the motion of a quadrotor. (a), off-line PSO optimal parameter setting of the controller. (b), online fuzzy modulated adaptive controller.

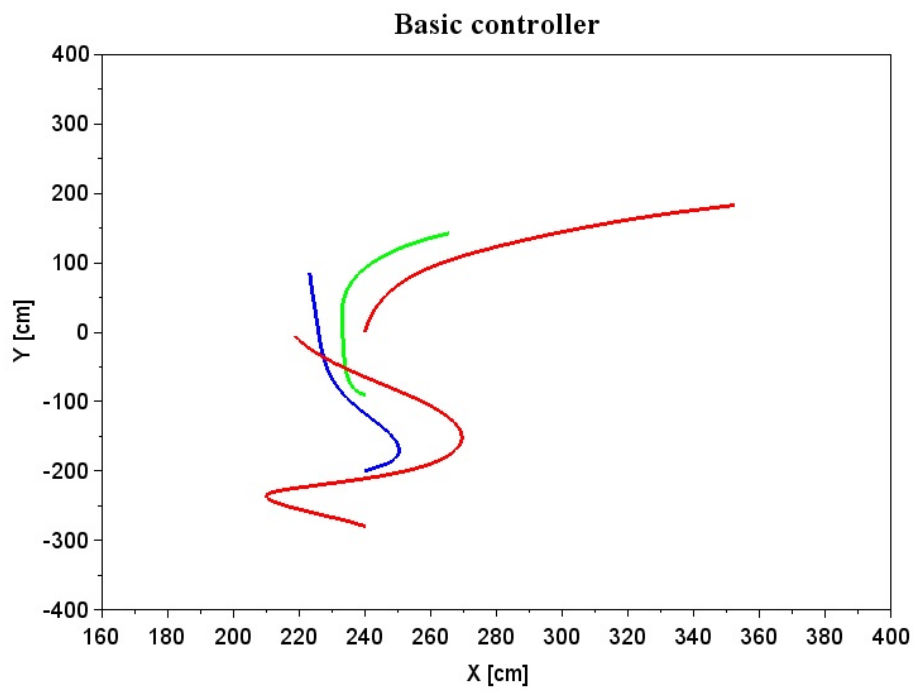
navigation error increases linearly with the number of quadrotors.

Another critical issue is the influence of the wind shear frequency. We have tested a range of wind shear frequencies affecting a system of four drones performing the task of *Experiment 3b*. Results are shown in Figure 5.16. The PSO optimized PD controller can not cope with frequencies greater than  $\frac{\pi}{2}$ , while the online fuzzy modulated adaptive controller is able to sustain much greater wind shear frequencies with small increase of navigation error. Figure 5.17 shows the time evolution of the desired and real angles of 3 quadrotors tuned by our online adaptive fuzzy controller in a realization of *Experiment 3b*. The figure shows how the fuzzy online adaptive control recovers from the initial oscillations in all the robots appearing in the transitory initial stages of the DLO transportation. Finally, Figure 5.18 presents the distance among quadrotors in *Experiment 3b* for a  $n = 3$  system under no wind conditions. Distance remains quite stable for the designed distances in the quadrotor formation.

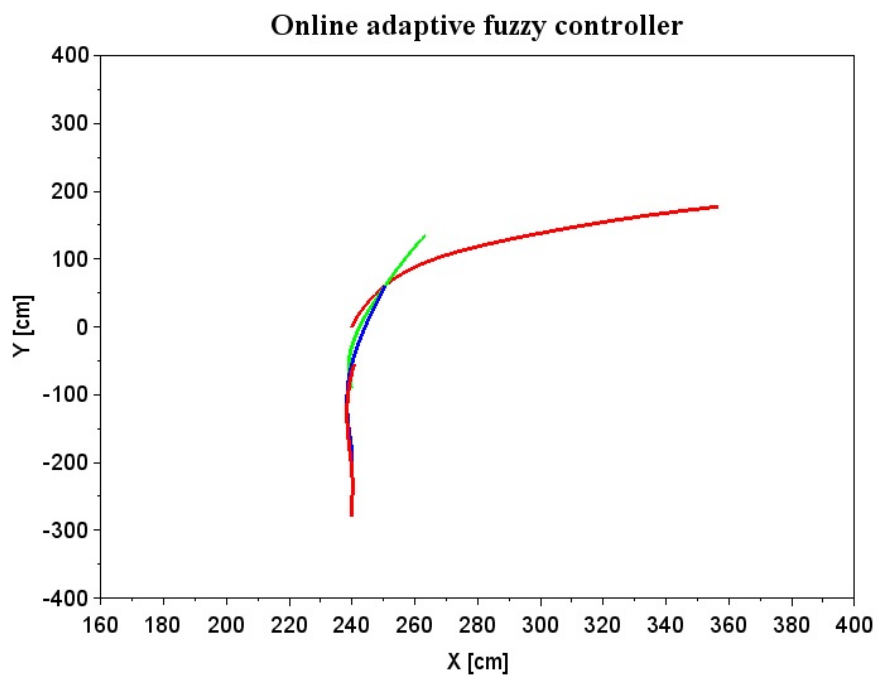
## 5.8 Conclusions

In this Chapter we have been able to show that quadrotors endowed with a novel adaptive fuzzy modulated tuning of PD controllers is able to deal with complex manoeuvres while performing the task of team DLO transportation. We have tested the approach under harsh wind conditions, and for increasing size of the team and the DLO and it clearly outperforms offline tuned PD controllers.



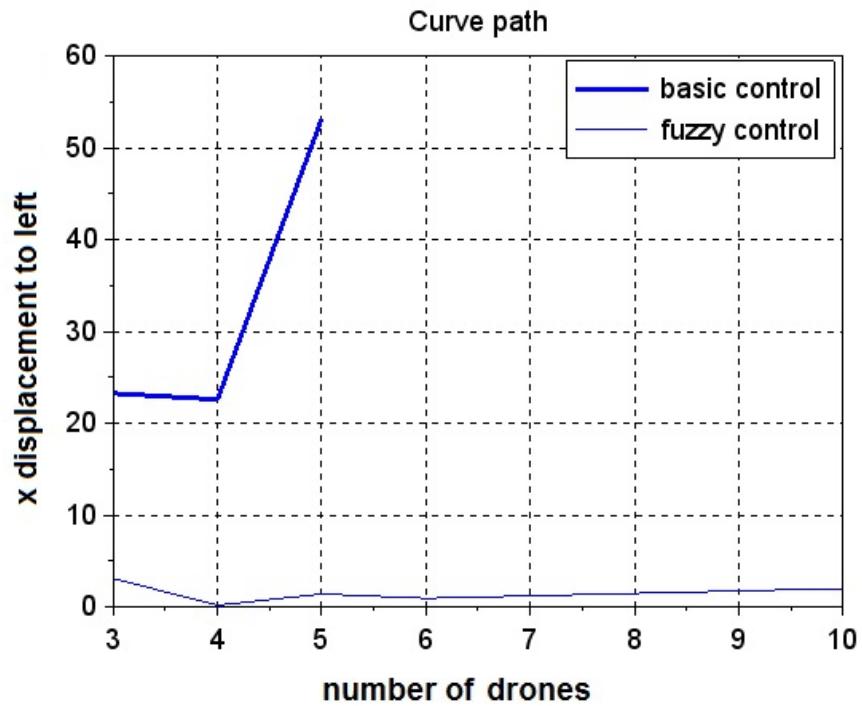


(a)

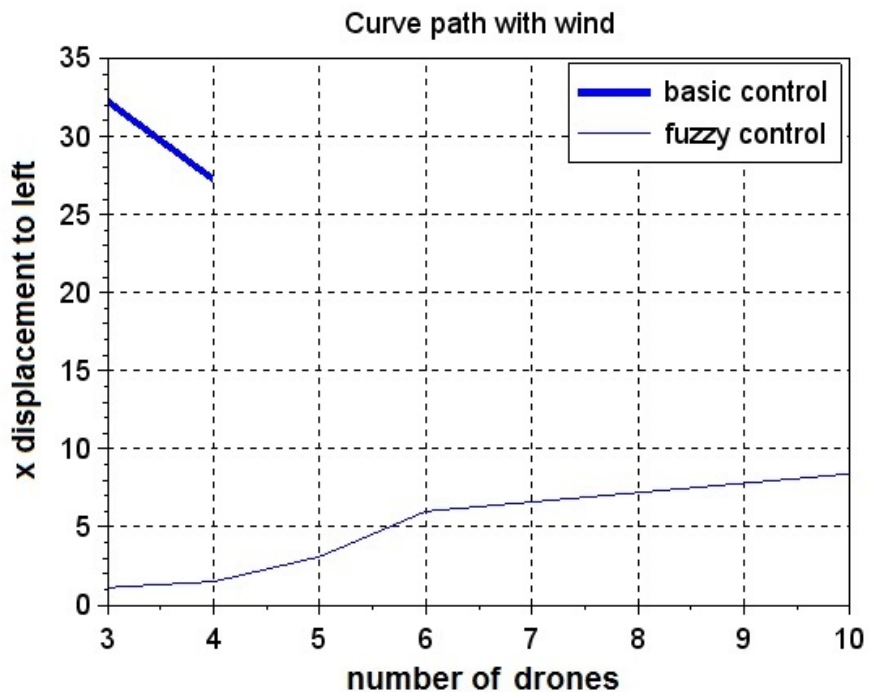


(b)

Figure 5.14: Trajectories of a system of four drones in *Experiment 3b*. (a), offline PSO optimal parameter setting. (b), online fuzzy modulated adaptive controller.



(a)



(b)

Figure 5.15: Error of offline PSO optimal parameter setting versus online fuzzy modulated adaptive controller following a curve path in *Experiment 3b*, increasing the number of quadrotors in the system. a) plot without wind shear influence. b) wind frequency perturbation is set to its nominal value.

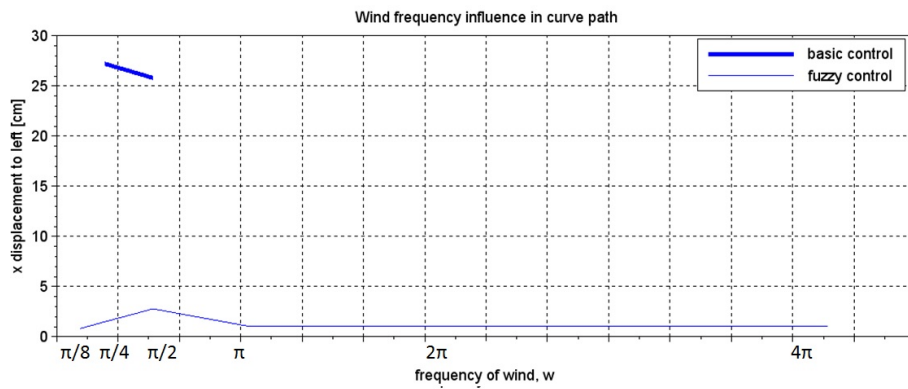


Figure 5.16: Exploration of wind shear frequency impact on navigation error of offline PSO optimal parameter setting versus online fuzzy modulated adaptive controller following the curve path in *Experiment 3b* with 4 drones

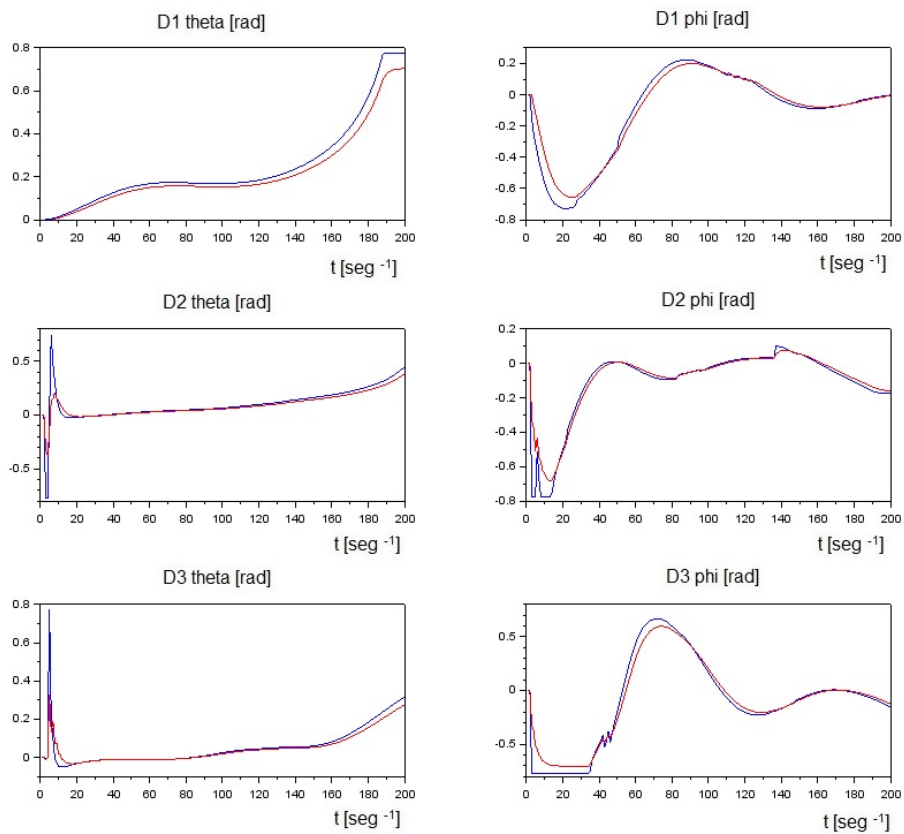


Figure 5.17: Time evolution of reference (blue) and real (red) values of the  $\theta$  and  $\phi$  angles in a system of 3 quadrotors controlled by the fuzzy online adaptive algorithm in the setting of *Experiment 3b*, for no wind conditions. Left and right column plots correspond to the  $\theta$  and  $\phi$  angles of each robot, respectively.

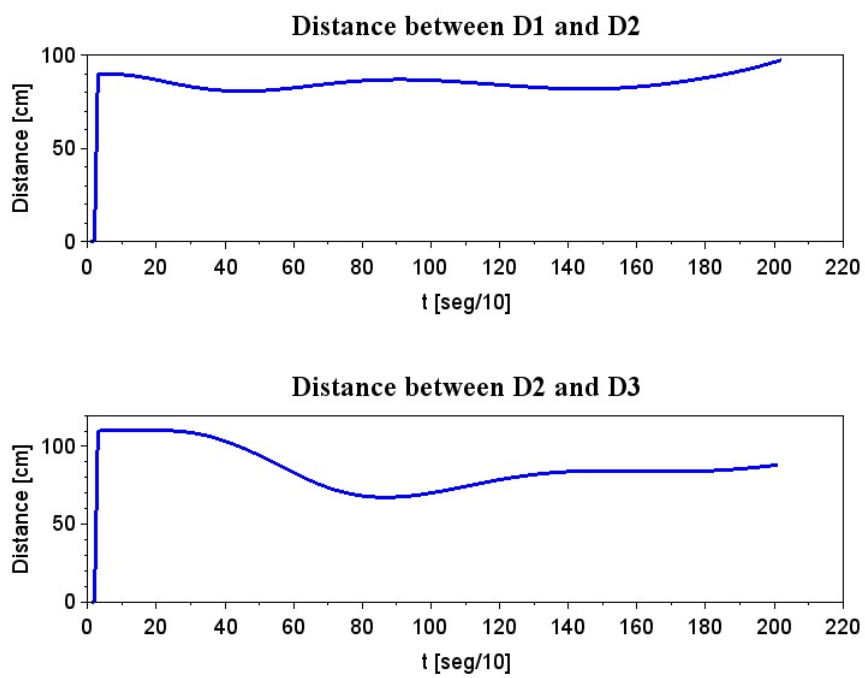


Figure 5.18: Time evolution of reference (blue) and real (red) values of the distance between 3 quadrotors controlled by the fuzzy online adaptive algorithm in the setting of *Experiment 3b*, for no wind conditions.



## Chapter 6

# Conclusions and Future Work

### 6.1 Conclusions

The general goals of the Thesis were proposed in the Introduction. Sections 6.1.1, 6.1.2 and 6.1.3 discuss our achievements of these goals.

#### 6.1.1 Aerial robots modeling for cooperative transportation of DLOs

In this Thesis a novel model of a system to transport DLO solids such as wires and ropes with some aerial robots has been proposed and validated and it represents a work aligned with the Linked Multi-Robot-Component-Systems that the research group of Computational Intelligence in UPV-EHU previously worked on. Being a quadrotor a non-linear system, a careful and precise modeling becomes indispensable. In our approach, the dofs of the system are related to body-centered frame angles (yaw, pitch, roll) and earth-frame Z coordinate. The proposal presents a novel way of representing DLO during transportation as catenaries, going a step further of the state of the art, as most researchers consider payload transportation with UAVs modelled as a pendulum. The dynamic parameters used for the experiments are standard drones' and do not require any modification excepting the ideal linking point between the catenary and the UAV. The simulations show feasible drone behaviour and torque-thrust values.

#### 6.1.2 Offline control strategy

Each quadrotor control was formed by two-loops circuits: attitude-control (inner-loop) and position-control circuits (outer-loop). We considered that all the quadrotors share the same values of inner controllers and that all the circuits related to the four dofs are equal. Offline control strategy was used in first phase for inner-loop tuning and in second, for outer-loop tuning.

We have compared two PID/PD offline tuning methods to adapt the quadrotor system for a smooth, fast and reliable behaviour. Firstly, we tested classical Ziegler-Nichols strategy, and later, we adopted an intelligent tuning method: PSO (Particle Swarm Optimization). Results showed that PSO tuning obtained a better performance, which also resulted to be robust to different quadrotor dynamic parameters and different catenary own weights, which turn the transportation system into an adaptable and robust system and PSO implementation showed good results even with only PD parameters. These experiments were carried out in a single axis direction.

In the second phase of the offline control tuning, horizontal motion of quadrotor system was implemented. Here, only PSO tuning was tested under different stress conditions, paths distances and catenary weights. Experiments resulted in a better performance of the UAV systems if the PSO tuning considered two moving directions rather than only one.

### 6.1.3 Online adaptive control strategy

Online adaptive strategy was applied to outer-loop PD tuning only. We considered inner-loop PD values fixed by PSO in previous step. An adaptive fuzzy strategy tuning method was implemented, inspired on Takagi-Sugeno controllers and *if – then* rules. This tuning strategy was tested in linear and curve paths for quadrotor transportation systems against basic offline control based on PSO algorithm. Effects of number of drone members was also studied and experiments were carried out under different stress conditions.

Besides, a proposal of quadrotors formation both in curve and straight paths was proposed, considering the distance constraints that catenary usage implies.

## 6.2 Future Work

Next, Sections 6.2.1, 6.2.2 describe the future work plan for the three main areas shown in this Thesis.

### 6.2.1 System modeling

Further work will involve testing new approaches to cope with transient states provoked by DLOs and their deformation during transportation process. As explained in State of Art Chapter, multiple proposals of deformable linear objects exist, but a further study on how these dynamic effects change the quadrotor transportation current behaviour should be studied.



Moreover, an experimental realization of the quadrotor DLOs transporting system is highly advisable in order to test the effectiveness and efficiency of current Thesis work. This step will drop loads of information about correct solids or perturbations modeling, control strategy and extra features.

Collision with ground surfaces render the catenary model inaccurate and they happen in the phases of take off and landing. In this Thesis work have not been taken into consideration, and thus an enhancement of the model to adopt this possibility appears as a challenging task.

### **6.2.2 Control strategy**

Implementation of Machine Learning Techniques to our system, focused on future implementation of professional routine works, such as the continuous transportation of cables from one point to another. We refer to adaptive systems when the system uses some intelligent algorithms to find the most suitable actions to its current situation, but we talk about "learning" machine or system once the system is not just able to find some efficient solutions by running some intelligent methods, but also through memorizing, comparing the result of "adaptive" algorithm. Sort of getting experience with time. Machine learning presents a wide horizon of possibilities to implement in drone applications such this.



# Bibliography

- [1] K. J. Aström and T. Hägglund. *PID Controllers: Theory, Design, and Tuning*. Instrument Society of America, Research Triangle Park, NC, 2 edition, 1995.
- [2] J. Acker and D. Henrich. Manipulation of deformable linear objects: From geometric model towards program generation. In *Robotics and Automation, 2005. ICRA 2005. Proceedings of the 2005 IEEE International Conference on*, pages 1541–1547, April 2005.
- [3] Ramzy S. Ali, Ammar A. Aldair, and Ali K. Almousawi. Article: Design an optimal pid controller using artificial bee colony and genetic algorithm for autonomous mobile robot. *International Journal of Computer Applications*, 100(16):8–16, August 2014. Full text available.
- [4] A. Andreu, L. Gil, and P. Roca. A new deformable catenary element for the analysis of cable net structures. *Computers & Structures*, 84(29-30):1882–1890, Nov 2006.
- [5] K.H. Ang, G.C.Y. Chong, and Y. Li. Pid control system analysis, design, and technology. *IEEE Trans Control Systems Tech*, 13(4):559–576, 2005.
- [6] L.M. Argentim, W.C. Rezende, P.E. Santos, and R.A. Aguiar. Pid, lqr and lqr-pid on a quadcopter platform. In *Informatics, Electronics Vision (ICIEV), 2013 International Conference on*, pages 1–6, May 2013.
- [7] H. Asama, A. Matsumoto, and Y. Ishida. Design of an autonomous and distributed robot system: Actress. In *Intelligent Robots and Systems '89. The Autonomous Mobile Robots and Its Applications. IROS '89. Proceedings., IEEE/RSJ International Workshop on*, pages 283–290, Sep 1989.
- [8] F. Augugliaro, S. Lupashin, M. Hamer, C. Male, M. Hehn, M.W. Mueller, J.S. Willmann, F. Gramazio, M. Kohler, and R. D'Andrea. The flight assembled architecture installation: Cooperative construction with flying machines. *Control Systems, IEEE*, 34(4):46–64, Aug 2014.

- [9] F. Augugliaro, A. Mirjan, F. Gramazio, M. Kohler, and R. D'Andrea. Building tensile structures with flying machines. In *Intelligent Robots and Systems (IROS), 2013 IEEE/RSJ International Conference on*, pages 3487–3492, Nov 2013.
- [10] N. Barakat and R. Rajagopalan. Speed control of a dc motor using a feedforward computed torque control scheme. In *Intelligent Control, 1996., Proceedings of the 1996 IEEE International Symposium on*, pages 432–437, Sep 1996.
- [11] G. Beni. The concept of cellular robotic system. In *Intelligent Control, 1988. Proceedings., IEEE International Symposium on*, pages 57–62, Aug 1988.
- [12] A. H. Bond and L. Gasse. Front matter. In Alan H. Bond Les Gasser, editor, *Readings in Distributed Artificial Intelligence*, pages iii –. Morgan Kaufmann, 1988.
- [13] John M. Borky. Payload technologies and applications for uninhabited air vehicles (uavs). In *Aerospace Conference, 1997. Proceedings., IEEE*, volume 3, pages 267–283 vol.3, Feb 1997.
- [14] Samir Bouabdallah, Roland Siegwart, Autonomous Systems, and Lab. Full control of a quadrotor. 2003.
- [15] S. Labiod Boubertakh, S. Bencharef. Pso-based pid and control design and for the stabilization and of a quadrotor. IEEE.
- [16] Gordon Bowden. Stretched Wire Mechanics. *eConf*, C04100411:038, 2004.
- [17] Tammaso Bresciani. Modelling, identification and control of a quadrotor helicopter. Master's Thesis ISRN LUTFD2/TFRT--5823--SE, Department of Automatic Control, Lund University, Sweden, October 2008.
- [18] Joel Brown, Jean-Claude Latombe, and Kevin Montgomery. Real-time knot-tying simulation. *The Visual Computer*, 20(2):165–179, 2004.
- [19] R.E. Brown, G.N. Maliotis, and J.A. Gibby. Pid self-tuning controller for aluminum rolling mill. *Industry Applications, IEEE Transactions on*, 29(3):578–583, May 1993.
- [20] P. Caloud, Wonyun Choi, J.-C. Latombe, C. Le Pape, and M. Yim. Indoor automation with many mobile robots. In *Intelligent Robots and Systems '90. 'Towards a New Frontier of Applications', Proceedings. IROS '90. IEEE International Workshop on*, pages 67–72 vol.1, Jul 1990.

- [21] Y.U. Cao, A.S. Fukunaga, A.B. Kahng, and F. Meng. Cooperative mobile robotics: antecedents and directions. In *Intelligent Robots and Systems 95. 'Human Robot Interaction and Cooperative Robots', Proceedings. 1995 IEEE/RSJ International Conference on*, volume 1, pages 226–234 vol.1, Aug 1995.
- [22] T.-O. Chan and D. D. Lichti. 3d catenary curve fitting for geometric calibration. *ISPRS - International Archives of the Photogrammetry, Remote Sensing and Spatial Information Sciences*, XXXVIII-5/W12:259–264, 2011.
- [23] Peng Cheng, Jonathan Fink, Soonkyum Kim, and Vijay Kumar. *Algorithmic Foundation of Robotics VIII: Selected Contributions of the Eight International Workshop on the Algorithmic Foundations of Robotics*, chapter Cooperative Towing with Multiple Robots, pages 101–116. Springer Berlin Heidelberg, Berlin, Heidelberg, 2010.
- [24] Shicong Dai, Taeyoung Lee, and Dennis S. Bernstein. Adaptive control of a quadrotor uav transporting a cable-suspended load with unknown mass. In *53rd IEEE Conference on Decision and Control December 15-17, 2014. Los Angeles, California, USA*. IEEE, 2014.
- [25] G.G. Denisov, V.V. Novilov, and M.L. Smirnova. The momentum of waves and their effect on the motion of lumped objects along one-dimensional elastic systems. *Journal of Applied Mathematics and Mechanics*, 76(2):225 – 234, 2012.
- [26] T. Dierks and S. Jagannathan. Output feedback control of a quadrotor uav using neural networks. *Neural Networks, IEEE Transactions on*, 21(1):50–66, Jan 2010.
- [27] Feng Ding, Jian Huang, Yongji Wang, and Lifei Mao. Vibration damping in manipulation of deformable linear objects using sliding mode control. In *Control Conference (CCC), 2012 31st Chinese*, pages 4924–4929, July 2012.
- [28] R.J. Duro, M. Graña, and J. de Lope. On the potential contributions of hybrid intelligent approaches to multicomponen robotic system development. *Information Sciences*, 180(14):2635–2648, 2010.
- [29] Z. Echeгойen, I. Villaverde, R. Moreno, M. Graña, and A. d Anjou. Linked multi-component mobile robots: Modeling, simulation and control. *Robotics and Autonomous Systems*, 58(12):1292–1305, Dec 2010.

- [30] Julian Estevez and Manuel Graña. *Bioinspired Computation in Artificial Systems: International Work-Conference on the Interplay Between Natural and Artificial Computation, IWINAC 2015, Elche, Spain, June 1-5, 2015, Proceedings, Part II*, chapter Robust Control Tuning by PSO of Aerial Robots Hose Transportation, pages 291–300. Springer International Publishing, Cham, 2015.
- [31] Julian Estevez, Jose Manuel Lopez-Guede, and Manuel Graña. Quasi-stationary state transportation of a hose with quadrotors. *Robotics and Autonomous Systems*, 63, Part 2(0):187 – 194, 2015. Cognition-oriented Advanced Robotic Systems.
- [32] B. Etkin. Stability of a towed body. *Journal of Aircraft*, 35(2):197–205, 1998.
- [33] Borja Fernandez-Gauna, Jose Manuel Lopez-Guede, and Ekaitz Zulueta. Linked multicomponent robotic systems: Basic assessment of linking element dynamical effect. In *Hybrid Artificial Intelligence Systems, 5th International Conference, HAIS 2010, San Sebastián, Spain, June 23-25, 2010. Proceedings, Part I*, pages 73–79, 2010.
- [34] T. Fukuda and S. Nakagawa. Dynamically reconfigurable robotic system. In *Robotics and Automation, 1988. Proceedings., 1988 IEEE International Conference on*, pages 1581–1586 vol.3, Apr 1988.
- [35] Deepak Gautam and Cheolkeun H. Control of a quadrotor using a smart self-tuning fuzzy PID controller. *International Journal of Advanced Robotic Systems*, page 1, 2013.
- [36] Xun Gong, Yue Bai, Cheng Peng, Changjun Zhao, and Yantao Tian. Trajectory tracking control of a quad-rotor uav based on command filtered backstepping. In *Intelligent Control and Information Processing (ICICIP), 2012 Third International Conference on*, pages 179–184, July 2012.
- [37] Greco. A procedure for the static analysis of cable structures following elastic catenary theory. *international jrnal of solids and structures*, 2014.
- [38] Lei Guo and Songyin Cao. Anti-disturbance control theory for systems with multiple disturbances: A survey. *{ISA} Transactions*, 53(4):846 – 849, 2014. Disturbance Estimation and Mitigation.
- [39] C.X. Habisohn. Method for damping load oscillations on a crane, October 5 1999. US Patent 5,960,969.

- [40] C.X. Habisohn. Method for inching a crane without load swing, April 18 2000. US Patent 6,050,429.
- [41] Jian Huang, Pei Di, T. Fukuda, and T. Matsuno. Dynamic modeling and simulation of manipulating deformable linear objects. In *Mechatronics and Automation, 2008. ICMA 2008. IEEE International Conference on*, pages 858–863, Aug 2008.
- [42] H. M. Irvine. *Cable Structures*. MIT Press, 1981.
- [43] Qimi Jiang and Vijay Kumar. Determination and stability analysis of equilibrium configurations of objects suspended from multiple aerial robots. *Journal of Mechanisms and Robotics*, 4(2):021005, 2012.
- [44] J.F. Jones, B.J. Petterson, and D.R. Strip. Methods of and system for swing damping movement of suspended objects, March 5 1991. US Patent 4,997,095.
- [45] Emery Jou and Weimin Han. 2. *Minimal-Energy Splines with Various End Constraints*, chapter 2, pages 23–40.
- [46] J. Kennedy and R. Eberhart. Particle swarm optimization. In *Neural Networks, 1995. Proceedings., IEEE International Conference on*, volume 4, pages 1942–1948 vol.4, Nov 1995.
- [47] Andrzej Koszewnik. The parrot UAV controlled by PID controllers. *Acta Mechanica et Automatica*, 8(2), Jan 2014.
- [48] K. Kozak, Qian Zhou, and Jinsong Wang. Static analysis of cable-driven manipulators with non-negligible cable mass. *Robotics, IEEE Transactions on*, 22(3):425–433, June 2006.
- [49] R.A. Krohling and J.P. Rey. Design of optimal disturbance rejection pid controllers using genetic algorithms. *Evolutionary Computation, IEEE Transactions on*, 5(1):78–82, Feb 2001.
- [50] Hyeonbeom Lee and H.J. Kim. Robust control of a quadrotor using takagi-sugeno fuzzy model and an lmi approach. In *Control, Automation and Systems (ICCAS), 2014 14th International Conference on*, pages 370–374, Oct 2014.
- [51] Julien Lenoir, Philippe Meseure, Laurent Grisoni, and Christophe Chailou. *Medical Simulation: International Symposium, ISMS 2004, Cambridge*,

- MA, USA, June 17-18, 2004. *Proceedings*, chapter A Suture Model for Surgical Simulation, pages 105–113. Springer Berlin Heidelberg, Berlin, Heidelberg, 2004.
- [52] Xiaohai Li and Jizhong Xiao. Robot formation and control in leader-follower and motion using and direct and lyapunov method. *INTERNATIONAL JOURNAL OF INTELLIGENT CONTROL AND SYSTEMS*, 10(3), 2005.
- [53] Yibo Li, Zitong Li, Yi Wang, and Wei Chen. Design of fuzzy neural network guidance law based on takagi-sugeno for uav. *International Journal of Control and Automation*, 7(12):133–142, 2014.
- [54] JoseManuel Lopez-Guede, Manuel Graña, JoseAntonio Ramos-Hernanz, and Fernando Oterino. A neural network approximation of l-mcrs dynamics for reinforcement learning experiments. In JoseManuel Ferrandez Vicente, Jose©Ramon Alvarez Sanchez, Felix Paz Lopez, and Fco.Javier Toledo Moreo, editors, *Natural and Artificial Computation in Engineering and Medical Applications*, volume 7931 of *Lecture Notes in Computer Science*, pages 317–325. Springer Berlin Heidelberg, 2013.
- [55] Angelo Luongo, Daniele Zulli, and Giuseppe Piccardo. On the effect of twist angle on nonlinear galloping of suspended cables. *Computers & Structures*, 87(15-16):1003–1014, Aug 2009.
- [56] S. Lupashin and R. D’Andrea. Stabilization of a flying vehicle on a taut tether using inertial sensing. In *Intelligent Robots and Systems (IROS), 2013 IEEE/RSJ International Conference on*, pages 2432–2438, Nov 2013.
- [57] M. Fanni A. Ramadan A. Abo-Ismail M. Elsamanty, A. Khalifa. Methodology for identifying quadrotor parameters, attitude estimation and control. Technical Report for, 2013.
- [58] T. Matsuno, D. Tamaki, F. Arai, and T. Fukuda. Manipulation of deformable linear objects using knot invariants to classify the object condition based on image sensor information. *Mechatronics, IEEE/ASME Transactions on*, 11(4):401–408, Aug 2006.
- [59] I. Maza, K. Kondak, M. Bernard, and A. Ollero. Multi-uav cooperation and control for load transportation and deployment. *Journal of Intelligent and Robotic Systems*, 57(1):417–449, 2009.



- [60] Midhun S. Menon, G.K. Ananthasuresh, and Ashitava Ghosal. Natural motion of one-dimensional flexible objects using minimization approaches. *Mechanism and Machine Theory*, 67(0):64 – 76, 2013.
- [61] D. A. Mercado, R. Castro, and R. Lozano. Quadrotors flight formation control using a leader-follower approach. In *2013 European Control Conference (ECC) July 17-19, 2013, Zürich, Switzerland.*, 2013.
- [62] J.-P. Merlet. The kinematics of cable-driven parallel robots with sagging cables: preliminary results. In *Robotics and Automation (ICRA), 2015 IEEE International Conference on*, pages 1593–1598, May 2015.
- [63] Nathan Michael, Jonathan Fink, and Vijay Kumar. Cooperative manipulation and transportation with aerial robots. *Autonomous Robots*, 30(1):73–86, Sep 2010.
- [64] M. Mohammadzaheri, Lei Chen, F. Behnia-Willison, and P. Aryan. A design approach for feedback-feedforward control systems. In *Control and Automation, 2009. ICCA 2009. IEEE International Conference on*, pages 2266–2271, Dec 2009.
- [65] Mohammed J. Mohammed, Mofeed T. Rashid, and Abduladhem A. Ali. Design optimal pid controller for quad rotor system. *International Journal of Computer Applications*, 106(3):15–20, November 2014. Full text available.
- [66] Mohd Ariffanan Mohd Basri, Abdul Rashid Husain, and Kumeresan A. Danapalasingam. Enhanced backstepping controller design with application to autonomous quadrotor unmanned aerial vehicle. *Journal of Intelligent & Robotic Systems*, 79(2):295–321, 2014.
- [67] M. Moll and L.E. Kavraki. Path planning for deformable linear objects. *IEEE Trans. Robot.*, 22(4):625–636, 2006.
- [68] M. Morari and E. Zafiriou. *Robust Process Control*. Prentice Hall, Englewood Cliffs, 1989.
- [69] Frédéric Muttin. Umbilical deployment modeling for tethered {UAV} detecting oil pollution from ship. *Applied Ocean Research*, 33(4):332 – 343, 2011.
- [70] C. Nicol, C.J.B. Macnab, and A. Ramirez-Serrano. Robust adaptive control of a quadrotor helicopter. *Mechatronics*, 21(6):927 – 938, 2011.

- [71] Mark W. Noakes and John F. Jansen. Generalized inputs for damped-vibration control of suspended payloads. *Robotics and Autonomous Systems*, 10(2 - 3):199 – 205, 1992.
- [72] Yaakov Oshman and Michael Isakow. Mini-uav altitude estimation using an inertially stabilized payload. *Aerospace and Electronic Systems, IEEE Transactions on*, 35(4):1191–1203, 1999.
- [73] P. Trivailo P. Williams, D. Sgarioto. Optimal control of an aircraft-towed flexible cable system. *Journal of Guidance, Control and Dynamics*, 29(2):401–410, 2006.
- [74] Dinesh K. Pai. STRANDS: Interactive Simulation of Thin Solids using Cosserat Models. *Computer Graphics Forum*, 2002.
- [75] I. Palunko, R. Fierro, and P. Cruz. Trajectory generation for swing-free maneuvers of a quadrotor with suspended payload: A dynamic programming approach. In *Robotics and Automation (ICRA), 2012 IEEE International Conference on*, pages 2691–2697, May 2012.
- [76] Lynne E. Parker. *Distributed Autonomous Robotic Systems 4*, chapter Current State of the Art in Distributed Autonomous Mobile Robotics, pages 3–12. Springer Japan, Tokyo, 2000.
- [77] Chao Peng, Zhenzhen Zhang, Jianxiao Zou, Kai Li, and Jian Zhang. Internal model based robust inversion feedforward and feedback 2dof control for {LPV} system with disturbance. *Journal of Process Control*, 23(10):1415 – 1425, 2013.
- [78] J. Phillips, A. Ladd, and L.E. Kavraki. Simulated knot tying. In *Robotics and Automation, 2002. Proceedings. ICRA '02. IEEE International Conference on*, volume 1, pages 841–846 vol.1, May 2002.
- [79] Hong Qin and Demetri Terzopoulos. D-nurbs: A physics-based geometric design framework. *IEEE Transactions on Visualization and Computer Graphics*, 2(1, 2):85–96, 1996.
- [80] Cesáreo Raimúndez and José Luis Camaño. *CONTROLO'2014 – Proceedings of the 11th Portuguese Conference on Automatic Control*, chapter Transporting Hanging Loads Using a Scale Quad-Rotor, pages 471–482. Springer International Publishing, Cham, 2015.
- [81] Kapseong Ro and James W Kamman. Modeling and simulation of hose-paradrogue aerial refueling systems. *Journal of guidance, control, and dynamics*, 33(1):53–63, 2010.

- [82] V. Roldao, R. Cunha, D. Cabecinhas, C. Silvestre, and P. Oliveira. A leader-following trajectory generator with application to quadrotor formation flight. *Robotics and Autonomous Systems*, 62(10):1597 – 1609, 2014.
- [83] Michael Rubenstein, Alejandro Cornejo, and Radhika Nagpal. Programmable self-assembly in a thousand-robot swarm. *Science*, 345(6198):795–799, 2014.
- [84] M. Saha and P. Isto. Manipulation planning for deformable linear objects. *Robotics, IEEE Transactions on*, 23(6):1141–1150, Dec 2007.
- [85] Atheer L. Sali. Flight pid controller design for a uav quadrotor. *Scientific Research and Essays Vol. 5(23)*, pp. 3660-3667, 4 December, 2010, 2010.
- [86] A.C. Satici, H. Poonawala, and M.W. Spong. Robust optimal control of quadrotor uavs. *Access, IEEE*, 1:79–93, 2013.
- [87] W.E. Singhose and D. Kim. Methods and systems for double-pendulum crane control, August 7 2012. US Patent 8,235,229.
- [88] J.M. Sousa, R. Babuska, and H. Verbruggen. Internal model control with a fuzzy model: application to an air-conditioning system. In *Fuzzy Systems, 1997., Proceedings of the Sixth IEEE International Conference on*, volume 1, pages 207–212 vol.1, Jul 1997.
- [89] K. Sreenath, N. Michael, and V. Kumar. Trajectory generation and control of a quadrotor with a cable-suspended load - a differentially-flat hybrid system. In *Robotics and Automation (ICRA), 2013 IEEE International Conference on*, pages 4888–4895, May 2013.
- [90] Koushil Sreenath and Vijay Kumar. Dynamics, control and planning for cooperative manipulation of payloads suspended by cables from multiple quadrotor robots. In *Robotics: Science and Systems (RSS)*, 2013.
- [91] G.P. Starr. Swing-free transport of suspended objects with a robot manipulator. In *Decision and Control, 1983. The 22nd IEEE Conference on*, pages 1484–1487, Dec 1983.
- [92] G.P. Starr. Swing-free transport of suspended objects with a path-controlled robot manipulator. *J. Dyn. Sys., Meas., Control*, 107(1):97–100, 1985.
- [93] D.R. Strip. Swing-free transport of suspended objects: a general treatment. *Robotics and Automation, IEEE Transactions on*, 5(2):234–236, Apr 1989.

- [94] Miguel Such, Jesus R. Jimenez-Octavio, Alberto Carnicero, and Oscar Lopez-Garcia. An approach based on the catenary equation to deal with static analysis of three dimensional cable structures. *Engineering Structures*, 31(9):2162 – 2170, 2009.
- [95] G. Szafranski and R. Czyba. Different approaches and of pid and control uav and type quadrotor. In *Proceedings of the International Micro Air Vehicles conference 2011 summer edition*, 2011.
- [96] Mazidah Tajjudin, Ramli Adnan, Norlela Ishak, Mohd Hashimah Ismail, Hezri Fazalul, Rahiman Faculty, and of Engineering. Model reference input for an optimal pid tuning using pso. In *2011 IEEE International Conference on Control System, Computing and Engineering*. IEEE, 2011.
- [97] T. Takagi and M. Sugeno. Fuzzy identification of systems and its applications to modeling and control. *Systems, Man and Cybernetics, IEEE Transactions on*, SMC-15(1):116–132, Jan 1985.
- [98] Wen Tan, Jizhen Liu, Tongwen Chen, and Horacio J. Marquez. Comparison of some well-known {PID} tuning formulas. *Computers & Chemical Engineering*, 30(9):1416 – 1423, 2006.
- [99] K.S. Tang, G.R. Chen, K.F. Man, and S. Kwong. *PID Control: New Identification and Design Methods*, chapter Fuzzy Logic and Genetic Algorithm Methods in PID Tuning, pages 339–360. Springer London, London, 2005.
- [100] Tanveer. Pid based controller design for attitude stabilization of quad-rotor. Technical Report research, 2014.
- [101] Demetri Terzopoulos, John Platt, Alan Barr, and Kurt Fleischer. Elastically deformable models. *SIGGRAPH Comput. Graph.*, 21(4):205–214, August 1987.
- [102] Huu-Tai Thai and Seung-Eock Kim. Nonlinear static and dynamic analysis of cable structures. *Finite Elements in Analysis and Design*, 47(3):237 – 246, 2011.
- [103] A. Theetten, L. Grisoni, C. Andriot, and B. Barsky. Geometrically exact dynamic splines. *Computer Aided Desisgn*, 40(1):35–48, 2008.
- [104] M. Tognon, S. S. Dash, and A. Franchi. Observer-based control of position and tension for an aerial robot tethered to a moving platform. *IEEE Robotics and Automation Letters*, 1(2):732–737, July 2016.

- [105] Marco Tognon. *Attitude and Tension Control of a Tethered Formation of Aerial Vehicles*. PhD thesis, 2014.
- [106] Van Tu Duong, Hak Kyeong Kim, Tan Tien Nguyen, Sea June Oh, and Sang Bong Kim. Position control of a small scale quadrotor using block feedback linearization control. *Lecture Notes in Electrical Engineering*, pages 525–534, 2014.
- [107] H. Wakamatsu, K. Takahashi, and S. Hirai. Dynamic modeling of linear object deformation based on differential geometry coordinates. In *Robotics and Automation, 2005. ICRA 2005. Proceedings of the 2005 IEEE International Conference on*, pages 1028–1033, April 2005.
- [108] Hideo Wakamatsu and Shinichi Hirai. Static modeling of linear object deformation based on differential geometry. *The International Journal of Robotics Research*, 23(3):293–311, 2004.
- [109] Jiangjiang Wang, Youyin Jing, and Chunfa Zhang. Robust cascade control system design for central airconditioning system. In *Intelligent Control and Automation, 2008. WCICA 2008. 7th World Congress on*, pages 1506–1511, June 2008.
- [110] Naifeng Wen, Lingling Zhao, Xiaohong Su, and Peijun Ma. Uav online path planning algorithm in a low altitude dangerous environment. *Automatica Sinica, IEEE/CAA Journal of*, 2(2):173–185, April 2015.
- [111] N. Yanai, M. Yamamoto, and Akira Mohri. Feedback control for wire-suspended mechanism with exact linearization. In *Intelligent Robots and Systems, 2002. IEEE/RSJ International Conference on*, volume 3, pages 2213–2218 vol.3, 2002.
- [112] A. Yavnai. Distributed decentralized architecture for autonomous cooperative operation of multiple agent system. In *Autonomous Underwater Vehicle Technology, 1994. AUV '94., Proceedings of the 1994 Symposium on*, pages 61–67, Jul 1994.
- [113] F.-K. Yeh. Attitude controller design of mini-unmanned aerial vehicles using fuzzy sliding-mode control degraded by white noise interference. *Control Theory Applications, IET*, 6(9):1205–1212, June 2012.
- [114] Bao-Lin Zhang, Yu-Jia Liu, Hui Ma, and Gong-You Tang. Discrete feed-forward and feedback optimal tracking control for offshore steel jacket platforms. *Ocean Engineering*, 91:371 – 378, 2014.

- [115] Hua Zhong, L. Pao, and R. de Callafon. Feedforward control for disturbance rejection: Model matching and other methods. In *Control and Decision Conference (CCDC), 2012 24th Chinese*, pages 3528–3533, May 2012.
- [116] Yingchun Zhong and Yan Luo. Comparative study of single-loop control and cascade control of third-order object. *Procedia Engineering*, 15:783 – 787, 2011. {CEIS} 2011.
- [117] M. Zhuang and D.P. Atherton. Automatic tuning of optimum pid controllers. *Control Theory and Applications, IEE Proceedings D*, 140(3):216–224, May 1993.
- [118] Andrew Zulu and Samuel John. A review of control algorithms for autonomous quadrotors. *Open Journal of Applied Sciences*, 224(14):547–556, 2014.